NONLINEAR ANALYSIS OF RC FRAMES RETROFITTED WITH STRUCTURAL STEEL ELEMENTS

A THESIS SUBMITTED TO
THE GRADUATE SCHOOL OF NATURAL AND APPLIED SCIENCES
OF
MIDDLE EAST TECHNICAL UNIVERSITY

BY

UĞUR AKPINAR

IN PARTIAL FULFILLMENT OF THE REQUIREMENTS
FOR
THE DEGREE OF MASTER OF SCIENCE
IN
CIVIL ENGINEERING

SEPTEMBER 2010

Approval of the thesis:

NONLINEAR ANALYSIS OF RC FRAMES RETROFITTED WITH STRUCTURAL STEEL ELEMENTS

submitted by **UĞUR AKPINAR** in partial fulfillment of the requirements for the degree of **Master of Science in Civil Engineering Department, Middle East Technical University** by,

Prof. Dr. Canan Özgen _____
Dean, Graduate School of **Natural and Applied Sciences**

Prof. Dr. Güney Özcebe _____
Head of Department, **Civil Engineering**

Assoc. Prof. Dr. Barış Binici _____
Supervisor, **Civil Engineering Dept., METU**

Examining Committee Members:

Assoc. Prof. Dr. Ahmet Yakut _____
Civil Engineering Dept., METU

Assoc. Prof. Dr. Barış Binici _____
Civil Engineering Dept., METU

Asst. Prof. Dr. Özgür Kurç _____
Civil Engineering Dept., METU

Asst. Prof. Dr. Afşin Sarıtaş _____
Civil Engineering Dept., METU

Mustafa Tan _____
Civil Engineer, PROTA

Date: 06.10.2010

I hereby declare that all information in this document has been obtained and presented in accordance with academic rules and ethical conduct. I also declare that, as required by these rules and conduct, I have fully cited and referenced all material and results that are not original to this work.

Name, Last name: Uğur AKPINAR

Signature :

ABSTRACT

NONLINEAR ANALYSIS OF RC FRAMES RETROFITTED WITH STRUCTURAL STEEL ELEMENTS

Akpınar, Uğur

M.Sc., Department of Civil Engineering

Supervisor: Assoc. Prof. Dr. Barış Binici

September 2010, 84 pages

Deficient concrete structures are serious danger in seismic zones. In order to minimize economical and human loss, these structures should be retrofitted. Selecting suitable retrofitting schemes requires detailed investigation of these systems. Considering these facts, this study aims to calibrate analytical models of systems with chevron braces and internal steel frames; and evaluate their seismic performances. First, analytical models of the frames with braces and internal steel frames were prepared and then their responses were compared with cyclic responses of experimental studies. Results of these models were used to determine performance limits by the methods proposed by TEC2007 and ASCE/SEI-41. Then, calibrated models were employed for time history analyses with various scales of Duzce ground motion and analytical results were compared with experimental findings. Seismic performance of these systems was also evaluated by using aforementioned codes. Finally, evaluated retrofitting schemes were applied to a 4-story 3-bay reinforced concrete frame that was obtained from an existing deficient structure and effectiveness of applied retrofitting schemes was investigated in detail.

Keywords: Chevron Brace, Internal Steel Frames, Infill Walls, Retrofitting, Nonlinear Dynamic Analysis

ÖZ

YAPISAL ÇELİK ELEMANLARLA GÜÇLENDİRİLMİŞ BETONARME YAPILARIN DOĞRUSAL OLMAYAN ANALİZLERİ

Akpınar, Uğur

Yüksek Lisans, İnşaat Mühendisliği Bölümü

Tez Yöneticisi: Doç.Dr. Barış Binici

Eylül 2010, 84 sayfa

Deprem bölgelerinde bulunan yetersiz betonarme yapılar ciddi tehlike oluşturmaktadır. Ekonomik zararların ve can kayıplarının en aza indirilmesi, bu yapıların güçlendirilmesini zorunlu kılmaktadır. Uygun güçlendirme yöntemini seçebilmek, bu yöntemlerin detaylıca araştırılmasını gerektirmektedir. Bu bilgiler ışığında, bu çalışmada çelik çaprazlar ve iç çelik çerçevelerin kullanıldığı betonarme çerçevelerin matematik modelleri oluşturulmuş ve bunların sismik performansları incelenmiştir. İlk bölümde çelik çaprazlı ve iç çelik çerçeveli betonarme çerçevelerin matematiksel modellerinden alınan sonuçlar deney sonuçlarıyla eşleştirilmiştir. Daha sonra analiz sonuçları kullanılarak yapının performansı TEC2007 ve ASCE/SEI-41'de önerilen yöntemlere göre belirlenmiştir. İkinci bölümde eşlenen modellerin Düzce depreminin farklı ölçeklerini kullanarak dinamik analizleri yapılmış, yapıların performansları aynı yöntemlerle belirlenmiştir. Son olarak oluşturulan matematik modelleri 4 katlı 3 açıklıklı betonarme bir yapıdan alınan çerçeveye uygulanmış, güçlendirme yöntemlerinin yapıya olan etkileri detaylıca incelenmiştir.

Anahtar Kelimeler: Çelik Çapraz, İç Çelik Çerçeve, Tuğla Duvarlar, Güçlendireme, Doğrusal Olmayan Dinamik Analiz

ACKNOWLEDGMENTS

This study was conducted under the supervision of Assoc. Prof. Dr. Barış Binici. I would like to express my appreciation for the help, expert guidance, suggestions that he has provided me throughout the study. It was a great honor and pleasure to work with him.

I would like to thank to my superiors for their important suggestions throughout my research. Ramazan Özçelik and Efe Kurt deserve thanks for their technical support. I also should thank my friends and my colleagues in K2-105 of the faculty for their greatest friendship and support.

I would like to express my deepest appreciation to my parents and my darling for their confidence in me and for the support, love and understanding that they have provided me throughout my life.

The financial support by the Scientific and Technological Research Council of Turkey (TÜBİTAK) is gratefully acknowledged.

TABLE OF CONTENTS

LIST OF TABLES

TABLES

LIST OF FIGURES

FIGURES

LIST OF SYMBOLS / ABBREVIATIONS

a	Effective Strut Area for Infill Walls
A_g	Gross Area of a Section
ACI	American Concrete Institute
ASCE	American Society of Civil Engineers
CP	Collapse Prevention
C_u	Compressive Strength of Braces at First Buckling
damage1	Damage due to Ductility
damage2	Damage due to Energy
DR	Drift Ratio
e	Initial Eccentricity at Center of a Brace Member
E	Young's Modulus
E_c	Young's Modulus of Concrete
E_{ms}	Young's Modulus of Plaster-Infill Composite
f_b	Compressive Strength of a Brick Element
f_c	Uniaxial Crushing Strength of a Material
f_t	Uniaxial Tensile Strength of a Material
f_{mv}	Shear Strength of a Bed Mortar/Plaster Mix
f_{cm}	Compressive Strength of a Strut Member
F_m’	Compressive Strength of Mortar
F_y	Yield Strength of a Material
FRP	Fiber Reinforcement Polymers
g	Gravitational Acceleration
h_{col}	Height of a Column
ISF	Internal Steel Frame
IO	Immediate Occupancy
L	Length of a Member

LS	Life Safety
M_{pb}	Plastic Moment Capacity of a Brace Member
P	Axial Force on a Cross-section
pinchX	Pinching Factor for Strain During Reloading
pinchY	Pinching Factor for Stress During Reloading
P_b	Buckling Load of a Brace Member
PSD	Pseudo-Dynamic
r_{inf}	Diagonal Length of a Infill Panel
RC	Reinforced Concrete
SP	Specimen
t_{in}	Thicknesses of a Brick Unit
t_p	Thicknesses of a Plaster
TEC	Turkish Earthquake Code
URM	Unreinforced Masonry
Δ_c	Axial Deformation at Buckling Load of Braces
$(\varepsilon_c)_{IO}$	Concrete Compression Strain Limit for IO
$(\varepsilon_c)_{LS}$	Concrete Compression Strain Limit for LS
$(\varepsilon_c)_{CP}$	Concrete Compression Strain Limit for CP
$(\varepsilon_s)_{IO}$	Longitudinal Reinforcement Strain Limit for IO
$(\varepsilon_s)_{LS}$	Longitudinal Reinforcement Strain Limit for LS
$(\varepsilon_s)_{CP}$	Longitudinal Reinforcement Strain Limit for CP
λ	Slenderness Parameter
φ	Reinforcement Diameter
ρ_s	Available Confining Steel Ratio
ρ_{sm}	Required Confining Steel Ratio
θ	Angle whose Tangent is Infill Height to Length Ratio

CHAPTER 1

INTRODUCTION

1.1 Problem Statement

Many existing concrete structures in Turkey do not satisfy the requirements of modern seismic codes. Therefore, these structures have poor ductility and lateral loading capacities, which make them vulnerable under seismic hazard. Inadequate detailing, poor material quality, insufficient section sizes, usage of plain bars, not providing strong column-weak beam connections are the frequently observed deficiencies in these structures. In addition to these, irregularities such as soft story, heavy overhangs or short columns also adversely affect the seismic response of the structures. Previous earthquakes showed that retrofitting of these structures is inevitable for minimizing both economical and human loss.

There are several retrofitting methods developed to act as a new lateral load resisting system or aim to upgrade existing deficient members. Using Fiber Reinforcement Polymers (FRP) for example, is one way of member strengthening. Such member upgrade methods are more effective if the number of members requiring strengthening is limited in number. Otherwise adding a new structural system, which is the focus of this thesis, is more efficient.

Shear walls are one of the widely used retrofitting techniques in Turkey. There is a wide range of experimental studies that signify the effectiveness of post-

installed RC walls on stiffness and strength enhancement of the structures. Although they are very effective as lateral load resisting systems, they have disadvantages such as requiring extensive workmanship, increasing the mass of structure and blocking free spaces inside frames.

The use of steel braces is another possible retrofitting technique for deficient structures. These systems have important advantages such as effective usage of openings; slight increase in mass and economical application especially due to rapid installation. Application on the outer plane of the structures is another way of retrofitting by steel braces. External bracing system is feasible due to minimal effect on serviceability of building during the construction. However, slenderness of steel sections should be carefully determined to meet the deformation demands. Buckling of the brace members has also a significant effect on the performance of these strengthening methods.

Integrating a new internal steel frame (ISF) as a strengthening system is not common in Turkey but an effective way of retrofitting methods. ISF's also support structures under the gravitational loads and could help in preventing gravity collapses under high lateral deformation demands. It could be used with or without anchors depending on the desired strength increase.

All these methods aim to keep the structure under the required safety limits while meeting the lateral load and ductility demands of the structure during an earthquake. Before applying any of these methods, existing seismic performance of the structures should be carefully examined. The feasible retrofitting schema then needs to be selected by paying attention to economy, ease of application and retrofitting time.

1.2 Literature Survey

In this section, analytical studies focusing on steel braces and steel retrofit of existing structures surveyed within the scope of this thesis will be briefly summarized.

Ikeda and Mahin (1986) developed a pin-ended brace model with a plastic hinge located at its mid-point (Figure 1.1). In the model, an analytical axial force-plastic hinge formulation was derived and the variation of tangent modulus of elasticity during cycles was studied. Cyclic analysis results of the braces and dynamic analysis results of braced frame structures were compared with the test data. Based on their studies following conclusions were drawn:

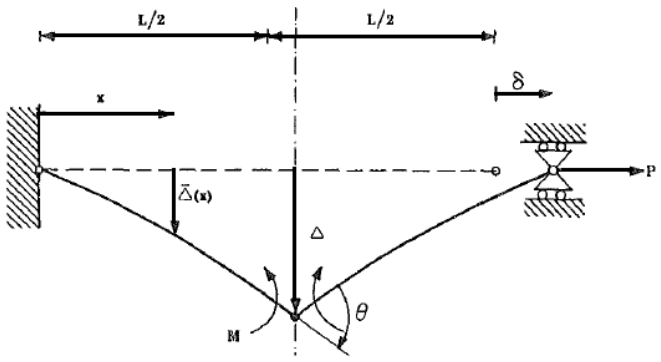

Figure 1.1: *Proposed brace model*

- Due to simplicity of the model center-plastic hinge approach is suitable for large scale structural system analyses.
- Model is capable of simulating the inelastic behavior of braces in cyclic and dynamic analysis.
- Modifications on the formulation by considering variation of the tangent modulus of elasticity and local buckling can lead a better estimation of cyclic inelastic behavior.

Badoux and Jirsa (1990) investigated the behavior of braced frames both analytically and experimentally. Retrofitted frame was prepared to have deep beams and short columns and tested under lateral cyclic loading. An analytical study was conducted by simulating an interior column in a braced frame loaded laterally (Figure 1.2). In addition to that, a parametric study was conducted to understand the effect of slenderness ratio of braces on the response of retrofitted frame.

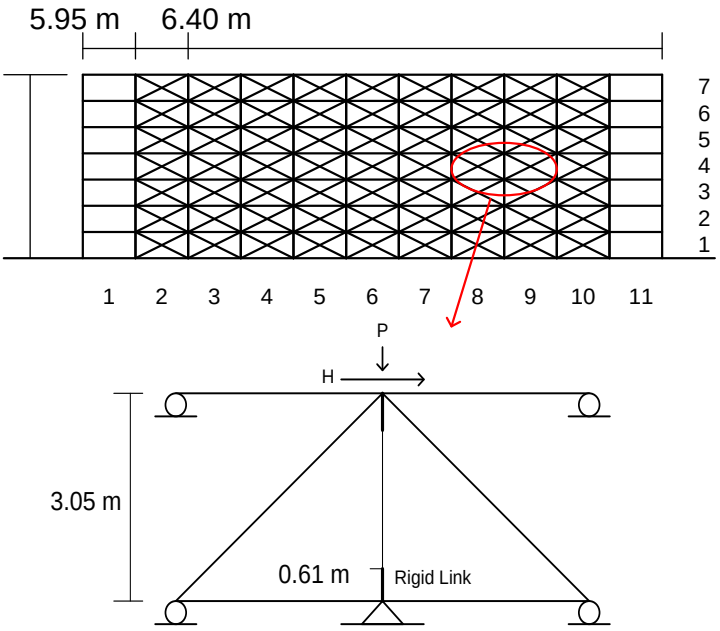

Figure 1.2: *Analytical model of analyzed sub-frame*

Studies showed that:

- RC frame and the bracing system could be taken as independent systems and designer can adjust desired strength and stiffness by changing brace sections.
- To have acceptable seismic behavior, brace sections should be designed to remain elastic because of the unpredictable nature of exposed seismic loading that can trigger buckling.
- Reducing slenderness ratio would help to prevent inelastic buckling effects on the brace sections.
- To prevent failure under gravity loads, failure mechanism of RC frame should be taken into account before designing the braces.

Pincheira and Jirsa (1995) examined the performance of three, seven and twelve story existing RC buildings for five earthquake ground motion records measured on firm and soft soils. Structures were rehabilitated with three different rehabilitation schemes; post tensioned bracing, X-bracing and addition of structural

infill walls (Figure 1.3). All methods were compared with the response of original structures in terms of stiffness and strength enhancement. According to analysis results:

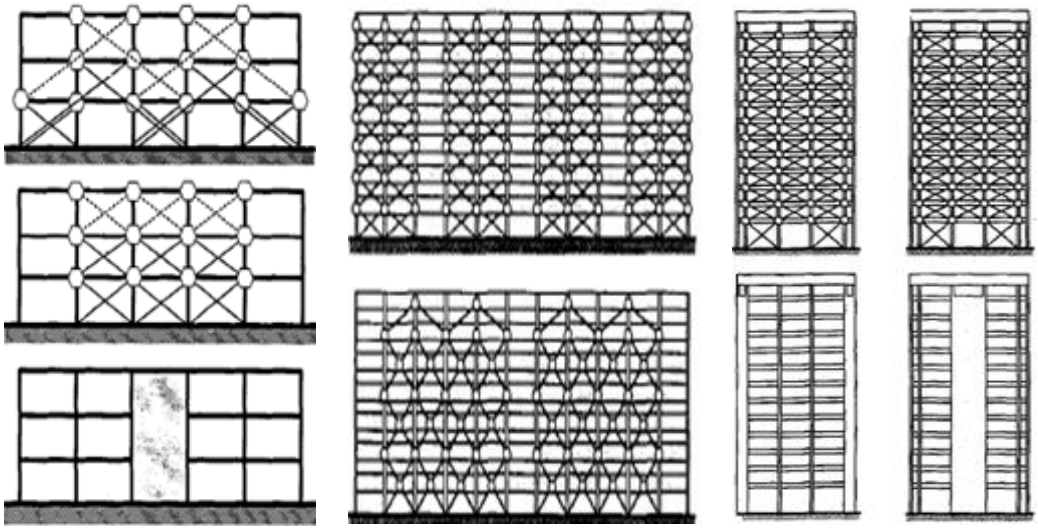

(a) Three-Story Building (b) Seven-Story Building (c) Twelve-Story

Figure 1.3: *Retrofitting schemes of examined buildings*

- In order provide acceptable seismic performance, it is possible to choose from several different brace arrangements whilst the solution being non-unique.
- For three-story building, all the retrofitting methods exhibited satisfactory performance for all ground motions.
- For seven- and twelve-story buildings, structural wall provided satisfactory performance however bracing systems did not provide the expected performance for all ground motion records.
- Brace systems could affect axial load levels on RC members adversely, so for such cases it could be important to improve axial load capacities of RC members.
- For the post tensioned brace case, distribution of internal forces on RC members are closely related with bracing pattern, brace sizes and initial level of brace pre-stress.

Tremblay (2001) examined several experimental studies on inelastic response of steel braces under cyclic loading (Figure 1.4). A wide range of brace parameters were investigated such as section type, dimensions, boundary conditions, slenderness, compactness and material properties. Effect of displacement histories and the buckling modes (in-plane, out-of-plane) of braces were also investigated. Equations were proposed for post-buckling, displacement and force relations. Recommendations of this study were;

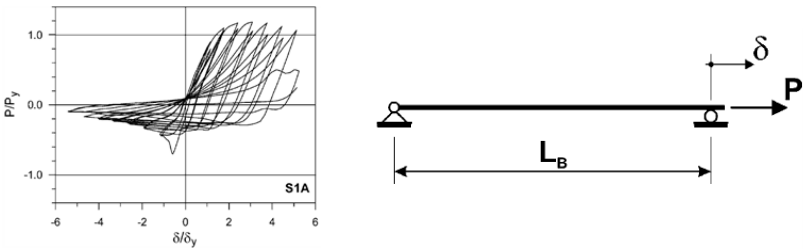

Figure 1.4: *Typical brace section and its hysteretic response*

- Actual yield strength of all the specimens exceeded the nominal properties and this effect should be included in design.
- The compressive strength of the braces at first buckling (C_u) generally exceeded the value founded from column design curves.
- For less slender braces ($\lambda = \frac{KL}{r}\sqrt{\frac{F_y}{\pi^2 E}} < 1$), compression and tension braces could develop simultaneously a compression force equal to C_u and a tension force equal to (A_g*F_y). For slender braces compression force can be taken as 0.8*C_u when tension braces have yielded.
- Applied loading history affects the maximum tension force that will develop in a brace section and highest loads being observed under large tension excursions applied early in the test.
- Proposed equations for investigated parameters agreed well with the test data and values specified in several codes should be modified in order to have better estimations.
- Fracture of bracing members was highly dependent on slenderness ratio and slender braces can sustain higher ductility levels prior to fracture.

Ghobarah and Elfath (2001) investigated the seismic performance of eccentric steel bracing by analyzing a low-rise non-ductile RC structure subjected to various ground motion records. In eccentric bracing systems, buckling is prevented by using ductile steel links that dissipates energy under seismic loads. Another advantage of this scheme is the ease of installation of eccentric braces compared to that of concentric braces. The claimed reason was braces needed only three connections with RC members. An existing three-story office building was rehabilitated using; (a) concentric inverted-V-bracing, (b) inverted-V bracing with vertical steel links (eccentric), (c) different orientation of second case (Figure 1.5). According to the analysis results:

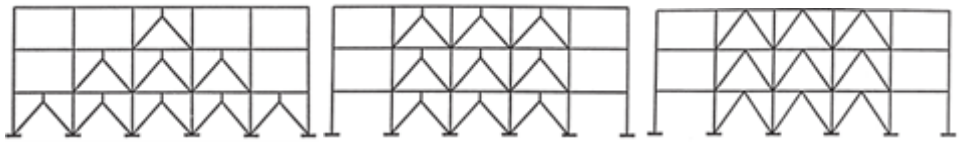

(c) E2 (b) E1 (a) V1

Figure 1.5: *Applied rehabilitation schemas*

- Concentric bracing case V1 provided the highest increase in stiffness. However eccentric bracing case E2 resulted in higher lateral loading capacity than V1 and E1 cases.
- Eccentric bracing cases suffered less damage and deformation under the load demanded by earthquake ground motions.
- Link deformation angle is an important factor for eccentric bracing systems and it should be kept under an allowable shear deformation limit.
- Plastic mechanism of the structure under seismic loads is significantly related with the distribution of braces over the structure.

Study conducted by Ghobarah and Elfath (2001) mainly suffers from being purely analytical without any experimental validation.

Dicleli and Mehta (2007) developed a nonlinear brace model and checked its performance by simulating seismic analysis with 1-bay, 1-story braced frames (Figure 1.6). They had an initial imperfection in the middle of brace members given by:

$$e = \frac{M_{pb}}{P_b}\left(1 - \frac{P_b L^2}{12EI}\right) \tag{1}$$

where e is the initial eccentricity at the center of the brace member, P_b is the buckling load of the brace member, M_{pb} is the reduced plastic moment capacity of the brace member and L is the total length of the brace member.

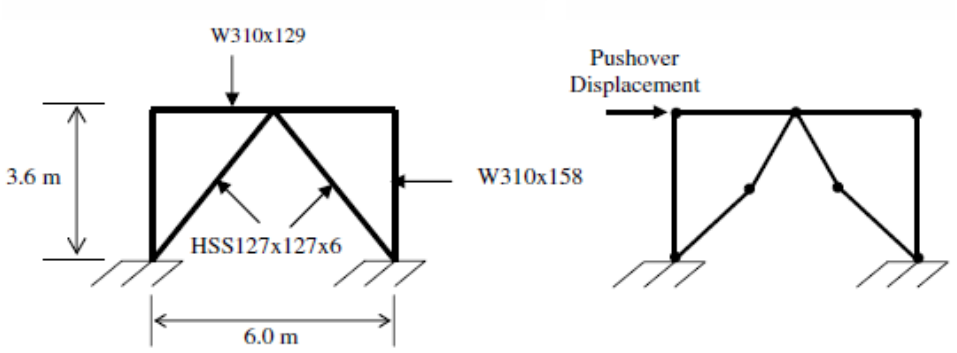

Figure 1.6: *Single-story frame and its structural model*

Brace sections were connected to frame as pinned connections and different slenderness ratios were investigated to understand the effect of brace slenderness on response of the frames. Results of this parametric study can be summarized as follows:

- Main effect of the slenderness of a brace section was the buckling load, after buckling occurs different values of slenderness did not provide any significant difference in absorbed energy.
- To have a better lateral loading capacity, frames should be designed with stronger beams.
- Frequency characteristics of ground motions were found to be important due to being detrimental for buckling of the braces.

Tsai et al. (2008) performed pseudo-dynamic test of a 3-story 3-bay braced frame with concrete-filed tube columns and prepared analytical models by using Pisa3D and Opensees structural analysis programs (Figure 1.7). They conducted static and dynamic time history analyses with selected earthquake ground motions. After that they prepared an error analysis between the experimental and analytical results to improve the accuracy of simulations. Finally, they calibrated their models according to results of error analysis. The results they concluded were:

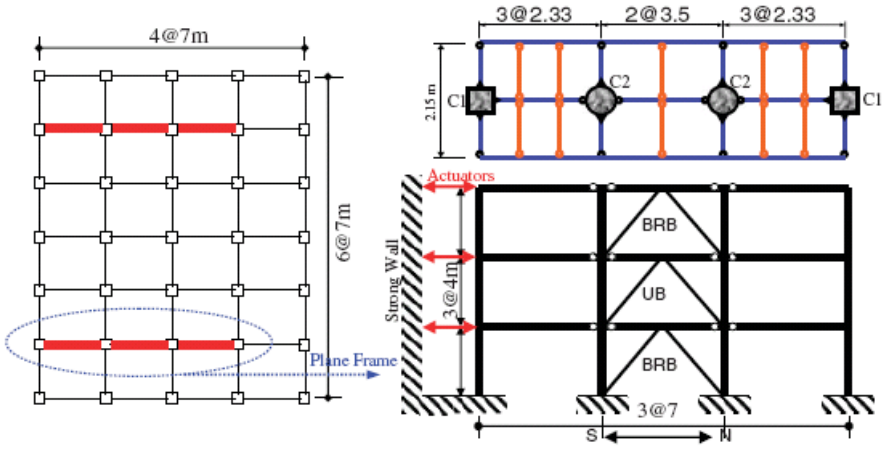

Figure 1.7: *Idealized prototype frame*

- Pseudo-dynamic test results could be satisfactorily simulated by both simulation tools.
- Buckling restrained bracing systems performed well in terms of maximum drift ratios under the effects of various numbers of earthquakes.
- Error analysis was beneficial for understanding the inadequacy of the analytical model and calibrating it.

Uriz et al. (2008) investigated the capability of inelastic beam-column element model with the Opensees simulation platform in modeling the hysteretic response of steel braces. A tubular section was analyzed with pin-pin support condition under cyclic loading (Figure 1.8). They used hysteretic model of Menegotto-Pinto as steel material and checked brace responses for both local and

global manner. They used an initial imperfection to the geometry of the system in the form of initial camber for including buckling in braces. Parametric studies were conducted by modifying the modeling parameters such as; initial deformation ratio, element number, support conditions and number of integration points. Different cross section shapes were also tested to understand the effect of section types and compactness. According to analysis results:

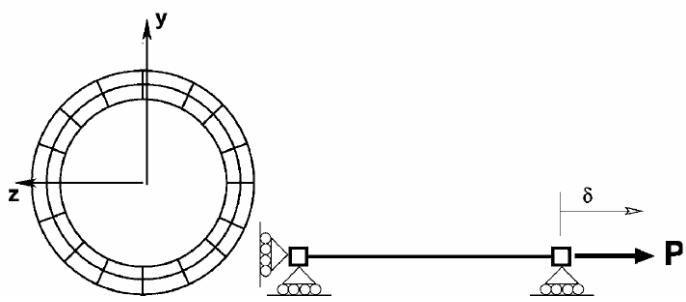

Figure 1.8: *Section geometry and analyzed brace element*

- To able to observe buckling, the brace member should at least be divided into two inelastic force-based beam-column elements.
- Increasing mesh did not improve the global response but affected the accuracy of local strains.
- Initial imperfection given at the brace mid-point should be 0.05-0.1% of the brace length and buckling load was very sensitive to value of selected initial imperfection.
- Three Gauss integration points was sufficient for an accurate result on hysteretic buckling behavior.
- Ten to fifteen layers lead to an adequate performance on estimating stress-strain distribution on brace sections. For I-sections, three-five lavers should be used in flanges.
- For compact sections, local buckling did not have a significant importance however, for non-compact sections local buckling did affect the hysteretic behavior of the braces.

Apart from studies focusing on analytical simulation of steel elements, study by Talaat and Mosalam (2009) requires citing due its relevance to this study (Chapter-3) while simulating as built specimen with infill walls. Talaat and Mosalam (2009) proposed an analytical formulation that implements automated removal of collapsed elements during an ongoing simulation. They tested one-story and five story structural systems that have deficient columns and infill walls with unreinforced masonry. Opensees simulation platform was used for modeling and removal algorithm (Figure 1.9). They compared the analytical results with shake table tests of one-story structural system. They used five-story structural system for investigating the performance of removal algorithm and the collapse progression of members.

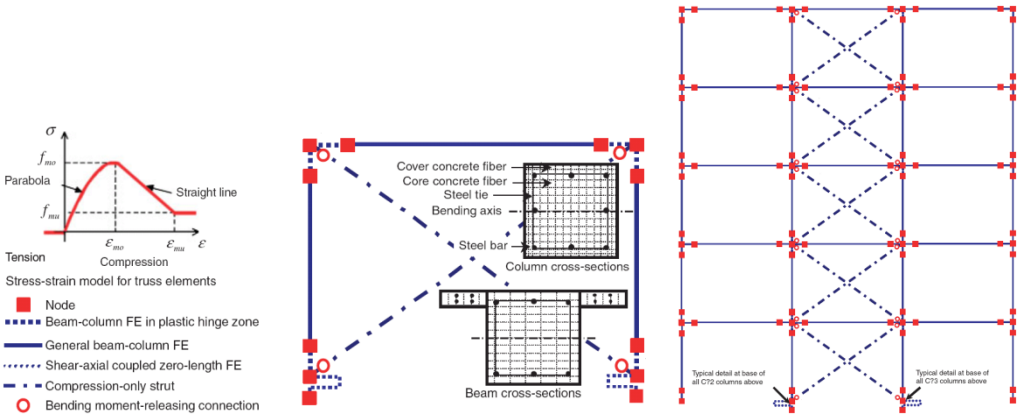

Figure 1.9: *Modeling of one-story and five-story frames*

According to their results:

- Intra-event variability is an important factor in determining the outcome of progressive collapse simulation.
- Uncertainty in earthquake intensity as the most important factor affecting the outcome, followed by URM wall stiffness for a given ground motion.
- Uncertainties in live load (occupancy level) and viscous damping ratio (excluding frictional damping due to damage) have moderate and minor influences, respectively.

1.3 Objective and Scope

Retrofitting methods should be carefully selected and applied to structures in the light of engineering knowledge. This could be ensured by the usage of prepared guidelines or codes with calibrated simulation tools. Understanding of the cyclic response of these systems is one of the important steps before proposing design methods and performance criteria for these systems. Studying all possibilities for a system experimentally is time consuming, difficult and expensive if not impossible. At this point, calibrated numerical models may serve to be very beneficial.

The objective of this study is:

- To calibrate numerical models in light of cyclic and pseudo-dynamic tests for steel retrofitted deficient RC frames.
- To evaluate the performance limit states of such retrofitted systems.
- To compare the performance of different retrofit schemes by conducting nonlinear time history analysis on a case frame building.

In Chapter 2, numerical models for retrofitted frames with steel braces and internal steel frames are proposed and cyclic simulation results are compared with test results. Results of these models are then used to investigate the performance of retrofitting methods by using TEC2007 and ASCE41. After validation of the modeling, parametric studies are conducted with various section sizes for braces and internal steel frames. In Chapter 3, time history analysis of two story retrofitted frames and frame with infill walls are conducted and simulation results are compared with PSD test results. Numerical results are used to evaluate the seismic performance and effectiveness of retrofitting methods. In Chapter 4, retrofitting methods are applied to a 4-story frame that is obtained from an existing RC building and time history analyses are conducted. Effectiveness of retrofitting methods is compared and structural damages are determined. Finally in Chapter 5, summary and main conclusions of the study are provided with further study recommendations.

CHAPTER 2

NUMERICAL SIMULATIONS OF CHEVRON BRACES AND INTERNAL STEEL FRAMES

2.1 Test Details

2.1.1 Chevron Braces

Ozcelik and Binici (2006) conducted a number of one-story one-bay frame tests to investigate various steel retrofit schemes. Retrofitted specimens had 1.4 m width and 1.0 m height with a scale of 1/3. Experiments were conducted at METU laboratory by employing the setup given in Figure 2.1. In these studies, columns and beam were detailed considering the frequent deficiencies of structures in Turkey such that low material strengths, excessive transverse reinforcement spacing at the column ends and insufficient RC member section sizes.

Columns of the test frames were bent about their strong axis and their dimensions were 100x150 mm with four 8 mm diameter longitudinal plain bars. Transverse reinforcement was 4 mm diameter plain bars and the spacing of the stirrups was 100 mm for the columns and 70 mm for the beams. The flange width and thickness of the beam section were 450 mm and 55 mm, respectively. Column and beam section sizes are shown in Figure 2.2. The yield strength of the longitudinal bars was 330 MPa and the transverse bars were 270 MPa. The yield

strength of the steel brace sections is presented in Table 2.1. The concrete had a 28-day cylinder compressive strength of about 8-10 MPa (Table 2.2). All the test frames were constructed with similar material properties and member dimensions with varying brace sizes. Steel blocks were placed on the RC beam to provide a total axial load of about 6 tons.

For the strengthened cases, square hollow box section chevron braces were connected to the bottom of the columns and the mid-span of the beam by gusset plates (internal inverted V-Braces). In order to prevent shear failure of the beams, extra steel plates were attached at both ends of the beam. Gusset plates were connected to RC members by anchor rods. Then the brace sections were welded to these plates. Details of the brace sections in terms of dimensions, slenderness and axial load levels on columns are given in Table 2.2.

In the experimental program, four different steel brace members with varying axial load levels were tested. Specimens were tested under constant gravity load and cyclic lateral displacement program. The details of the tested frame are shown in Figure 2.2.

Table 2.1*: Brace's yield and ultimate strengths*

Brace Dimension (mm)	Yield Stress (Mpa)	Yield Strain	Ultimate Stress (Mpa)	Ultimate Strain
30x30x2	397	0.0020	414	0.0439
30x30x2.5	415	0.0021	415	0.0114
40x40x3	397	0.0020	414	0.0439

Table 2.2*: Details of experimental program (Chevron Brace)*

Specimen Name	Specimen Type	Brace Dimension (mm)	Brace Slenderness	Concrete Compressive Strength (Mpa)	Axial Load Ratio
SP1	Bare	-	-	10.0	0.10
SP2	Bare	-	-	8.1	0.18
SP3	Strengthened	30x30x2.5	90.4	10.0	0.10
SP4	Strengthened	30x30x2.5	90.4	8.5	0.18
SP5	Strengthened	30x30x2	88.0	8.5	0.18
SP6	Strengthened	40x40x3	66.7	8.5	0.18

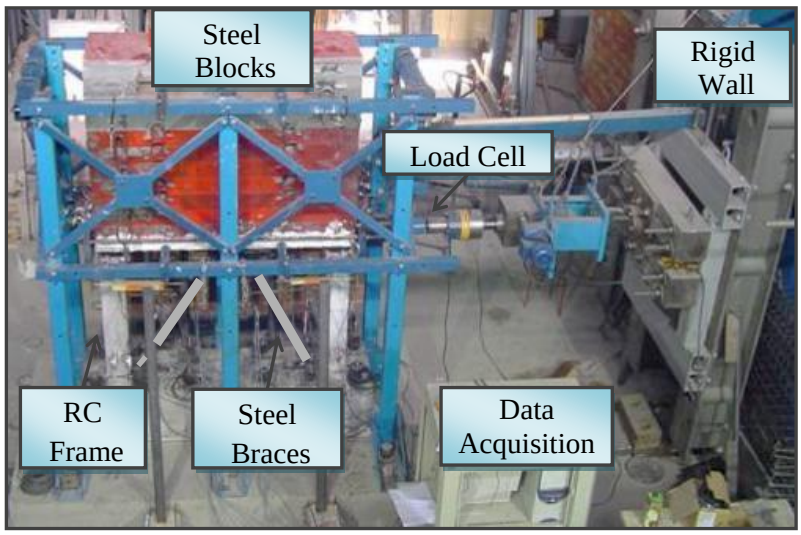

Figure 2.1: *Chevron braces test setup*

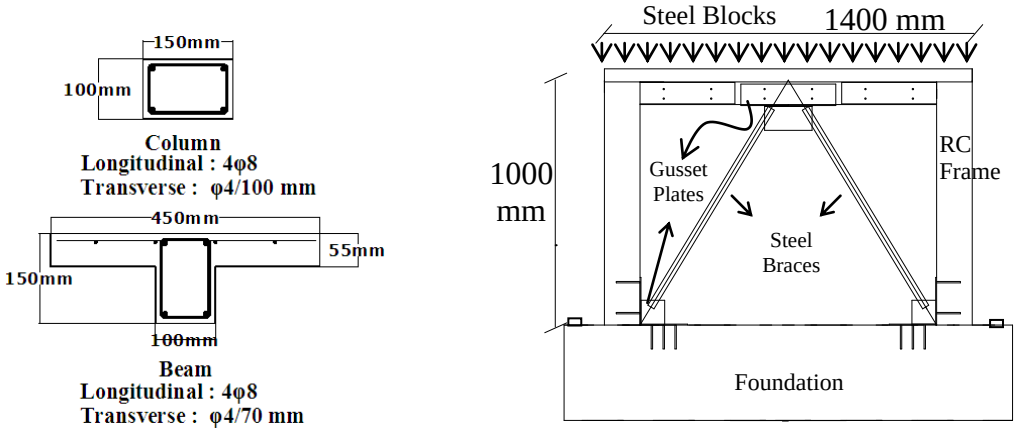

Figure 2.2: *Beam, column details and tested frame*

2.1.2 Internal Steel Frames

Identical deficient RC frames were employed for Internal Steel Frame (ISF) retrofit tests (Figure 2.3). The ISFs were constructed in the form of rigidly connected steel beams and columns; and they were placed into RC frames as shown in Figure 2.4.

Ozcelik and Binici (2006) used mainly two different methods to install the ISFs. In the first method (Figure 2.5.a), no anchors were used between the RC frame

and internal steel frames. In this way, installation of ISFs was conducted with less workmanship. To have a smooth bonding surface, a thin layer of repair putty was applied on the entire surface of RC frame. The individual steel members were attached to the RC frame by using epoxy. After the epoxy had cured, the steel beams at the bottom and top were welded to the steel columns. In the second method (Figure 2.5.b), steel anchors were used between the RC frame and internal steel frames. It was aimed to have composite action between the RC frame and ISF. Until mounting of anchor rods, similar procedure was followed as in method-I. In total, 42 (21x2) column and 32 beam anchor rods were used to provide the shear force transfer between the RC and steel frames. Specimens were tested under constant gravity load and cyclic lateral displacement program. Dimensions and strengths of the internal steel frame sections and corresponding axial load levels are given in Table 2.3.

Table 2.3: *Details of experimental program (ISF)*

Specimen Connection Type	Column Dimension (mm)	Beam Dimension (mm)	Column Yield Strength (MPa)	Beam Yield Strength (MPa)	Concrete Compressive Strength (Mpa)	Axial Load Ratio
Method-1	80x80x4	70x70x3	398	385	7.5	0.19
Method-2	I-140	I-80	313	373	7.5	0.19

Figure 2.3: *ISF test setup*

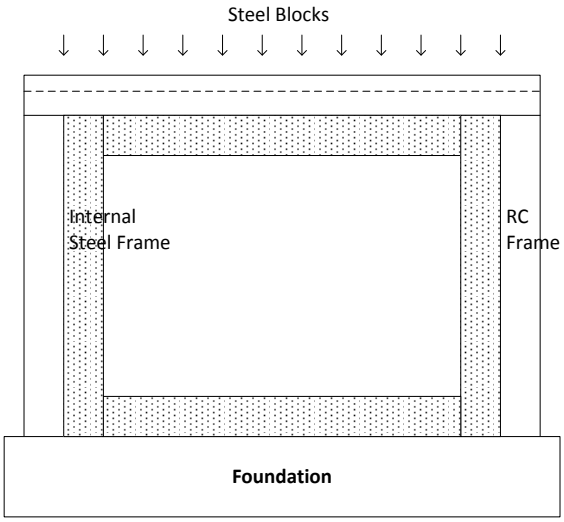

Figure 2.4: *ISF and RC frame*

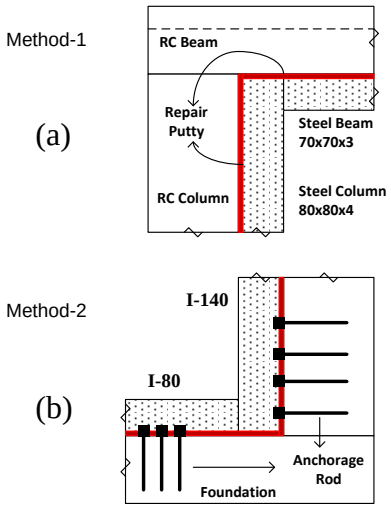

Figure 2.5: *Connection methods for ISFs*

2.2 Numerical Models

2.2.1 RC Frame Modeling

Pushover and cyclic analyses of test specimens were performed utilizing Opensees Simulation Platform version 2.2 (Mazzoni et.al. 2010). Dimensions of the numerical model were identical to those of the test specimens (Figure 2.2). Force based fiber frame elements (*nonlinearBeamColumn*) were used to model RC beam and columns.

The material model used for concrete (*Concrete01*) follows the rules of the confined and unconfined concrete models proposed by Kent and Park (1972) with the Karsan and Jirsa (1972) plastic offset rules (Figure 2.6.a). Bond slip effects of reinforcements on the column ends were taken into account by using Clough type hysteretic material model having a bilinear monotonic envelope with cyclic strength degradation (Figure 2.6.b). Further discussion of this approach is presented in the next paragraph. Fiber sections were used to generate all the members which were discretized into smaller regions (Figure 2.7). Number of layers was determined considering suggestions of Uriz et al. (2008). For RC columns second order effects

were also taken into account. Linear geometric transformation was used for RC beams due to insignificant effect of geometric nonlinearity on the results. First story level nodes were constrained for horizontal deformations. Load on frame was distributed to the upper corner nodes as point loads. Self-weight of the beam and columns were also taken into account.

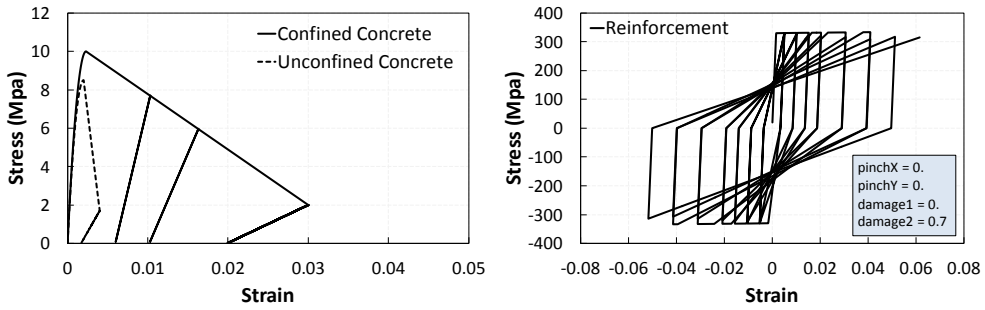

(a) (b)

Figure 2.6: *Material properties of concrete and reinforcement*

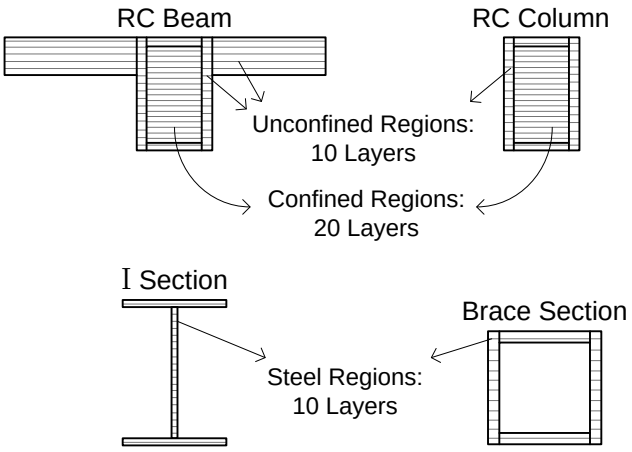

Figure 2.7: *Number of layers*

Material model of the steel members had a strong influence on the cyclic response of the test frames. Several simulations employing kinematic hardening models for steel material was found to be inadequate to simulate the overall response of specimens with stiffness degradation. Presence of bond slip in the column's longitudinal reinforcement bars causes rapid stiffness degradation during unloading while previously opened cracks are being closed. Two material models included in

Opensees namely *Steel02* and *Hysteretic Material* were compared in terms of cyclic responses (Figure 2.8). Although *Steel02* considers Bausinger effect with Giuffre-Menegotto-Pinto rules; it cannot exhibit any in cycle degradation and pinching. The way of unloading stiffness of the *hysteretic material* provides the desired performance on simulating bond slip in the column ends (Figure 2.8.a).

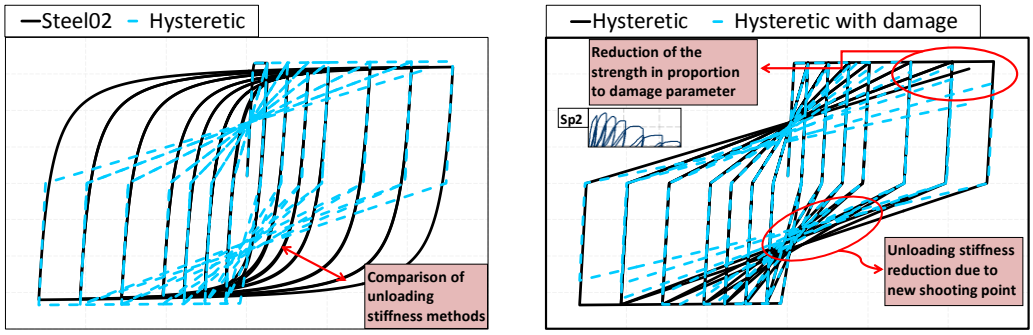

(a) (b)

Figure 2.8: *Comparison of material models and effect of damage factor*

Another problem is the strength degradation due to the formation of fractures on beam and column connections. Cyclic tests (Figure 2.8.b Sp2) showed that there was significant reduction in strength which cannot be simulated with kinematic hardening models. To overcome this problem, damage parameter (*damage2=0.7*) was used with hysteretic material where *pinchX* is pinching factor for strain during reloading, *pinchY* is pinching factor for stress during reloading, *damage1* is damage due to ductility, *damage2* is damage due to energy (Figure 2.8.b).

2.2.2 Brace Modeling

For the modeling of the brace sections it was aimed to have accurate buckling and post buckling predictions. For this purpose, the effective length of the braces was adjusted properly by introducing rigid end zones at brace ends. These connections were modeled with simple elastic frames (*elasticBeamCoulmn*) which had high rigidity with respect to braces and RC frame. To capture the brace buckling as observed during test, braces were divided into four equal elements as proposed by

Uriz et al. (2008). Instead of straight brace member, a sinusoidal curved member was used with an initial imperfection (0.5-1 mm) at mid-span of the brace. In this way buckling mode could be simulated in the plane of the frame as opposed to the tests where buckling was out of plane.

RC Frame had fixed boundary conditions at the base of columns. However, brace members were tied to the RC frame and the foundation with pin connections. The reason of using pin connections was able to simulate observed buckling deformation mode accurately during the test. Test results showed that gusset plates deformed (out of plane) significantly under the axial forces and braces buckled similar to a pin-pin connected mode. The summary of the modeling is presented in the Figure 2.9. The material model of the brace members was assigned a bilinear kinematic hardening model (*Steel02*) having 1% hardening slope (Figure 2.10).

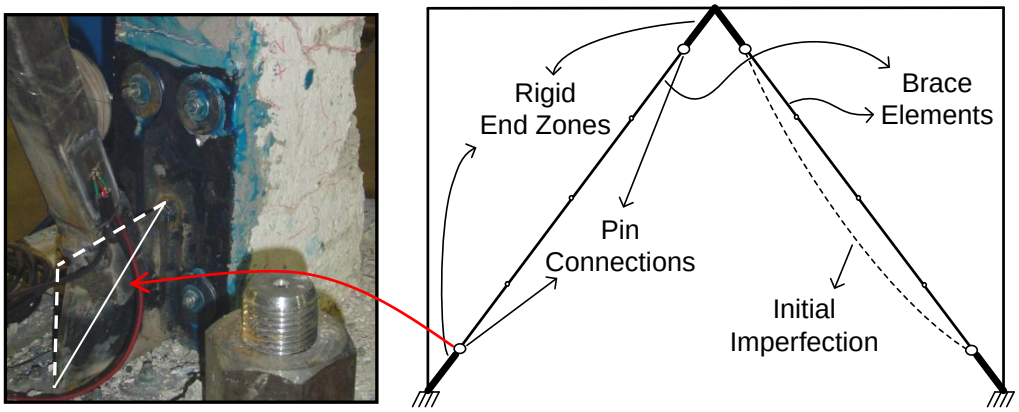

Figure 2.9: *Modeling strategy for chevron braces*

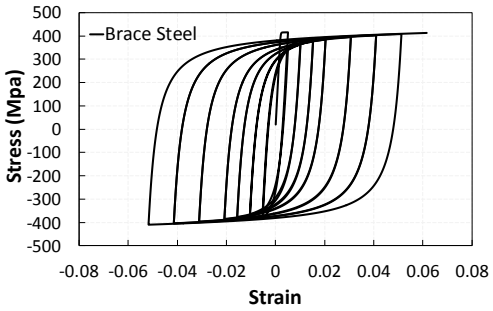

Figure 2.10: *Material properties of brace sections*

Analyses were conducted in two parts. First gravity loads were imposed to the frame. Newton's algorithm was performed with 0.1 step sizes. Buckling of the braces was not observed at this moment. Then cyclic load pattern was imposed to the frame at the beam level. *KrylovNewton* algorithm was used with displacement control integrator that had 0.0001 step sizes.

2.2.3 ISF Modeling

In the construction of the analytical model for ISF, a similar way discussed in the previous part was followed. As mentioned already, there were two different installing methods of ISFs existed therefore two different modeling approaches were developed.

In the first method, namely non-composite section method, RC frame members and ISF elements were defined individually. Columns and beams were divided into 10 and 14 equal parts, respectively. Displacement based fiber frame elements (*dispBeamColumn*) were used due to easy convergence of members with multiple segments (Figure 2.7). Afterwards, all the joints between RC frame and ISF were connected by rigid beams (*rigidLink*) and spring elements (*zeroLength*). In order to simulate the interaction between these members, material model of the spring elements were defined as elastic with no tensile strength. Shear and moment transfer between RC frame and ISF was not included in this model. RC columns were fixed under the column ends whereas steel frames had pinned and roller connections. Illustration of the modeling strategy is given in Figure 2.11.a.

Second approach was the modeling of RC frame and the internal steel frame as composite section. To simulate the similar conditions with the test, concrete and steel sections were defined with appropriate steel and concrete fibers as a simple section. In this way full composite action was ensured. Force based fiber frame elements (*nonlinearBeamColumn*) were used to model beam and columns. As shown in Figure 2.11.b, the composite section is formed from reinforced concrete and steel I-sections. RC columns and steel frames were mounted to foundation with fixed connections. Modeling of the weight blocks, material models and the other solution

strategies were similar to those explained in the previous section. However, the material model of the internal steel frame members was assigned as hysteretic material model having a bilinear monotonic envelope with cyclic stiffness degradation in order to simulate severe pinching due to slippage of the two sections as observed in the experiments (Figure 2.12).

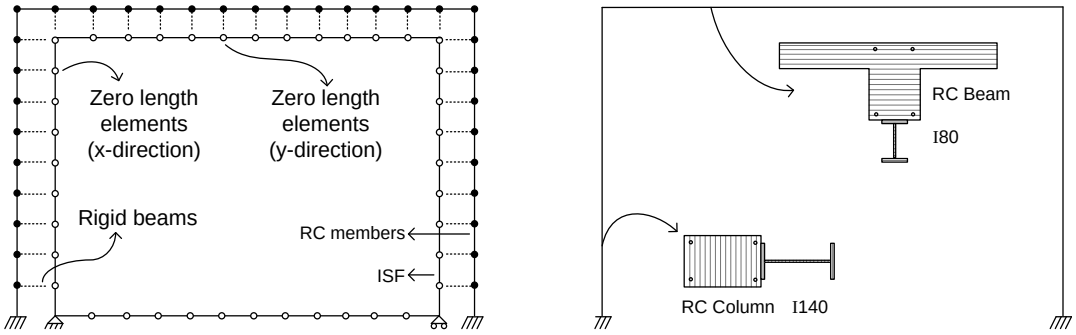

Figure 2.11: *Modeling strategy for ISFs*

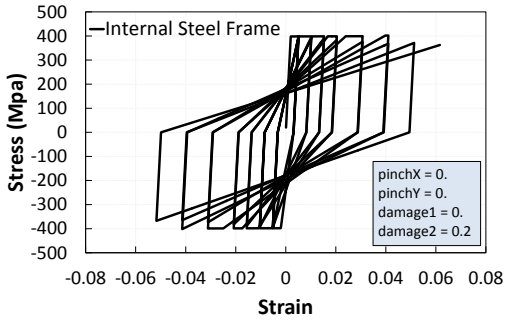

Figure 2.12: *Material properties of ISFs*

2.3 Analysis Results

2.3.1 Comparison of Test Results with Analytical Models

2.3.1.1 Chevron Braces

Six experiments were analyzed to investigate the ability of reproducing strengthened specimens. Pushover and cyclic analysis results of the numerical models were compared with the load-deformation response of the tested frames (Figure 2.13). Error estimation for lateral loading capacity, post buckling response of the braces and further evaluation of the results are presented in the next paragraph.

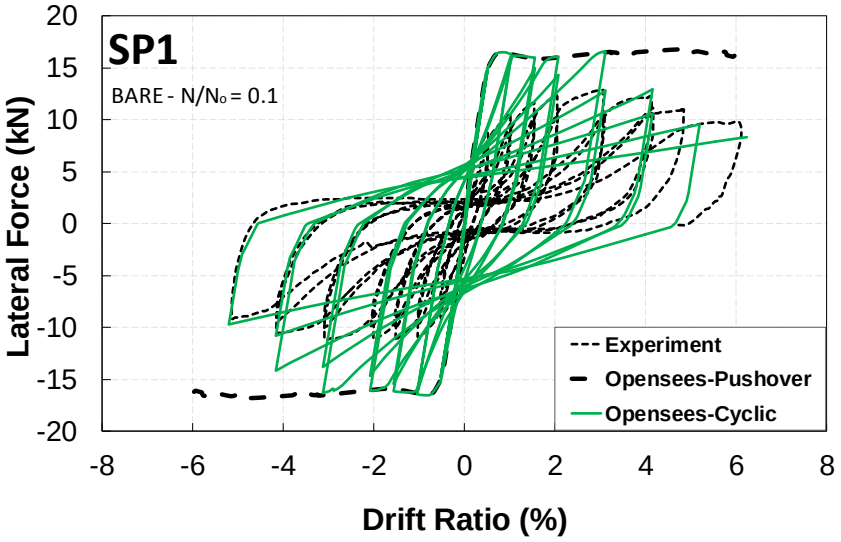

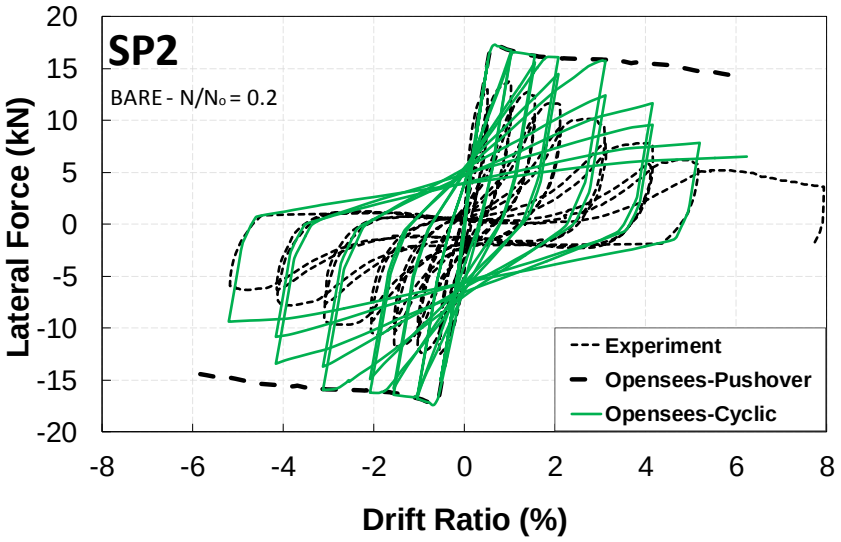

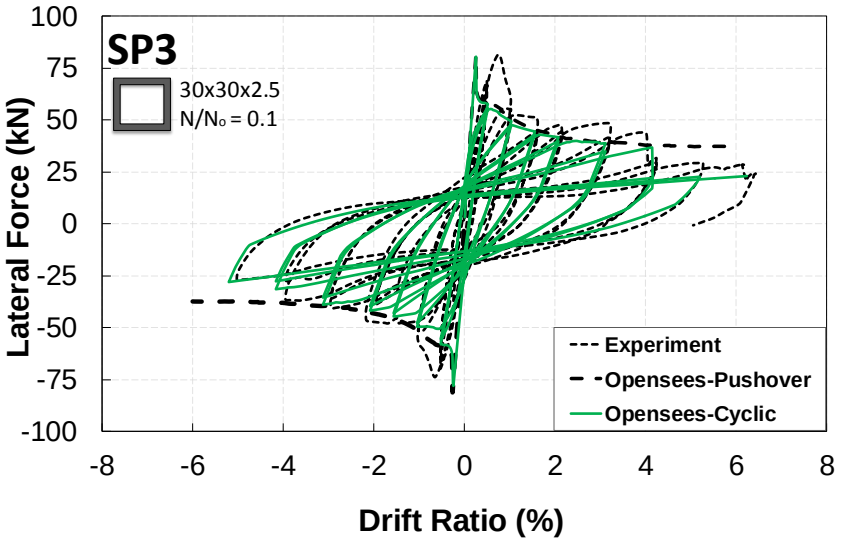

Figure 2.13: *(Continued)*

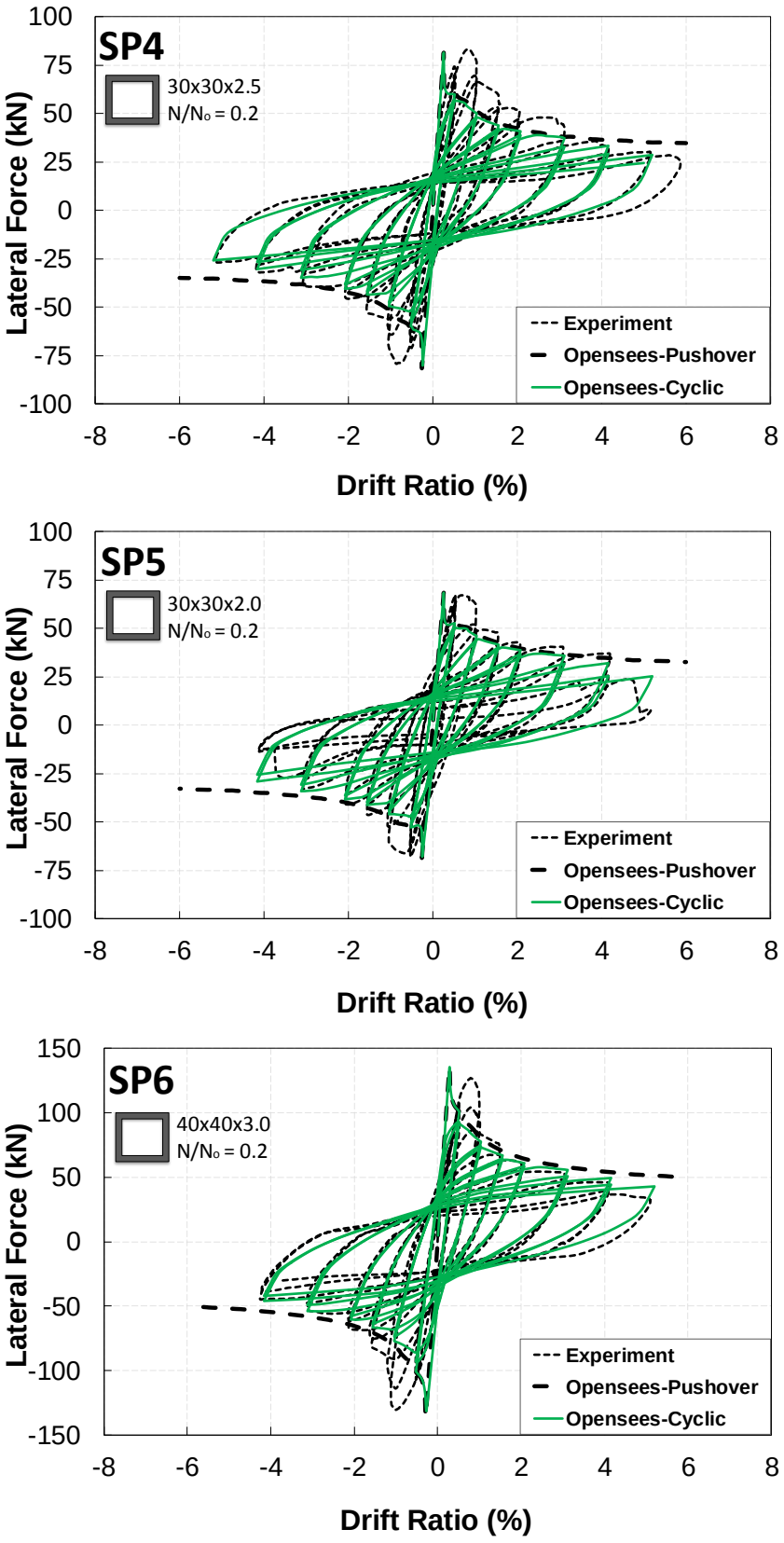

Figure 2.13: *Cyclic comparison of numerical model and test results of braces*

According to the results, initial stiffness of the test frames matched well with the numerical simulations. However, softening of stiffness in the initial loading branch of test frames could not be simulated adequately. In the numerical model, previously explained rigid elements were used as steel gusset plates and gusset elongations were not taken into account (Figure 2.9). Furthermore, the initial crookedness of the braces may not have been reflected accurately. These two reasons are thought to be the sources of error in the loading stiffness. Except Sp1 and Sp2 specimens' results, lateral load capacities of the test frames were simulated well. Errors in lateral load capacity of test frames are given in Table 2.4. According to the results of strengthened cases, braces dominate the overall behavior of the test frames and accurate estimation of buckling load of the braces lead a satisfactory estimation of lateral load capacity for the test frame. However, for the cases without braces (Sp1 and Sp2) this is not the case. In order to investigate the source of error, a parametric study was conducted (Figure 2.14). Three parameters that affect moment capacity of the columns were investigated namely yield capacity of the longitudinal bars, clear cover and axial load level. All three parameters were assumed to have a 20% swing and possible limiting values are given in Figure 2.14.a. Cyclic analyses were conducted with limiting parameters and results for worst, default and best parameter conditions were compared (Figure 2.14.b). According to the results, lower bound parameters seem to produce more accurate results.

Table 2.4: *Error estimation of lateral load capacity (Chevron Brace)*

Specimen Name	Specimen Type	Brace Dimension (mm)	Test Max. Base Shear (kN)	Analysis Max. Base Shear (kN)	Error (%)
SP1	Bare	-	12.88	16.80	30.4
SP2	Bare	-	13.75	17.32	26.0
SP3	Strengthened	30x30x2.5	81.55	81.14	0.5
SP4	Strengthened	30x30x2.5	83.53	81.55	2.4
SP5	Strengthened	30x30x2	68.06	68.52	0.7
SP6	Strengthened	40x40x3	130.39	135.63	4.0

Case	-20%	+20%
Long. Reinf. Capacity (Mpa)	264	396
Clear Cover (mm)	12	8
Axial Load (kN)	4800	7200

(a)

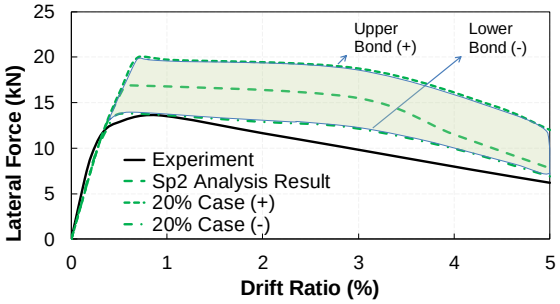

(b)

Figure 2.14: *Parametric study on bare frame*

For the strengthened cases numerical simulation agreed well with the experimental results in terms of cyclic response and reloading/unloading stiffness. Post buckling behavior of the braces was simulated with minimal error. Similarly to the test results, analytical study showed that buckling of the braces affected significantly the cyclic performance of the braced frames.

2.3.1.2 Internal Steel Frames

Pushover and cyclic analysis of the numerical models were compared with the test results. Lateral load versus lateral displacement results and estimated errors are shown in Figure 2.15 and Table 2.5, respectively.

For the first method (non-composite sections), satisfactory agreement with the test data was obtained with the employed modeling technique. Both initial stiffness and softening of system were accurately simulated. In the analytical model, friction forces between RC member and internal steel frame elements were not taken into account. As a result of this, lateral load capacity of the test frame was underestimated with slight error. Using cyclic degradation with hysteretic material as the material model of ISF led to satisfactory agreement with reloading/unloading response of the test frame.

For the second method (composite sections), lateral load capacity of the test frames agreed well with the simulation results. According to the analysis results, initial stiffness of the system was similar to that observed in the test. However,

softening and the reloading/unloading response of the system were calculated with some error. In the modeling of test frame fixed boundary conditions were assumed under the columns. In the actual test setup, RC columns were fixed to foundation whereas internal steel frames were connected as shown in Figure 2.3. Thereby, assuming RC column and steel column as single frame member and having fixed support caused overestimation of the calculated stiffness. In order to understand the effect of the supports under columns another analysis was conducted with slightly modified boundary conditions (Figure 2.16). In the test; columns were connected to a steel beam that was fixed to foundation by steel anchors (Figure 2.5.b). To simulate this behavior, additional steel sections were connected to the column ends. These elements were taken as elastic sections using the reported material and section properties. Simulation results showed that modification of the boundary conditions resulted in a softer behavior with more pronounced pinching. As can be seen from Figure 2.16, this approach could provide a better estimation of cyclic behavior in terms of stiffness estimation and reloading/unloading curves.

It should be noted that for both installing methods strength degradation could not be observed in the pushover analysis results. That's because the cyclic degradation factor that was used in hysteretic material were not effective for monotonic envelopes.

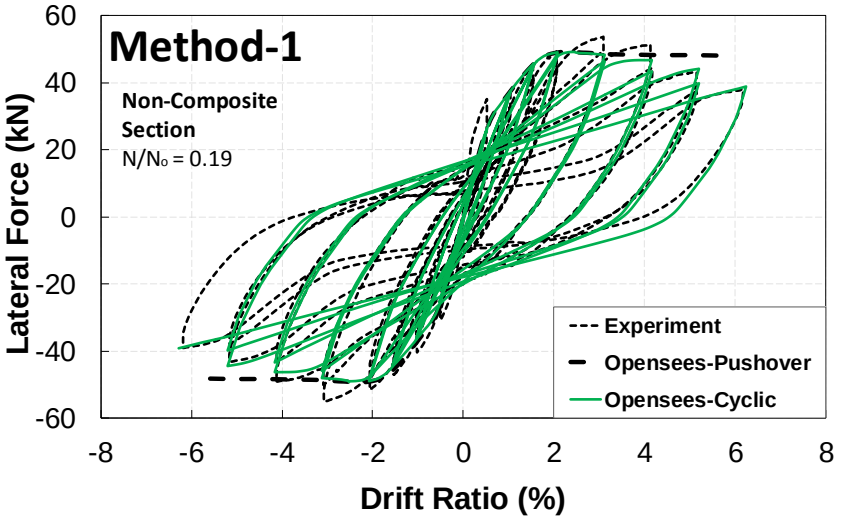

Figure 2.15: *(Continued)*

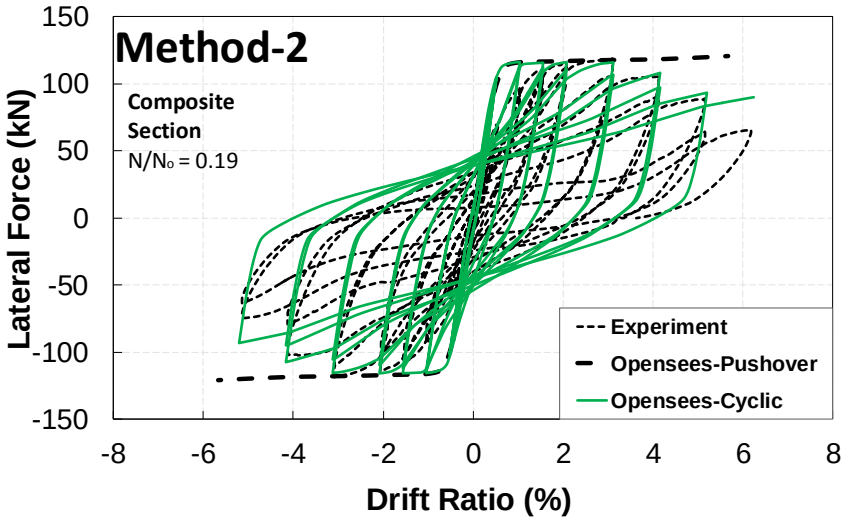

Figure 2.15: *Cyclic comparison of numerical model and test results of ISFs*

Table 2.5: *Error estimation of lateral load capacity (ISF)*

Specimen Connection Type	Column Dimension (mm)	Beam Dimension (mm)	Test Max. Base Shear (kN)	Analysis Max. Base Shear (kN)	Error(%)
Method-1	80x80x4	70x70x3	53.74	49.21	8.43
Method-2	I-140	I-80	118.89	116.35	2.14

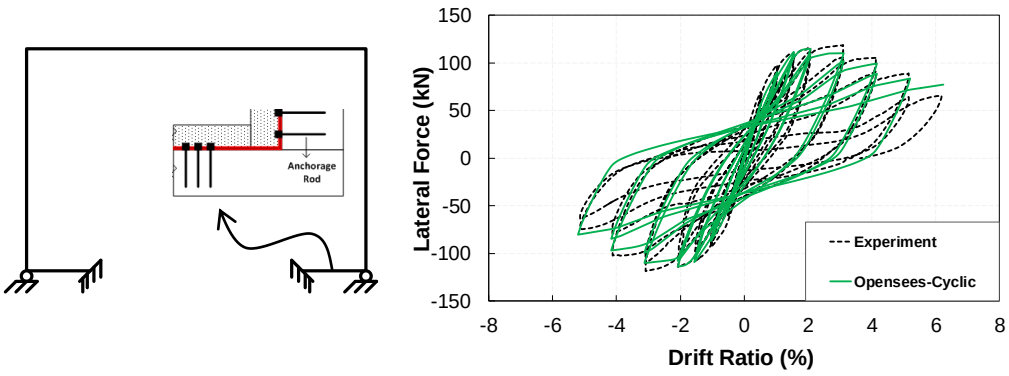

Figure 2.16: *Results with alternative boundary conditions for Method-2*

2.3.2 Performance Evaluations of Strengthening Methods and Parametric Study

2.3.2.1 Chevron Braces

Results of the numerical simulations were used to determine performance limit states of RC members and braces. RC column and beams performance levels were determined by the method suggested in Turkish Earthquake Code (2007). TEC method designates the strain limits for concrete in compression at stirrup level for three performance limit states (immediate occupancy (IO), life safety (LS) and collapse prevention (CP)), in the following form: $\varepsilon_{IO}=0.0035$, $\varepsilon_{LS}=0.0035+0.01(\rho_s/\rho_{sm})$, $\varepsilon_{CP}=0.004+0.01(\rho_s/\rho_{sm})$ where ρ_s is the available confining steel volume and ρ_{sm} is the required confining steel volume according to TEC2007. Also the strain limits for the longitudinal reinforcement are: $\varepsilon_{IO}=0.010$, $\varepsilon_{LS}=0.040$, $\varepsilon_{CP}=0.060$. Performance limits of the braces were taken from ASCE/SEI-41. ASCE/SEI-41 defines the axial deformation at the expected buckling load of the braces (Δ_c) and determines performance limit states IO, LS and CP as: $0.25\Delta_c$, $5\Delta_c$, $7\Delta_c$ for slender braces and $0.25\Delta_c$, $4\Delta_c$, $6\Delta_c$ for stocky braces. Figure 2.17 shows the detailed investigation of the pushover analyses of test specimens. Total base shear of the frame and the axial forces of compression and tension braces are given along with hinge patterns for the test frames. Obtained performance range for the RC members and the braces are also shown in the same figure.

According to estimated results, performance limits of the RC members in frames without any strengthening are closely related with axial loads on members and strengthening did not have significant influence on these limits. For all retrofitted cases, buckling of the braces occurred before RC members went beyond IO limits. However, IO limit of the braces was observed before the buckling point as expected. For both RC members and compression brace sections LS and CP limit states almost coincide for the cases with high axial load ratios. Although changing brace size did not influence RC limit states significantly, it affected the brace performance limits. These results imply that post buckling compression capacity of braces can be relied on at IO and LS limit states provided that the seismic displacement demands are kept below DRs critical for axial load bearing RC members.

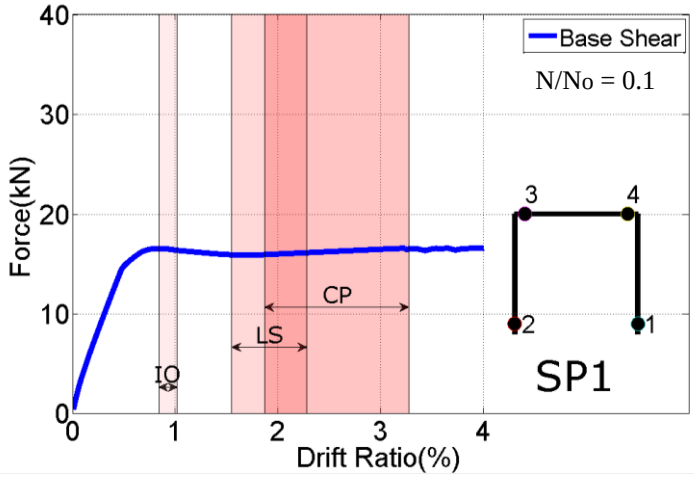

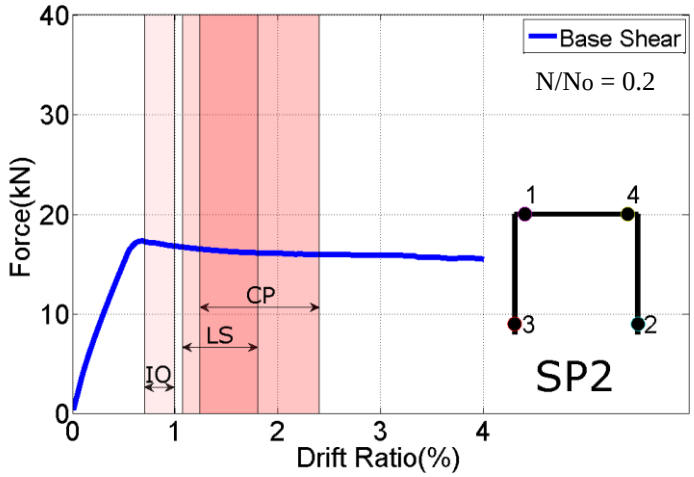

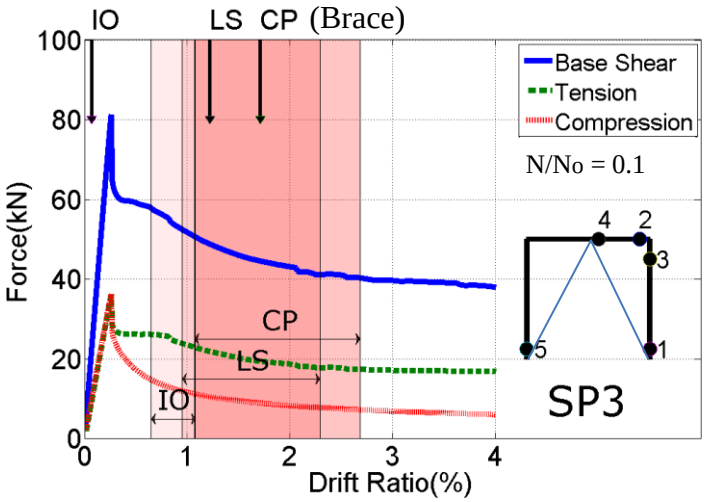

Figure 2.17: *(Continued)*

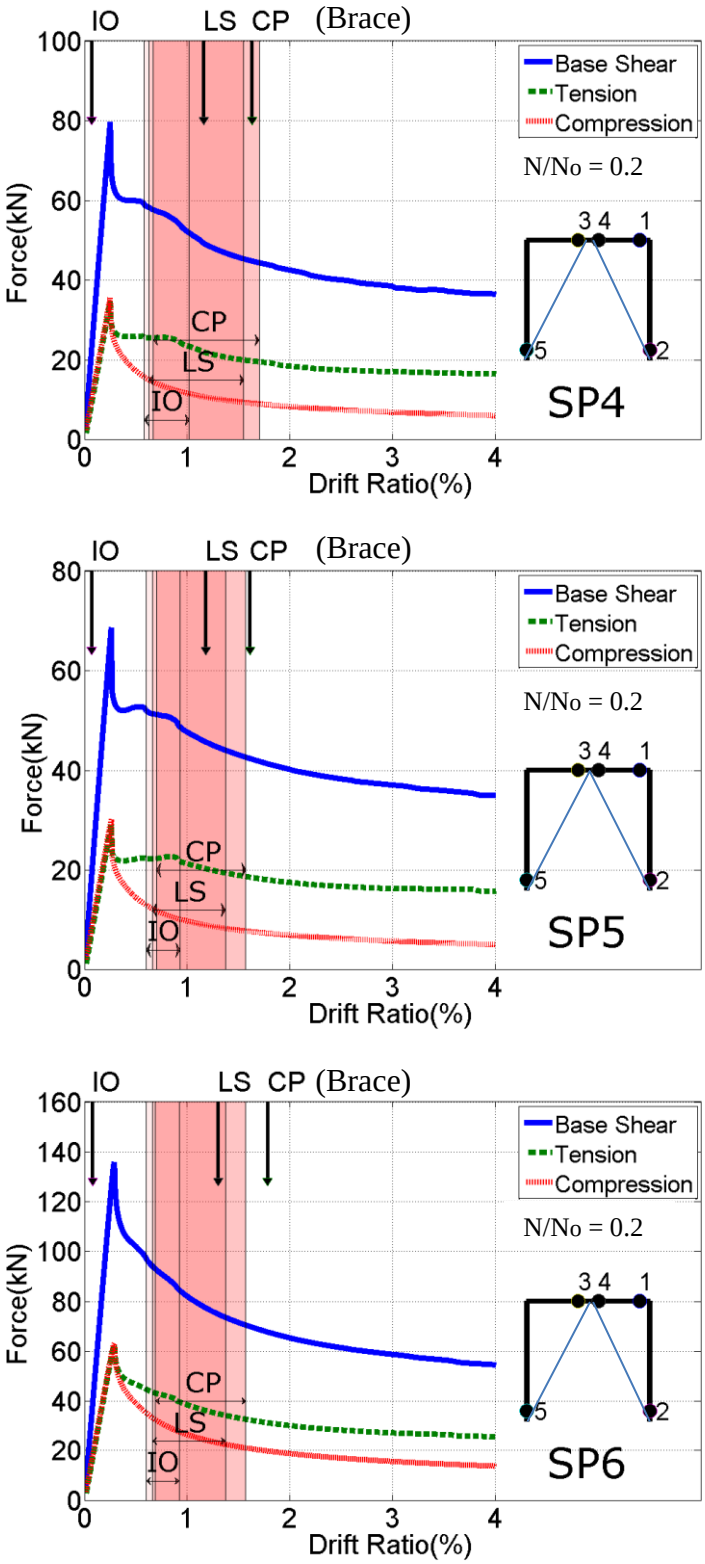

↔ RC Sections Performance Limits

↓ Brace Performance Limits (ASCE/SEI-41)

Figure 2.17: *Performance assessments of braces and RC frame members*

To examine the relation between slenderness ratio and ductility, a parametric study was conducted. RC frames having the same properties as the test frames were analyzed by using twelve different brace sections (with $N/N_0 = 0.2$). Brace sections were categorized according to their sizes, slenderness and compactness. To find a normalized force ratio, lateral components of the brace forces from the analysis were divided by the lateral components of the calculated yield forces of the braces.

The boundaries of the performance points based on RC members were determined using the strain based procedure of TEC2007. It is clearly seen from results given in Figure 2.18 that decreasing slenderness would increase the ductility of the braces. All the braces provide at least 30% of their buckling capacity before RC frame had passed beyond the CP performance limit. This value obviously increased with the decreasing slenderness of braces. For the 140x6 and 120x6 brace sections buckling was not observed during the analysis. The RC frame members reached their IO and LS states at about 0.8% and 1.1% DRs, respectively. Furthermore the average CP limit state was observed to be around 1.5%. As long as the displacement demands are kept below such drift ratios, use of relatively slender braces may be possible for economical designs on the grounds of relatively low deformability of RC deficient members.

In order to examine the effect of axial loads on limit states of RC members same parametric analysis were conducted with two different axial load ratios: $N/N_0 = 0.1$ and $N/N_0 = 0.3$ (Figure 2.19). According to results, decreasing axial loads on RC members affected both LS and CP limits of RC members. The average LS and CP limit states were observed to be around 1.7% and 2.3% DRs, respectively for the 10% axial load. However higher axial loads did not affect these limits significantly.

Finally, possibility of developing high shear forces on the brace-beam connections was investigated. The joint that connects braces with mid-span of the beam were statically analyzed for SP3 and SP6 results (Figure 2.20). Equilibrium of the systems was considered at the time that buckling occurred. It can be observed that the differences of the vertical components of tension and compression braces are balanced with the shear forces on beams. Hence, designer needs to ensure that this unbalanced shear force can be safely resisted by the existing RC beam.

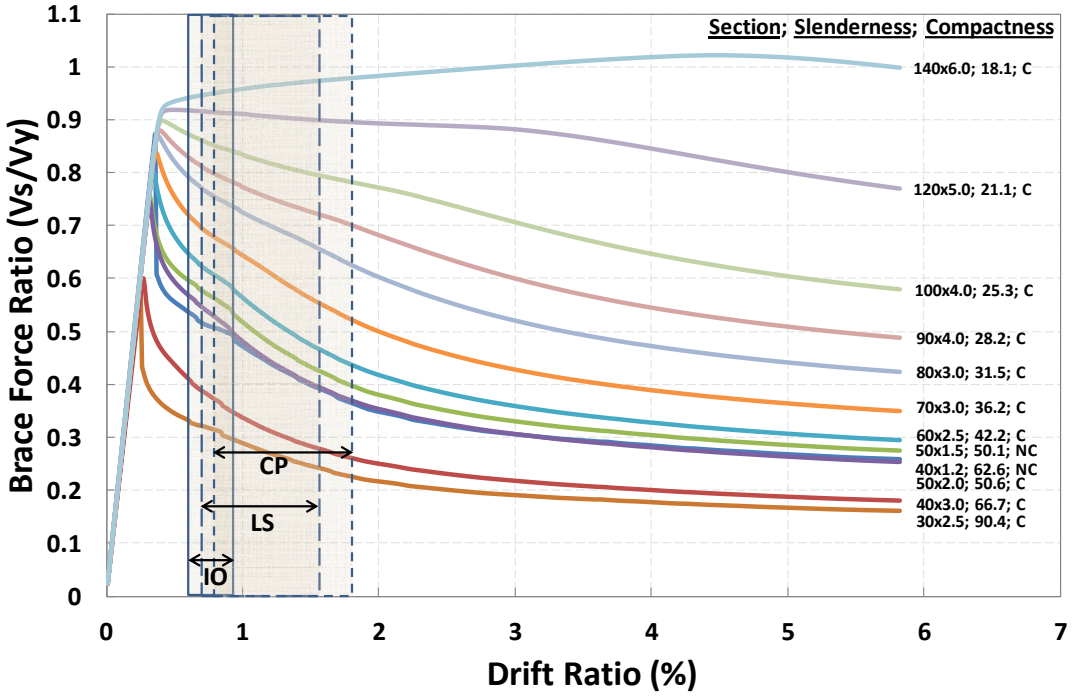

Figure 2.18: *Parametric comparison of varying steel braces (N/N_0 = 0.2)*

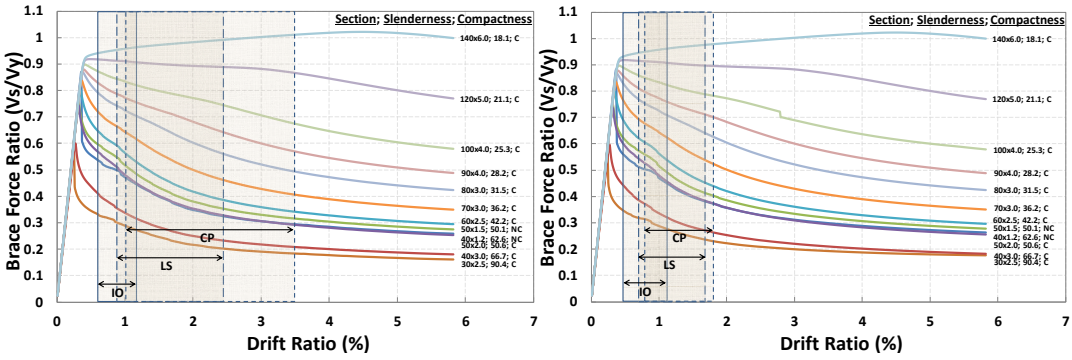

(a) N/N_0 = 0.1 (b) N/N_0 = 0.3

Figure 2.19: *Parametric comparison with varying axial loads (Chev. Braces)*

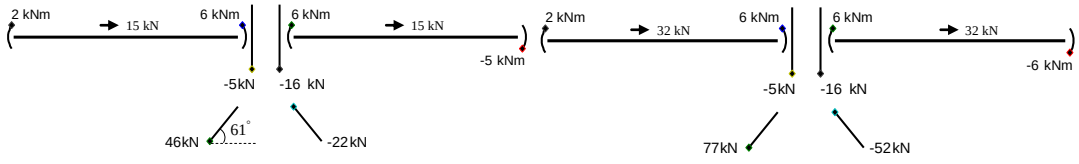

(a) Sp3 (b) Sp6

Figure 2.20: *Shear force on mid-span of the beams*

2.3.2.2 Internal Steel Frames

Since, no guidelines exist on performance estimation of such composite sections, performance points were determined solely based on concrete and reinforcement strains. Strain limits were taken from TEC2007 as explained previously. Results are presented on pushover curves along with performance limits and hinge patterns in Figure 2.21. Results of non-composite and composite ISFs showed that ISF may provide wider boundaries for RC member's performance limits. For method-1, hinging of steel members occurred on beam section as expected and yielding of ISF members started after the longitudinal reinforcement of RC member passed beyond their yield stress. Results of method-2 showed that ISF installed with anchors provides better deformability than the other strengthening methods considered in this study.

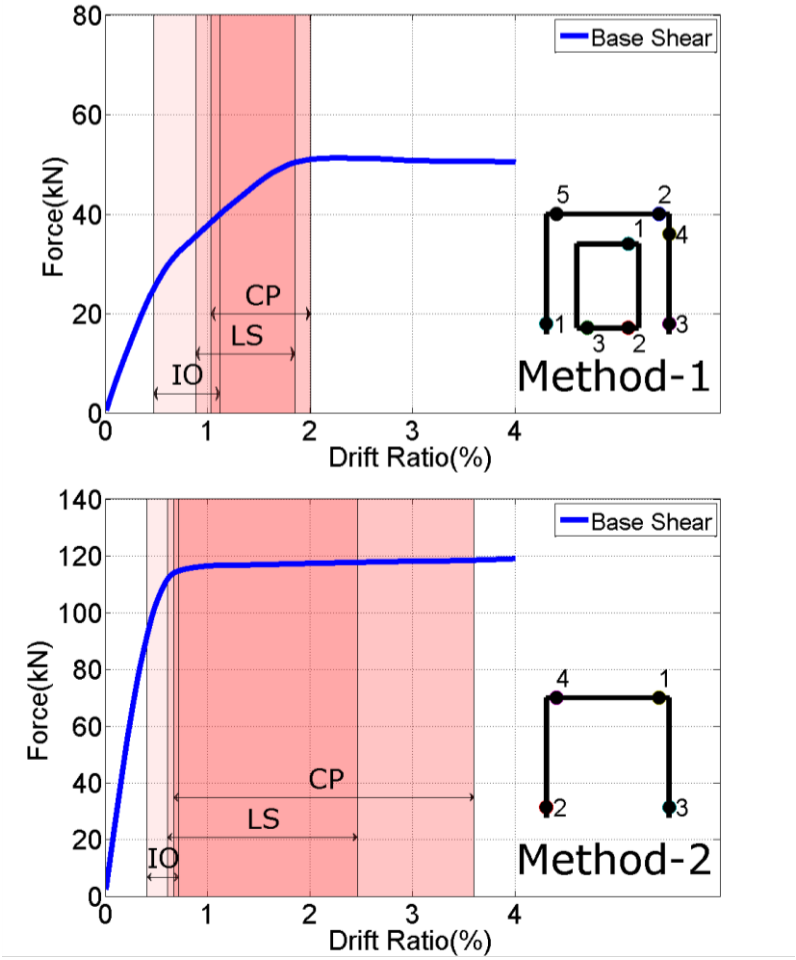

Figure 2.21: *Performance evaluation of ISFs*

A parametric study was conducted by employing various sizes of steel sections. Material properties were kept same with the original model to see the effect of member sizes on the response of retrofitting methods. Box sections and I-sections were used for non-composite and composite simulations, respectively. Parametric study results of the non-composite and composite sections are given in Figure 2.22 and Figure 2.24, respectively.

For the non-composite simulation results, increasing the steel column size while keeping steel beams same did not increase the lateral load capacity of the frame significantly. Due to dependency on the strength of the steel beams, steel column could not reach their strength limits. In addition to that, possibility of using steel sections with higher sizes were limited by the joint shear strength of RC beam-column connections which obviously cannot be provided with the current simulation procedure. Average DRs for IO, LS and CP performance limits were found as 0.7%, 1.3% and 1.4%. Analyses were repeated with $N/N_0 = 0.1$ and $N/N_0 = 0.3$ axial load ratios (Figure 2.23). Increasing axial load ratio on columns led to a similar result to the case with $N/N_0 = 0.2$. However decreasing axial loads on RC members shifted IO, LS and CP limits to 1.0%, 1.6% and 1.7% DRs, respectively.

For the composite simulation results, both steel beam and column section sizes had influence on the lateral load capacity of strengthened frames. Enhancement in deformability of the system is again observed in the parametric study. Hence composite section retrofit method is favored as it increases both strength and deformability of the system, while extending the damage region on RC members at low to moderate inter-story deformations. Average DRs for IO, LS and CP performance limits were found as 0.8%, 1.6% and 2.2%. For composite sections, effects of $N/N_0 = 0.1$ and $N/N_0 = 0.3$ axial load ratios remained limited (Figure 2.25). Increasing axial load ratio did not lead to any significant difference on the results however decreasing axial load ratio shifted IO, LS and CP limits to 0.9%, 1.8% and 2.3% DRs, respectively.

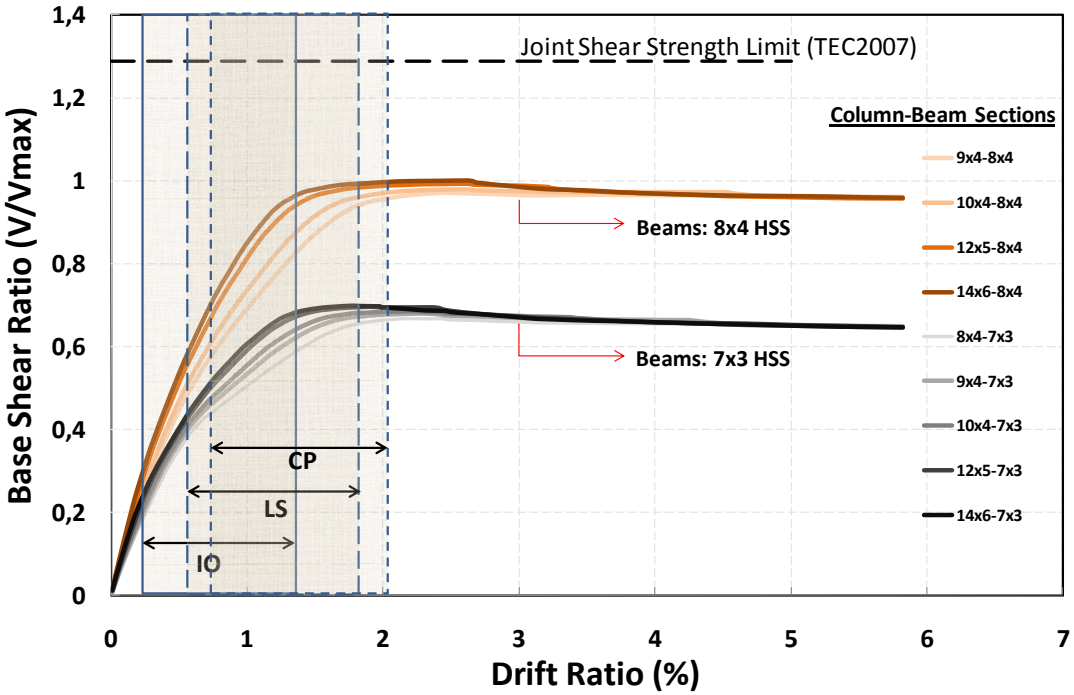

Figure 2.22: *Parametric study on non-composite sections (N/N_0 = 0.2)*

(a) N/N_0 = 0.1

(b) N/N_0 = 0.3

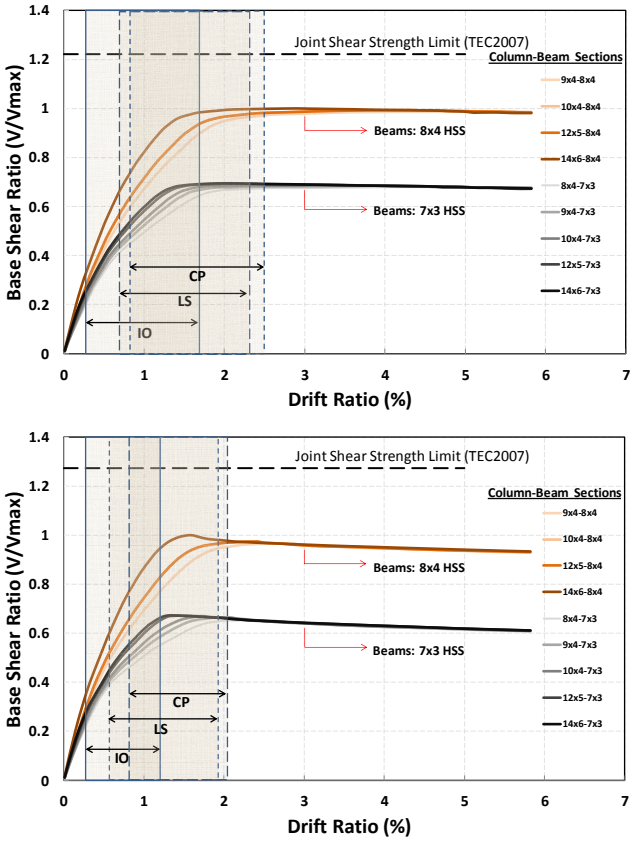

Figure 2.23: *Parametric comparison with varying axial loads (Method-1)*

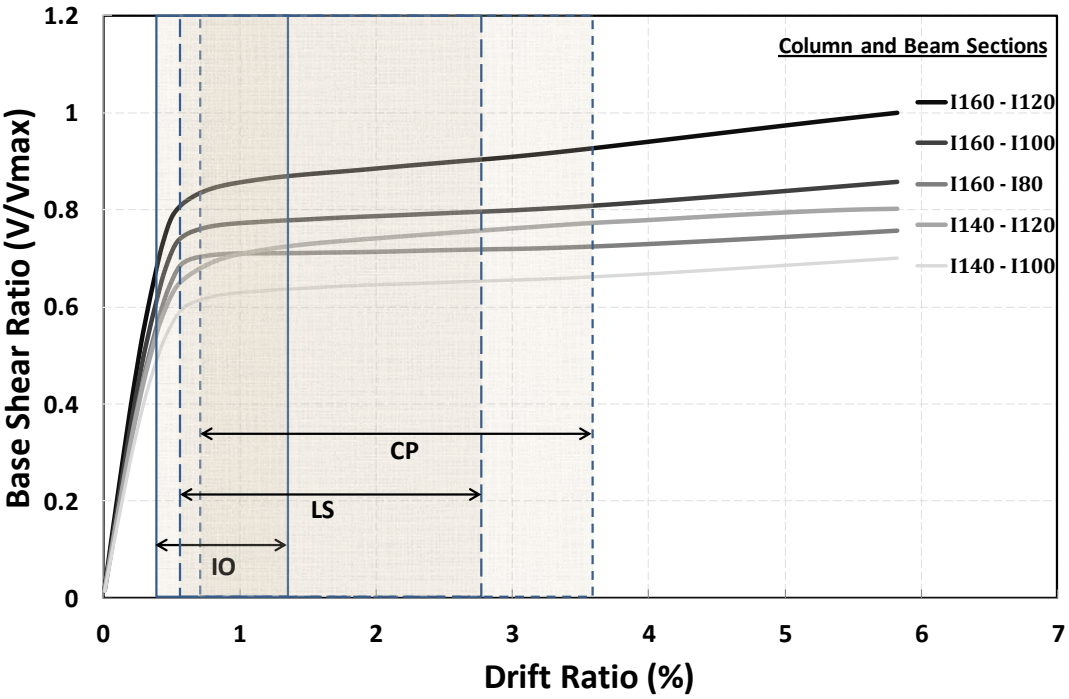

Figure 2.24: *Parametric study on composite sections (N/N_0 = 0.2)*

(a) N/N_0 = 0.1

(b) N/N_0 = 0.3

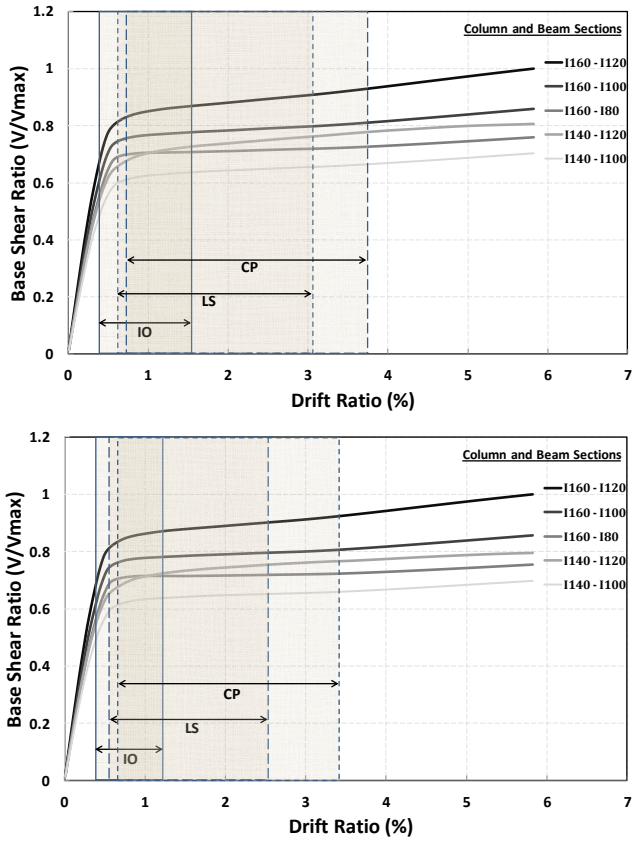

Figure 2.25: *Parametric comparison with varying axial loads (Method-2)*

CHAPTER 3

NUMERICAL SIMULATIONS OF REINFORCED CONCRETE FRAMES TESTED WITH PSEUDO-DYNAMIC TEST METHODS

3.1 Test Details

In order to validate the capability of numerical modeling discussed in the previous chapter on frame systems, analyses of two story three bay frames were conducted. This chapter explains in detail these simulations.

3.1.1 Case 1: RC Frame with Infill Walls

In this experiment, 3.6 m high and 6.45 m wide, two story-three bay ½ scaled RC frame was tested using continuous pseudo dynamic test method by applying Duzce ground motion. Ground motion record was applied in three scale levels namely 50%, 100% and 140%. During the test, the original ground motion was compressed in time by a factor of $1/\sqrt{2}$ to incorporate scale effects according to similitude law (Elkhoraibi and Mosalam, 2007). Complete details of the experiment can be found in Kurt (2010).

The test structure had deficiencies commonly observed in the Turkish building stock. For example, low strength concrete, insufficient confining steel and plain reinforcement bars were used in the test. In addition, the frame had inadequate transverse reinforcement at beam-column joints according to limits of latest version of Turkish Earthquake Code (2007). Another important deficiency that required mentioning was the violation of the strong column weak beam concept.

Uniaxial compressive strength of brick and the mortar that was used in infill wall were 12 MPa and 14 MPa. Longitudinal reinforcement and stirrups had yield strength of 330MPa and 290 MPa. The longitudinal reinforcement ratio of the columns was 1.14%. Plain bars with a diameter of 8 mm and 4 mm were used as longitudinal and transverse reinforcement, respectively. Concrete uniaxial compressive strength was 7.3 MPa. The building frame had uniform distributed loads on first and second story summing up to a total load of about 5 and 7 tons, corresponding to 600 and 650 kg/m^2, respectively. The details of the columns, beams and the RC frame are shown in Figure 3.1.

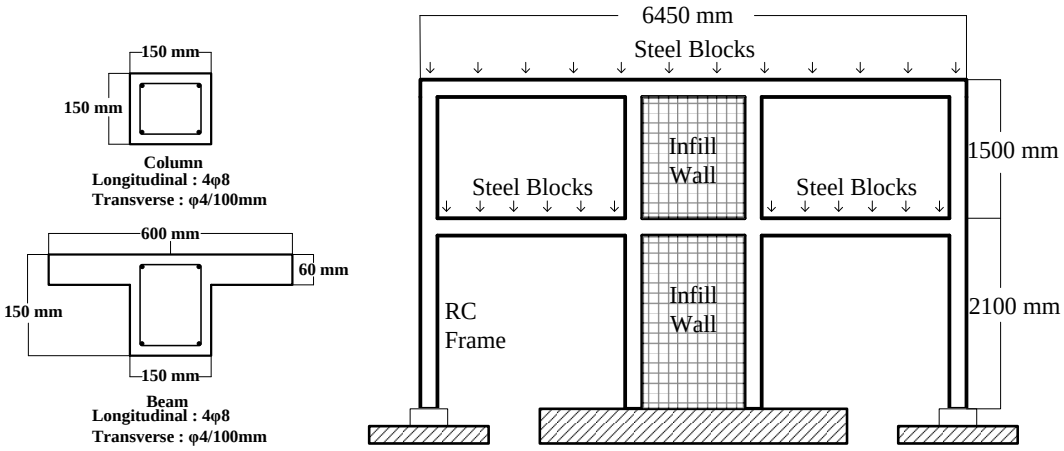

Figure 3.1: *RC frame with infill walls and beam-column details*

North-South component of 7.14 magnitude Duzce ground motion having a peak ground acceleration of 0.37g with three different scale factors was employed for the tests. Various damage states were observed by scaling the acceleration time series by 50%, 100%, 140% and additional 180%. Acceleration time series of the motion

and pseudo acceleration spectrum of the motion is shown in Figure 3.2. Estimated periods of the frame before and after the execution of ground motions are also given in the figure.

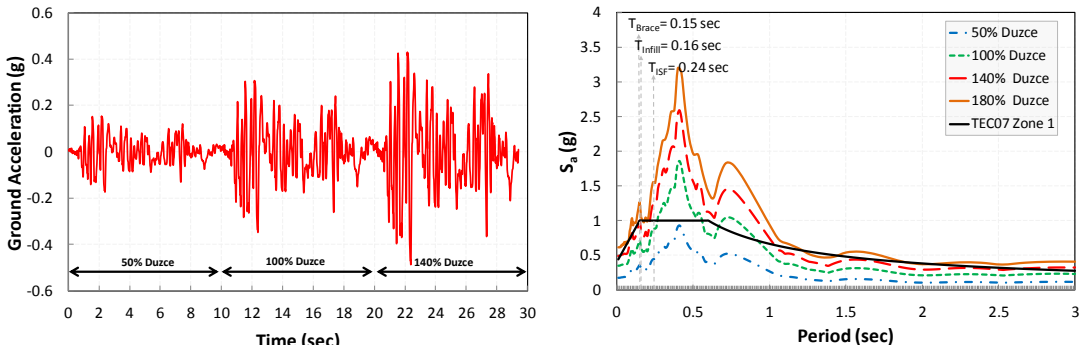

Figure 3.2: *Duzce ground motion and acceleration spectrum*

3.1.2 Case 2: RC Frame with Chevron Braces

An identical RC frame as described in the previous section was strengthened with chevron braces and pseudo dynamic tests were conducted for same (i.e 50%, 100%, 140%) and additional 180% scales of Duzce ground motion (Ozcelik 2010). RC member details and material strengths were kept constant to understand the effectiveness of applied retrofitting method. Details of the specimen are given in Figure 3.3.

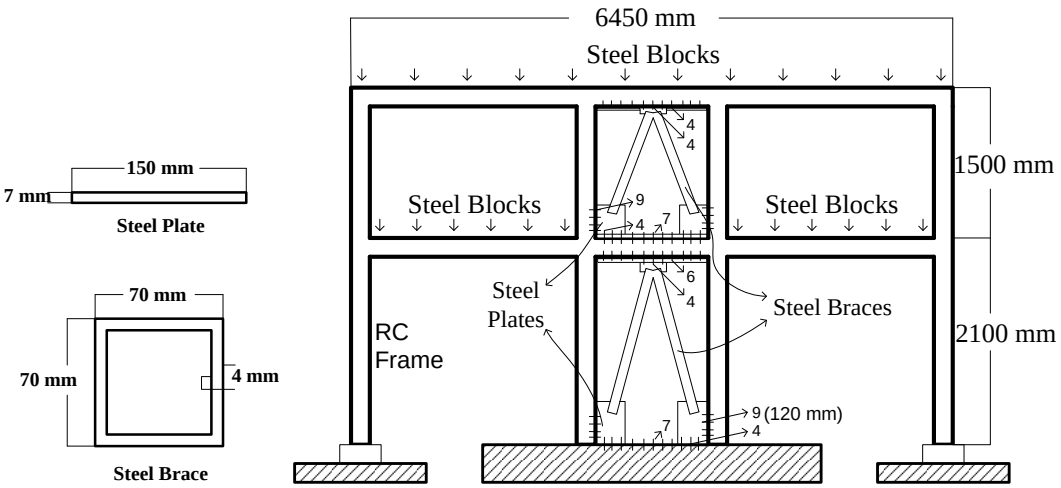

Figure 3.3: *RC frame with braces and brace section details*

Inverted V-braces were mounted into the interior bay of the test frame for both first and second stories. Steel plate sections with 7 mm thickness were connected via thru bolts along the center span of RC beam as shown in Figure 3.3. Gusset plates were attached by using anchorage rods to the RC column ends, foundation and middle length of the RC beams. The depth of anchor holes was 120 mm and number of anchor rods is shown in Figure 3.3. These plates were welded to steel brace sections. 70x70x4 steel box sections were used as brace members with yield strength of 400 MPa. Gusset plates and the steel plates under and top of the beams had yield strength of 350 MPa. Concrete and the other material strengths were approximately the same with the previously examined systems; i.e. concrete uniaxial compressive strength: 7.5 MPa, steel reinforcement: 330 MPa.

3.1.3 Case 3: RC Frame with Internal Steel Frames

A similar test specimen was prepared to investigate the effectiveness of internal steel frame retrofit by Ozcelik (2010). Test setup and specimen details were again kept unchanged and 180% scale of ground motion was also tested for this retrofitting method. Implementation of internal steel frames and steel section details are given in Figure 3.4.

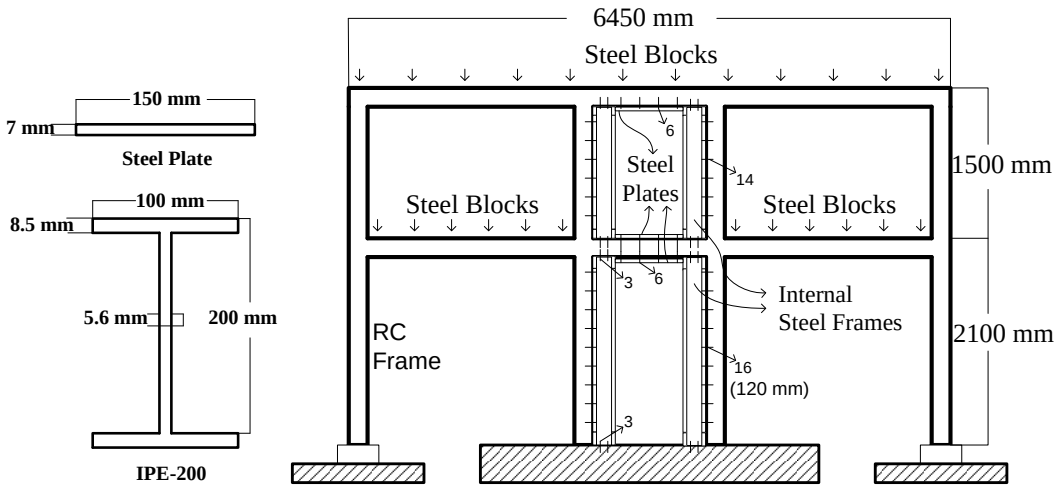

Figure 3.4: *RC frame with ISF and steel section details*

IPE 200 steel sections were installed inside the central bay using dowels having a depth of 120 mm. Individual anchors were used between the RC columns and internal steel frames to achieve full composite action. Steel plate sections with 7 mm thickness were bonded at the bottom and the top of interior beams. In this way, bending capacity of beams was enhanced significantly. The design was conducted such that the structural elements in the central bay act as full composite sections. Furthermore, strong column weak beam requirement was satisfied for these elements. IPE-200 sections and steel plates had yield strength of 235 MPa and 350 MPa, respectively. Concrete and the other material strengths similar with the reference test. Same testing procedure had been applied to the system and seismic performance was investigated.

3.2 Numerical Modeling

3.2.1 Case 1: RC Frame with Infill Walls

Nonlinear time history analyses of test structure were performed utilizing Opensees Simulation Platform version 2.2 (Mazzoni et.al. 2010) to observe the ability of estimating the dynamic response of the test frame. These analyses were conducted in 2D as Multi Degree of Freedom (MDOF) systems. Modeling strategy and material models employed for the MDOF analysis are summarized in Figure 3.5. Complete details of the analysis can also be found at Kurt et. al. (2010).

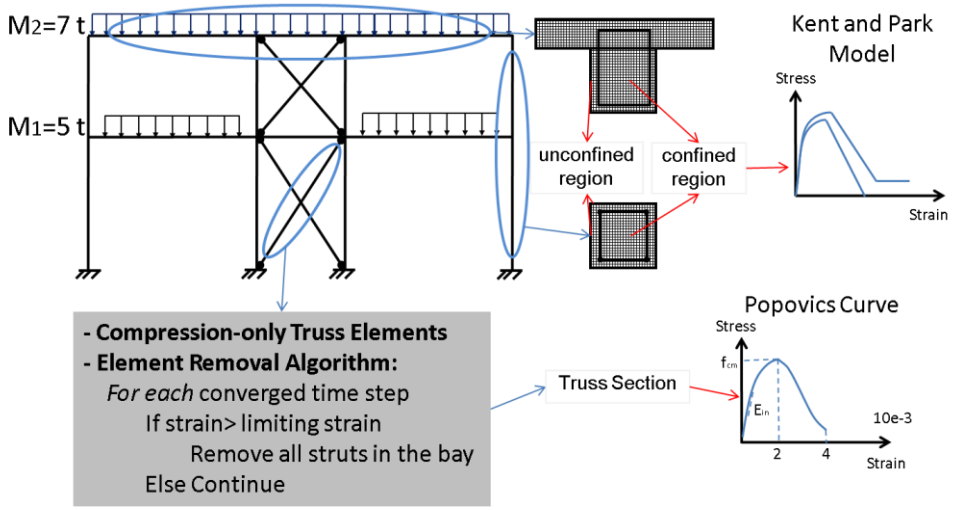

Figure 3.5: *Modeling strategy of infill walls*

Force based fiber frame elements were used to model beams and columns. The material model used for concrete (*Concrete01*) follows the rules of the confined and unconfined concrete models proposed by Kent and Park (1972) with the Karsan and Jirsa (1972) plastic offset rules. Due to welding of longitudinal reinforcements to the foundation in the column ends, bond-slip was not observed. Hence, reinforcing steel was modeled using a bilinear elasto-plastic model (*Steel 02*) with a kinematic hardening slope of 1%. The infill walls were modeled using compression only truss elements connected to the diagonal nodes of the boundary frame.

It was decided to employ recommended material properties and relevant equations from ASCE/SEI-41 guidelines. In this way it was possible to observe the success of estimating the natural period of the test structure with these stiffness values. Effective strut area for the infill walls was calculated according to ASCE/SEI-41 guidelines and found as 0.025 and 0.021 m^2 for the first and second stories using the following equations:

$$a = 0.175\ (\lambda_1 h_{col})^{-0.4} r_{inf} \tag{1}$$

$$\lambda_1 = \left[\frac{E_{ms}(t_{in}+t_p)sin2\theta}{4E_c I_c h_{in}}\right]^{1/4} \tag{2}$$

Above, h_{col} is the column height, r_{inf} is the diagonal length of infill panel, θ is the angle whose tangent is the infill height to length ratio, E_c and E_{ms} are the modulus of elasticity of concrete and the plaster-infill composite and t_{in} and t_p are the thicknesses of brick units and the plaster. The modulus of elasticity of the plaster-brick composite, E_{sm} was computed as 10000 MPa from (Binici and Ozcebe 2006):

$$E_{ms} = \frac{E_{in}t_{in}+E_m t_p}{t_{st}} \tag{3}$$

where E_{in} and E_m are the modulus of elasticity of the infill wall and mortar/plaster, and t_{in} and t_m are the thickness of the infill wall and mortar. Accordingly, E_{in} was taken as 7700MPa ($550F_m^{'}$) based on ASCE/SEI-41 recommendations and t_u was calculated as 16200 MPa ($4700\sqrt{F_c^{'}}$) using ACI 318-05 equation.

The observations made during the test showed that diagonal cracks formed in the central region of the infill in both directions. Later these cracks extended in a step pattern indicating the failure of bed joints along the diagonal. Consequently,

compressive strength of the strut (F_{cm}) was computed from ASCE/SEI-41 assuming that bed-joint shear strength governs the strength of the diagonal strut either in the form of a diagonal crack or a single horizontal bed joint by using equations:

$$V_{ss} = f_{mv}\, L\, (t_{in} + t_p) \tag{4}$$

$$f_{cm} = V_{ss}\, /(a\, cos\theta) \tag{5}$$

in which V_{ss} is the total shear resistance along the wall length, L is the length of the infill wall, f_{mv} is the shear strength of bed mortar/plaster mix which was taken from ASCE/SEI-41 as 0.25 MPa for masonry in good condition.

Popovics equation (1973) was employed for the compressive stress-strain behavior of the infill struts (*Concrete 04*) as suggested by Madan et. al (1997). The strain at peak compressive strength and diagonal strut failure were taken as 0.002 and 0.004. Lumped mass approach with a Rayleigh critical damping of 2% was utilized during the analyses by also incorporating the second order nonlinear geometric effects.

Although the infill diagonal strut fails in one direction in the numerical simulation, the strut in the opposite direction at the first story had significant capacity and stiffness. Hence the frame could not deform in the opposite direction upon failure of only one diagonal strut. In order to overcome this modeling error, element removal algorithm as suggested by Talaat and Mosalam (2009) was adopted as shown in Figure 3.5. When the failure strain of the diagonal strut is exceeded in one direction, the struts in both directions are removed from the model. In this way, failure of the strut in one direction results in complete failure of the infill wall.

3.2.2 Case 2: RC Frame with Chevron Braces

Numerical model of chevron brace retrofitted specimens was prepared by the procedure described in Chaper-2. Rigid end zones and the section properties were assigned based on the test conditions. However, stiffness of elements (used to account for the gusset plate lengths) at base level were modified due to uplift of gusset plates that was observed during the test. Axial force on brace elements versus

uplift displacements of gusset plates were sketched form the test data (Figure 3.7). Effective stiffness's of link elements were calculated by using trend lines of different scales of ground motion. By including element property change method, corresponding stiffness's were modified and analysis were conducted with updated stiffness's prior to the beginning of each ground motion. Rayleigh critical damping of 5% was utilized and a similar successive analysis method with the first case was followed for rest of the time history analysis. Summary of the modeling strategy is given in Figure 3.6.

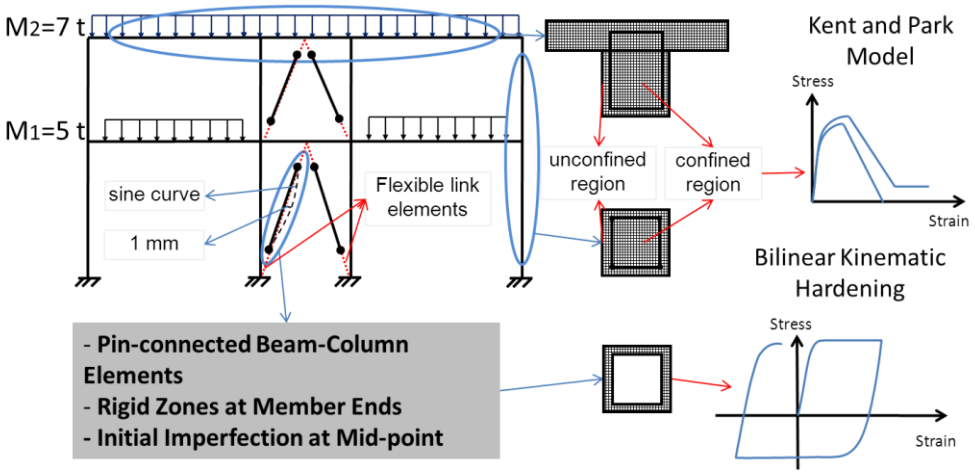

Figure 3.6: *Modeling strategy of chevron braces*

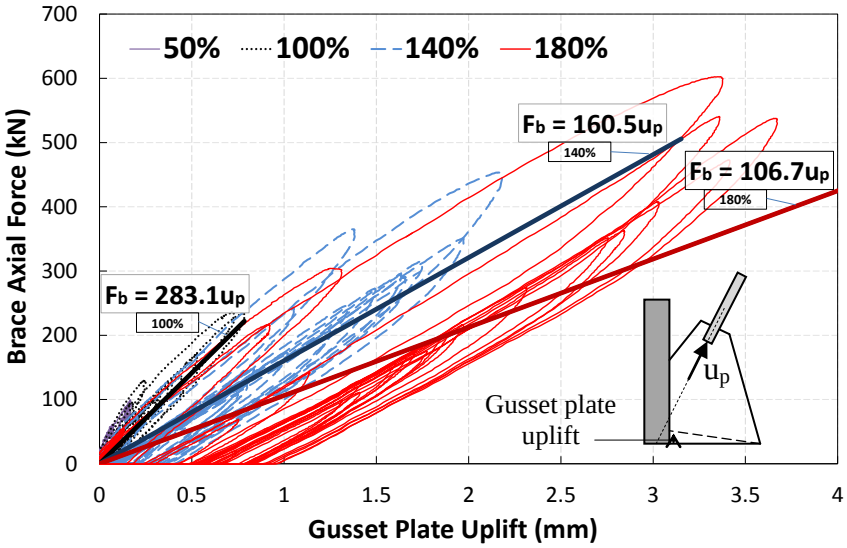

Figure 3.7: *Brace axial force versus gusset plate deformation*

3.2.3 Case 3: RC Frame with Internal Steel Frames

Same strategy described in Chapter-2 was used with slightly modifications due to modeling of steel plates top and bottom of the interior beams. These plates were taken as additional longitudinal reinforcement for the interior beams. In the fiber section model of the beams, corresponding longitudinal reinforcement with equivalent cross-section area was placed at top and bottom of the sections. Rest of the modeling was similar to previous cases and its details are given in Figure 3.8.

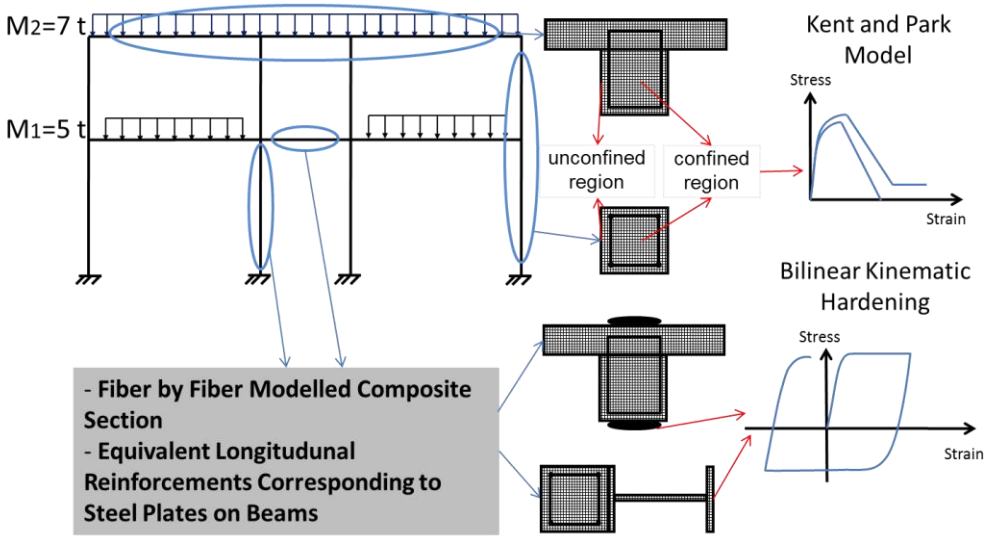

Figure 3.8: *Modeling strategy of ISFs*

3.3 Analysis Results

3.3.1 Case 1: RC Frame with Infill Walls

Firstly, pushover analysis of the frame using the first mode shape lateral load profile was conducted (Figure 3.9). In the same graphs, experimental and numerical comparisons of base shear versus top and first story displacement responses are also given. It could be observed that initial stiffness and lateral load carrying capacity was estimated with adequate accuracy. Infill wall failure was estimated to take place at about 1% overall drift ratio. After this displacement level, lateral strength of the system degraded rapidly and reduced to that of the bare frame.

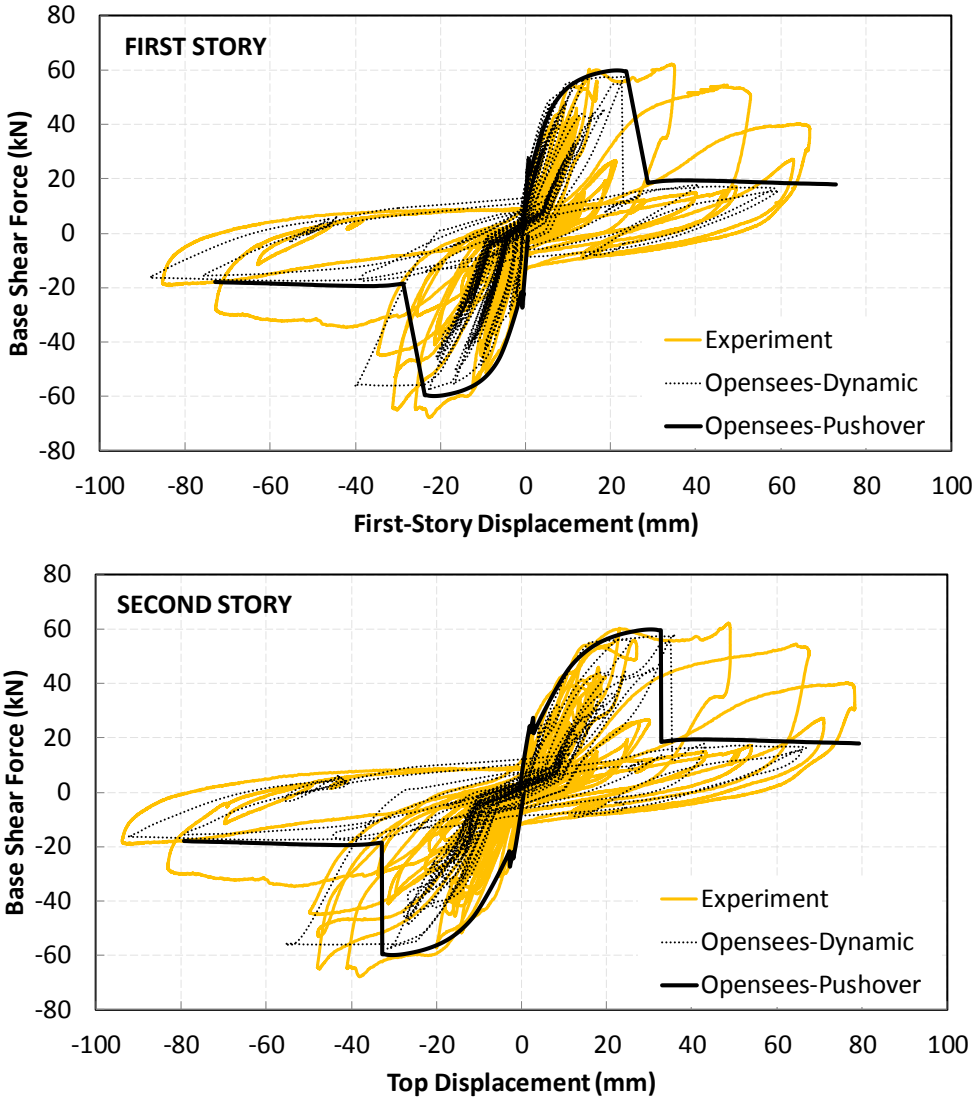

Figure 3.9: *Load-deformation response of infill system*

During the analyses all scale levels of the Duzce ground motions were given one after the other. In this way softening of the structure due to previous ground motion could be taken into account. The nonlinear time history analyses results are presented in Figure 3.10. It could be observed that numerical simulation results agreed well with the experimental results for the analytical model. For the 140% scale, the experimental results were not capable of simulating the reversed cyclic behavior accurately if no element removal was used. This is because of the fact that upon failure of one composite strut, the stiffness and strength of the other strut is observed to completely degrade. It can be observed that, time series response for

story deformation could now accurately be predicted upon using previously discussed element removal algorithm.

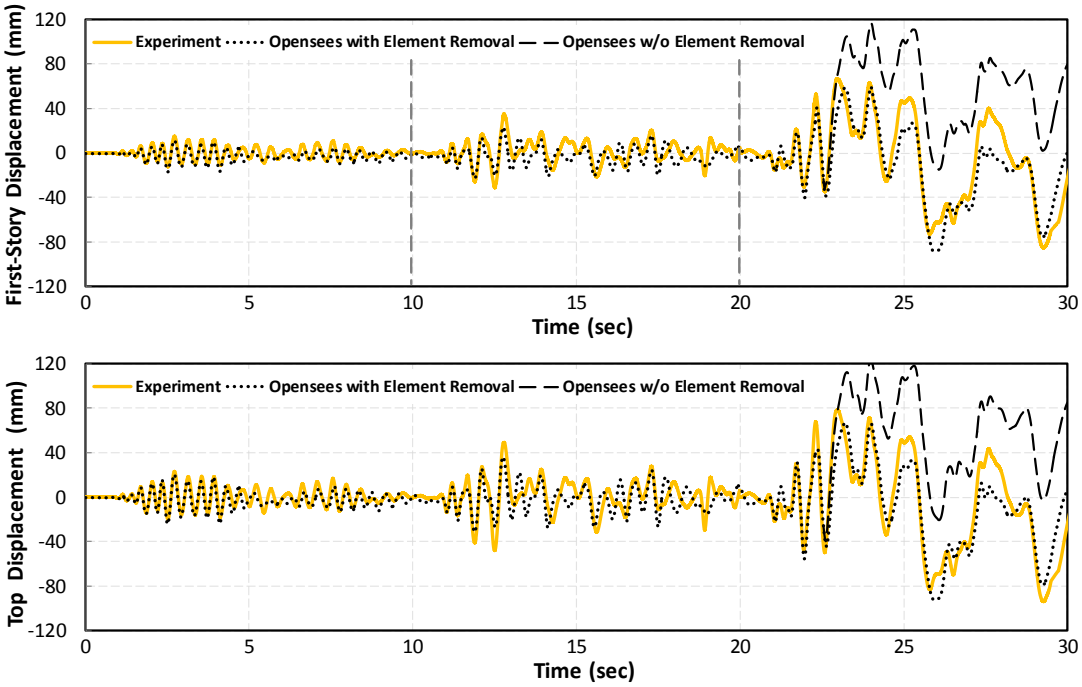

Figure 3.10: *Simulation results for infill system*

Conducting an eigenvalue analysis at each converged analysis step, period change was determined and compared with the identified period as reported with the method by Kurt et al. (2010) in Figure 3.11. Estimated period change, although shows significant jaggedness, it follows the experimental trend. Furthermore, period jumps observed at 140% scale due to the significant strength deterioration of the first story infill wall was reproduced with the numerical simulations.

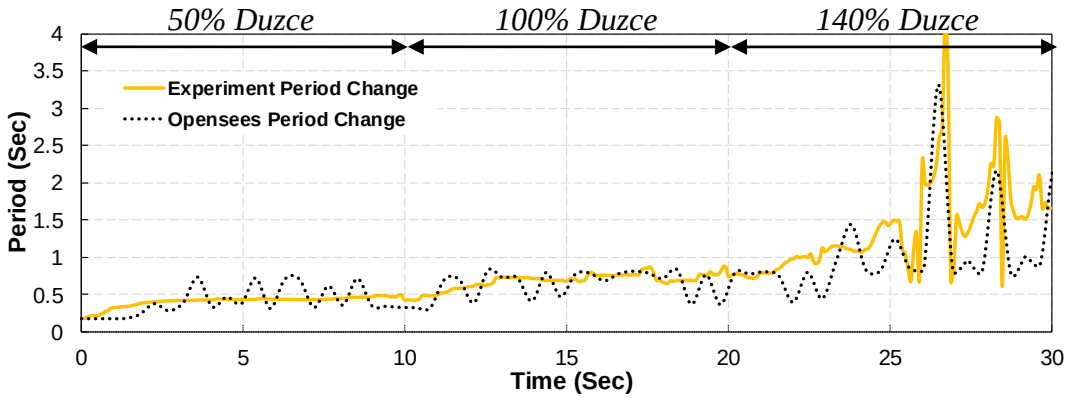

Figure 3.11: *Comparison of period change for infill system*

Errors in peak displacements and lateral loading capacity of the system are given in Table 3.1. According to results observed peak displacement in 140% scale of the test was estimated with 31.51% error if element removal algorithm was not used. However error was calculated as 1.44% by including element removal algorithm in the analysis.

Table 3.1: *Error estimation of peak base shear and displacements (Infill Wall)*

Analysis Type	GM Scale	Story	Test Max. Disp. (mm)	Analysis Max. Disp. (mm)	Error (%)	Test Max. Base Shear (kN)	Analysis Max. Base Shear (kN)	Error (%)
With Element Removal	50%	1	15.02	17.01	13.31	60.35	55.80	7.54
		2	23.01	24.27	5.46			
	100%	1	31.22	23.25	25.52	62.24	57.67	7.34
		2	47.98	36.22	24.51			
	140%	1	85.34	88.30	3.48	54.54	55.09	1.01
		2	93.84	92.49	1.44			
Without Element Removal	50%	1	15.02	17.01	13.31	60.35	55.80	7.54
		2	23.01	24.27	5.46			
	100%	1	31.22	23.25	25.52	62.24	57.67	7.34
		2	47.98	36.22	24.51			
	140%	1	85.34	116.89	36.97	54.54	56.04	2.76
		2	93.84	123.41	31.51			

Column moment-curvature responses of the exterior columns were compared to those measured experimentally (Figure 3.12.a). Hysteretic behavior of the analytical and numerical results showed similar energy dissipation characteristics. Although the moment capacity of the section was accurately predicted, ultimate curvature demands in one direction were overestimated. Following the exact loading and unloading cycles measured experimentally was found to be extremely challenging. Curvature variation of the interior columns during the time history analysis also pointed out a similar outcome (Figure 3.12.b). Although the response was matched well for 50% scale, trend was getting worst with 100% and 140%

scales. Results showed that estimating local demand parameters such as column plastic rotations remains to be a more difficult task compared to global parameters such as inter-story drift ratio or base shear capacity.

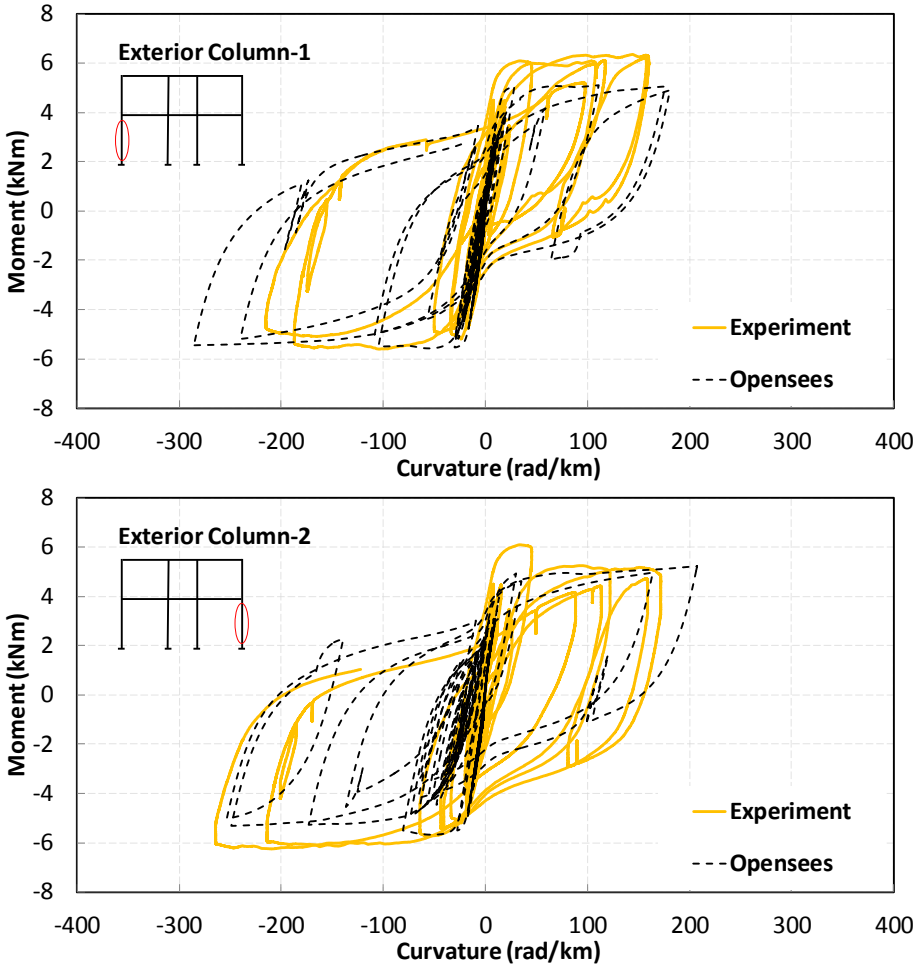

(a) Moment-Curvature relationship of interior columns

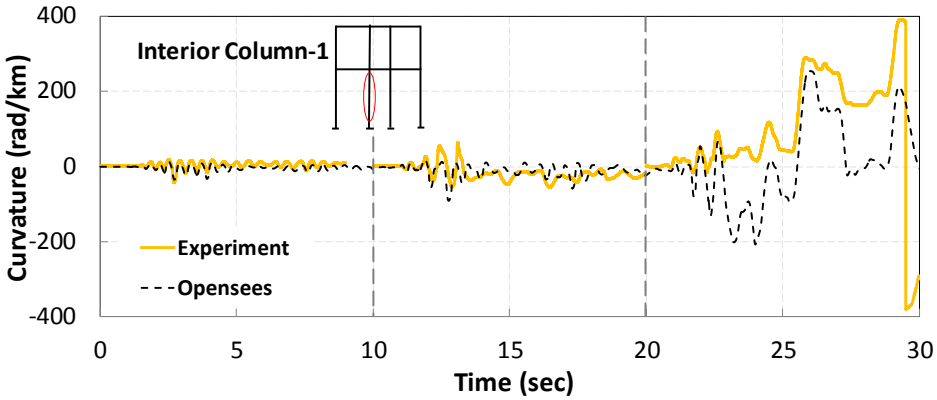

Figure 3.12: *(Continued)*

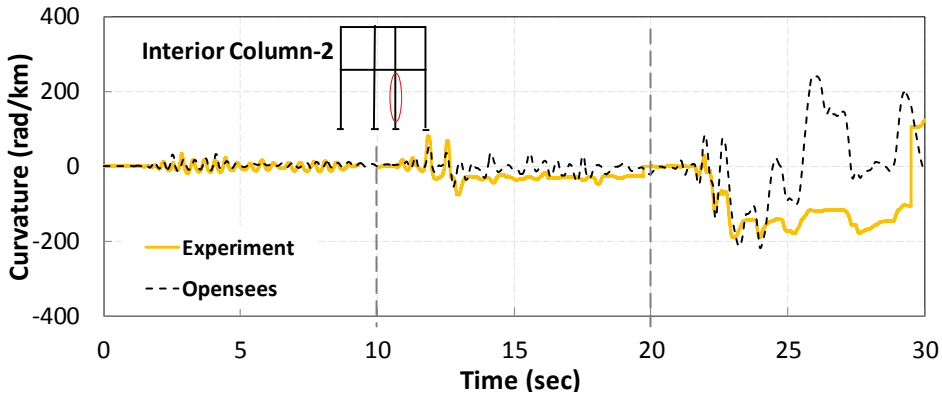

(b) Curvature history of exterior columns

Figure 3.12: *Comparison of sectional responses of columns*

3.3.2 Case 2: RC Frame with Chevron Braces

For the case with chevron braces, there was no buckling observed in the braces for any scales of applied ground motion. This condition resulted in events such as observing relatively low drift ratios, high initial stiffness and lack of softening in the system. Base shear versus top and first story displacement responses and nonlinear time history analyses results are given in Figure 3.13 and Figure 3.14, respectively. Errors in peak displacements and lateral loading capacity of the braced frame models are given in Table 3.2.

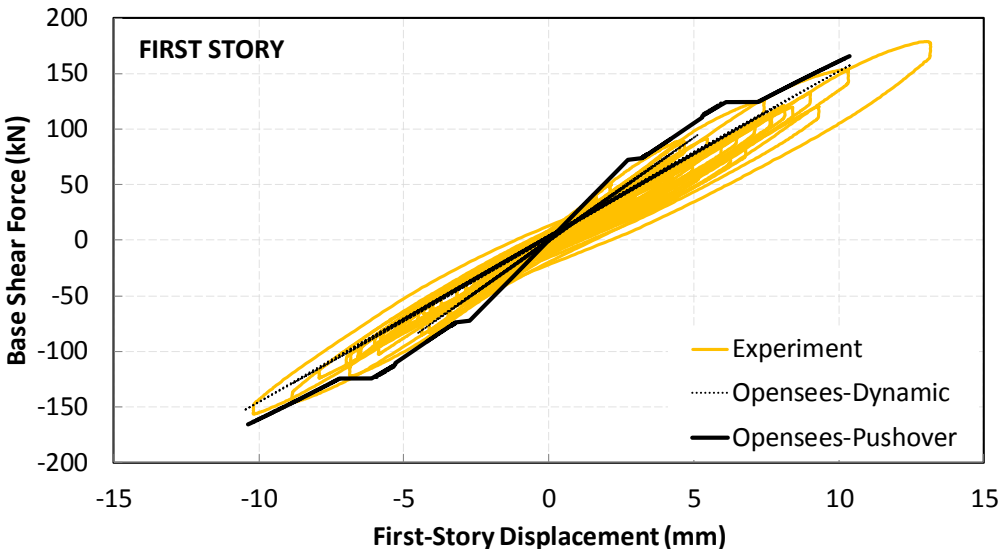

Figure 3.13: *(Continued)*

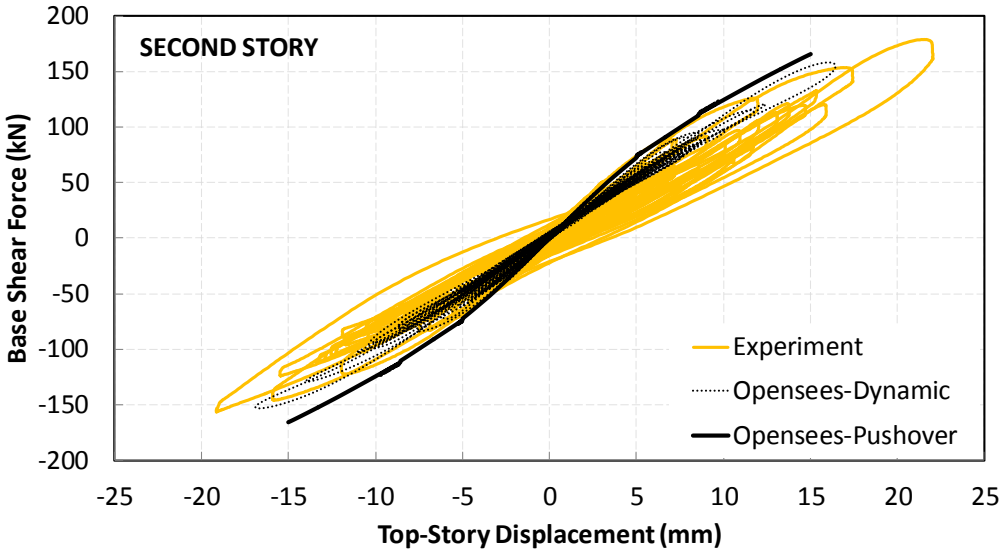

Figure 3.13: *Load-deformation response of braced system with flexible links*

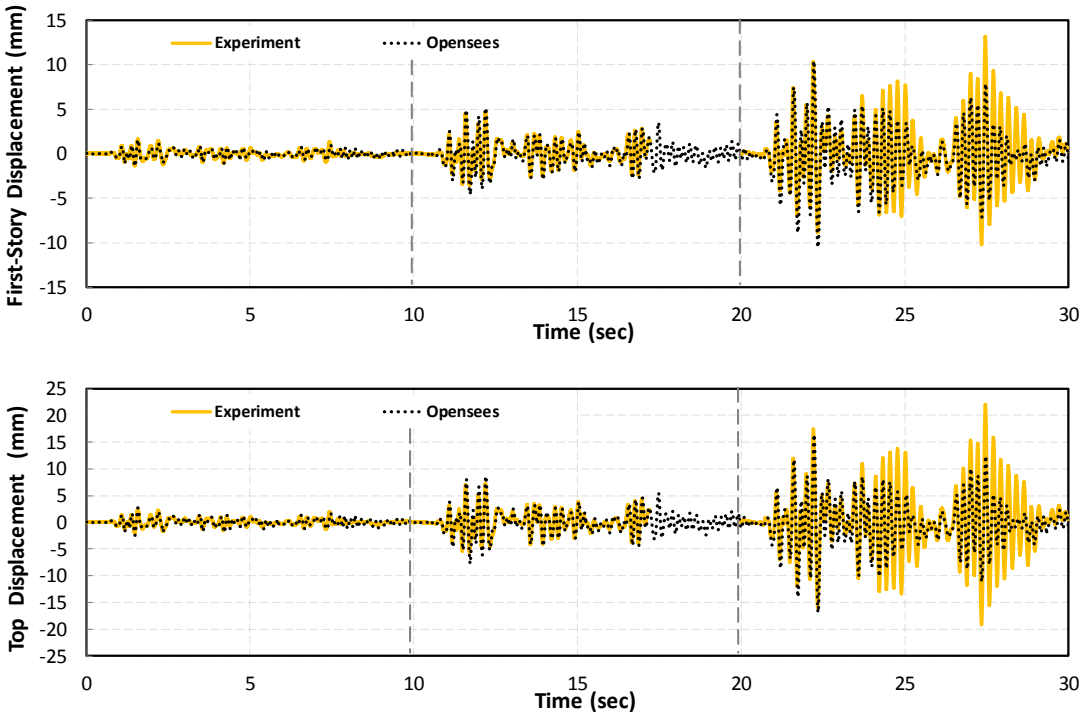

Figure 3.14: *Simulation results for braced system with flexible links*

The initial stiffness and displacement response of the numerical simulation results agree well with those of test measurements. However displacement response was underestimated for the end of 140% scale of test results. Top story displacement

versus base shear and displacement response results of the system that had been connected with rigid links is also given in Figure 3.15. According to results excluding uplift of gusset plates prevented system to soften for 100% and 140% scales. For both scales, model underestimated the peak displacements and unable to matched the cyclic response of the test results. According to error estimation results of this case, error increased with increasing earthquake scale and this effect became more critical.

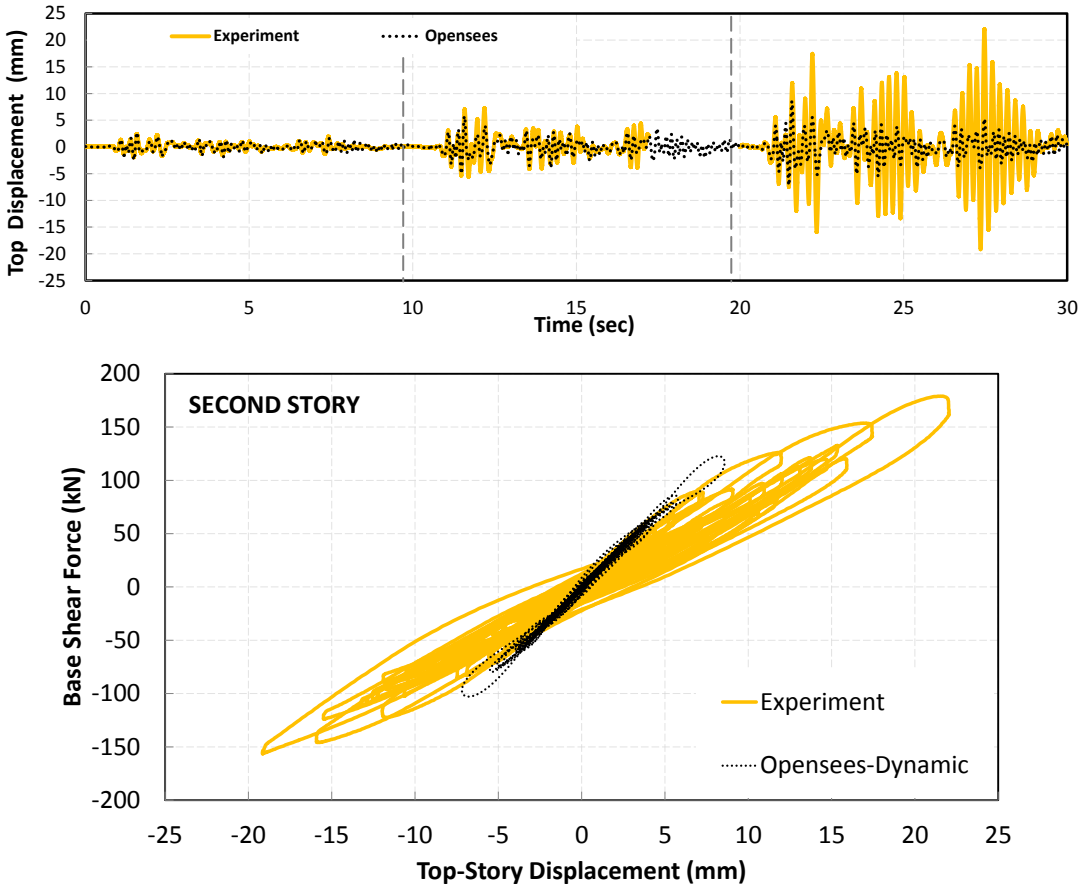

Figure 3.15: *Simulation results for braced system with rigid links*

Comparison of eigenvalue analysis results with identified period change are shown in Figure 3.16. The general trend of period change seems to be matching well with identified period change, implying the success of damage estimation.

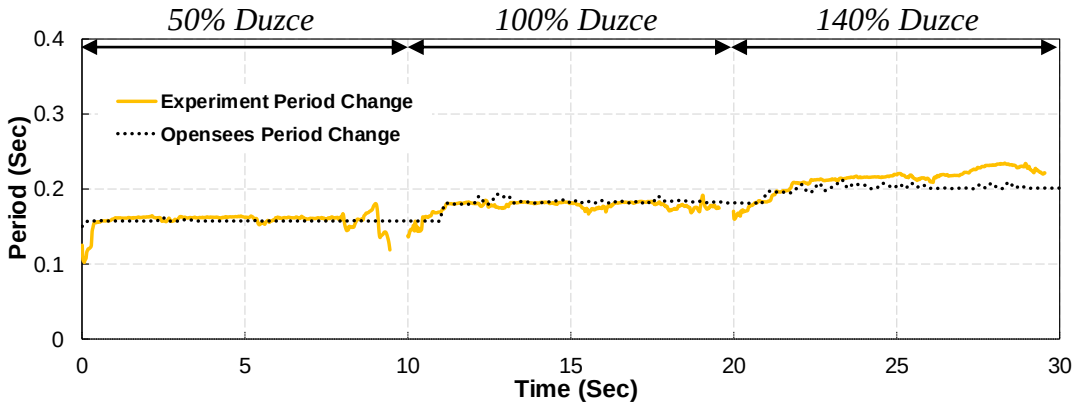

Figure 3.16: *Comparison of period change for braced system with flexible links*

Table 3.2: *Error estimation of peak base shear and displacements (Chevron Braces)*

Analysis Type	GM Scale	Story	Test Max. Disp.(mm)	Analysis Max. Disp. (mm)	Error (%)	Test Max. Base Shear (kN)	Analysis Max. Base Shear (kN)	Error (%)
Model With Flexible Links	50%	1	1.66	1.57	5.68	39.94	42.66	6.82
		2	2.45	2.42	1.01			
	100%	1	4.69	5.15	9.94	89.13	95.15	6.76
		2	7.29	8.64	18.46			
	140%	1	13.18	10.52	20.17	178.98	153.29	14.36
		2	22.06	16.91	23.34			
	180%	1	18.17	17.73	2.42	206.06	197.37	4.22
		2	34.92	31.36	10.19			
Model With Rigid Links	50%	1	1.66	1.57	5.68	39.94	42.66	6.82
		2	2.45	2.71	10.66			
	100%	1	4.69	3.17	32.43	89.13	85.81	3.72
		2	7.29	5.78	20.76			
	140%	1	13.18	4.54	65.53	178.98	102.84	42.54
		2	22.06	8.58	61.12			
	180%	1	18.17	5.98	67.09	206.06	161.04	21.85
		2	34.92	11.55	66.92			

Although model is not fully capable of matching 140% scale, it simulates the time history response of the system perfectly for 180% scale (Figure 3.17). Analytical model estimates the peak deformation of first and second story very accurately. Cyclic behavior of the system was also matched better than 140% scale results.

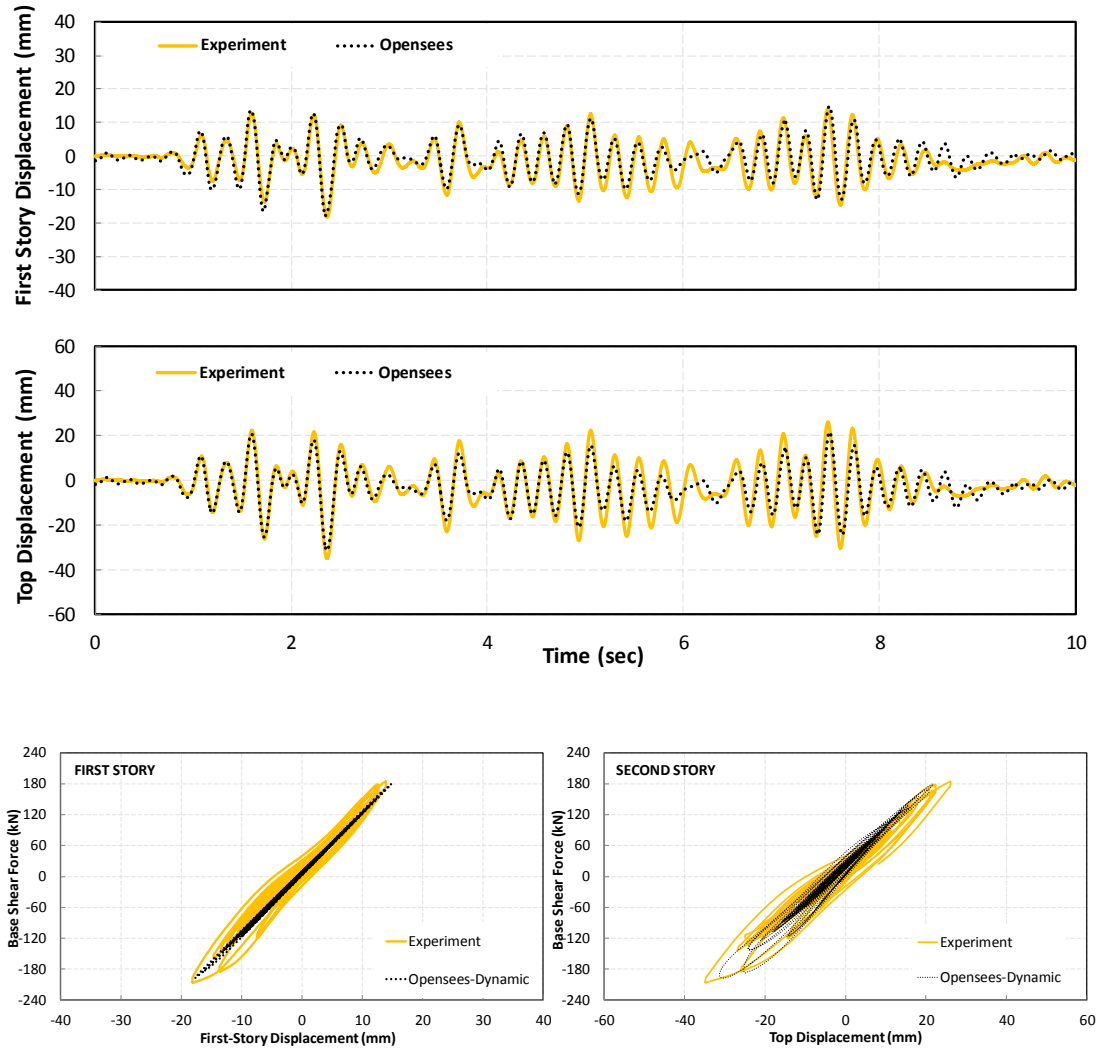

Figure 3.17: *Time-history and base shear force results of 180% scaling*

3.3.3 Case 3: RC Frame with Internal Steel Frames

Inelastic pushover analysis of the ISF and base shear versus top and first story displacement history responses are given in Figure 3.18. Although initial

stiffness was estimated accurately, model underestimated the degradation of stiffness of the system. Estimated errors for ISF system are given in Table 3.3. Peak lateral load capacity of the frame, on the other hand, was simulated with little error. For 50% and 100% scales, model was almost perfectly capable of capturing the displacement history achieved by the test. However for 140% scale, there was significant error observed in terms of maximum displacements between the simulation and the test results (Figure 3.19).

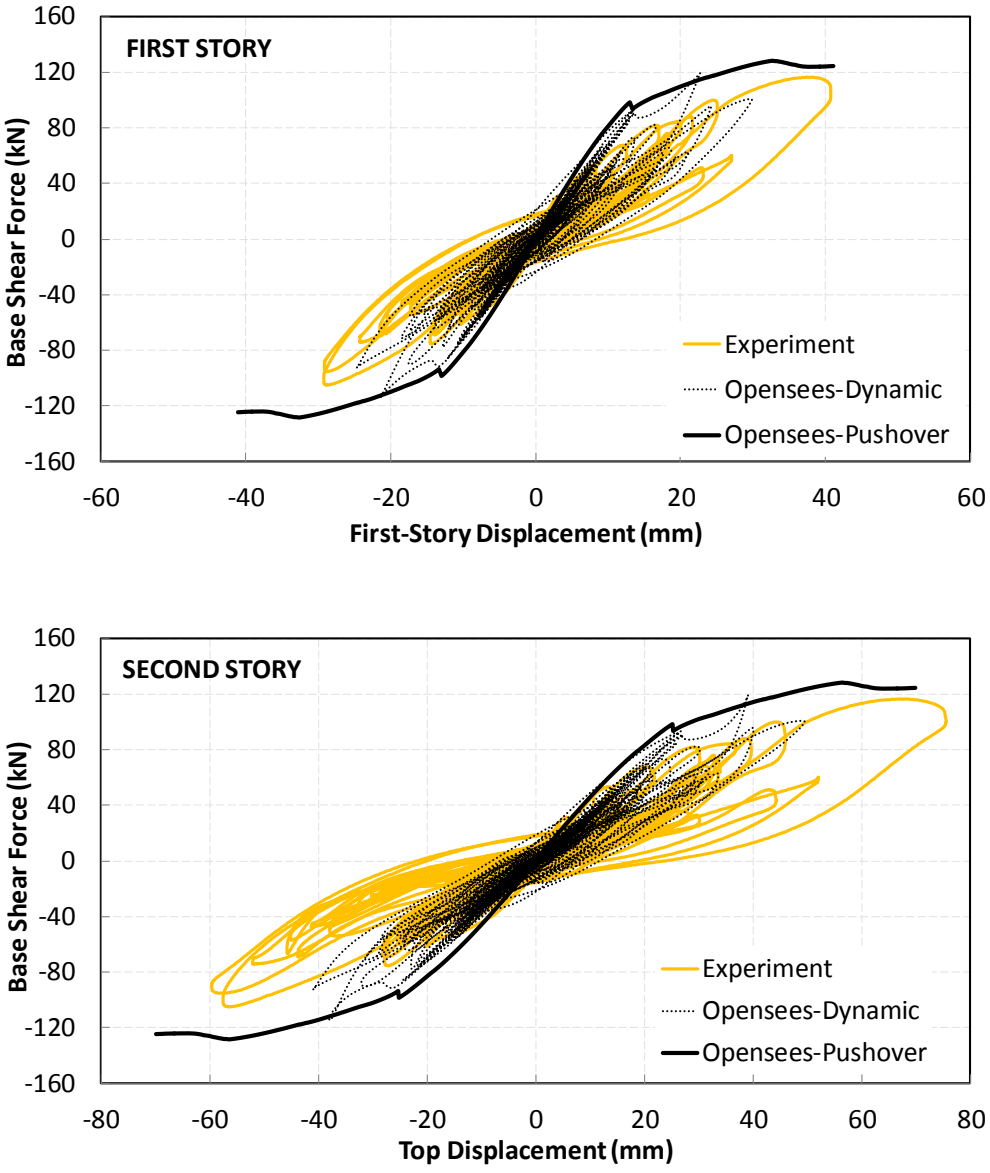

Figure 3.18: *Load-deformation response of ISF system*

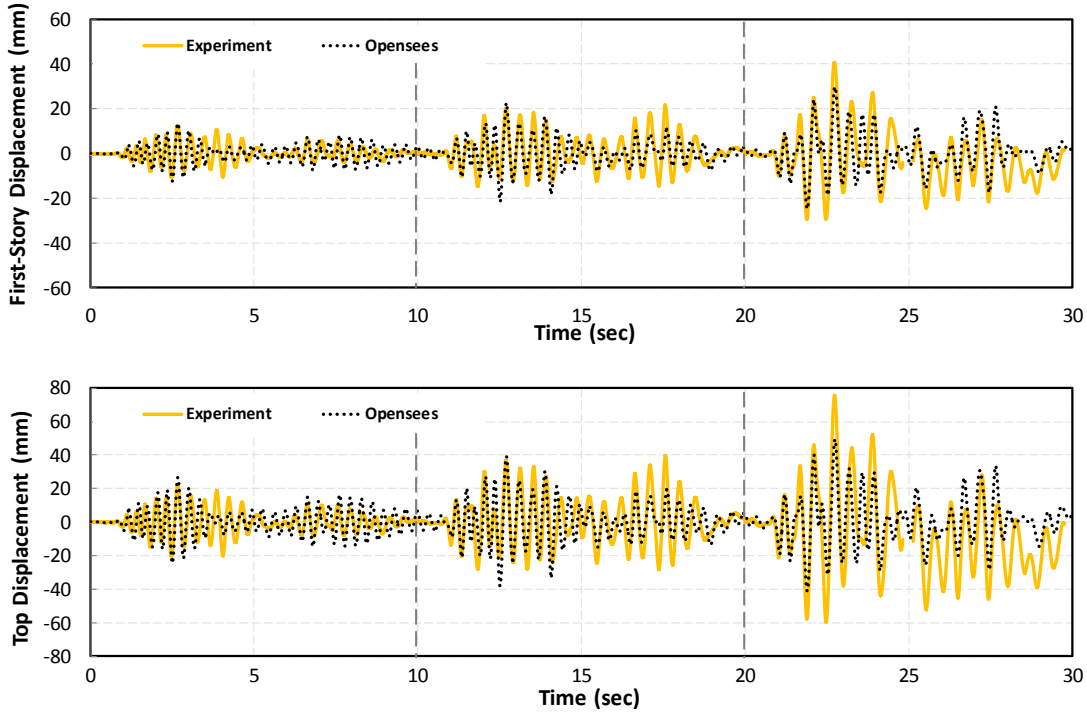

Figure 3.19: *Simulation results for ISF system*

Comparison of period change during the ground motion excursion is another important parameter on identifying the performance of numerical model (Figure 3.20). According to results initial period was found 0.21 sec in the test and 0.24 sec in the analysis. Up to 20th second, simulation estimation of period was below that obtained from the test results. However, estimated period change matched well with the 140% ground motion scale results.

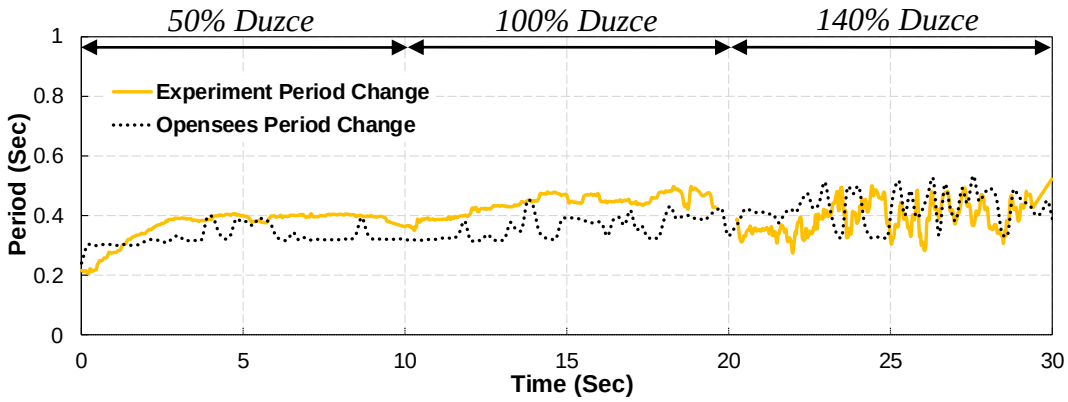

Figure 3.20: *Comparison of period change for ISF system*

Table 3.3: *Error estimation of peak base shear and displacements (ISF)*

Analysis Type	GM Scale	Story	Test Max. Disp. (mm)	Analysis Max. Disp. (mm)	Error (%)	Test Max. Base Shear (kN)	Analysis Max. Base Shear (kN)	Error (%)
ISF	50%	1	12.56	13.57	8.08	67.62	86.00	27.17
		2	21.80	24.44	12.14			
	100%	1	21.68	22.73	4.83	88.20	114.66	30.01
		2	39.71	39.12	1.50			
	140%	1	40.76	29.87	26.71	116.63	100.85	13.53
		2	75.56	49.51	34.48			
	180%	1	57.61	59.77	3.75	123.18	108.71	11.75
		2	111.90	94.26	15.76			

Next 180% scale of ground motion was used to analyze the strengthened frames. Time history analysis results showed that model was capable of capturing peak displacement of first story accurately and second story with an acceptable error (Figure 3.21). Analysis results matches with test results in terms of general cyclic behavior however model underestimates the lateral load capacity of the system.

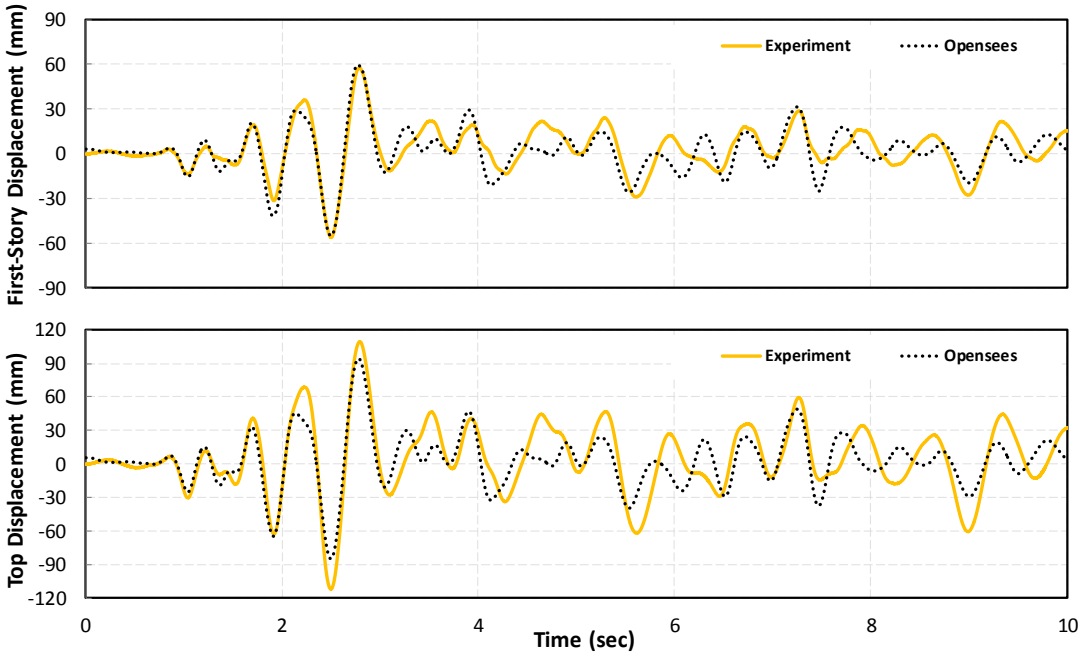

Figure 3.21: *(Continued)*

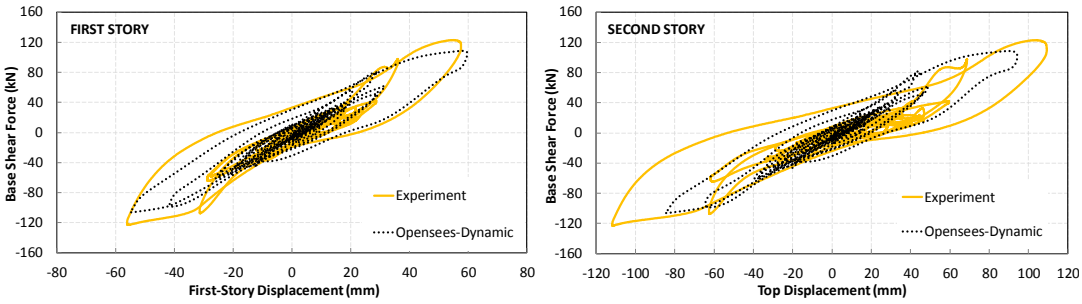

Figure 3.21: *Time-history and base shear force results of 180% scaling*

3.4 Performance Evaluation of Reinforce Concrete Frames

3.4.1 Case 1: RC Frame with Infill Walls

RC column and beams' performance levels were determined by the method suggested in Turkish Earthquake Code (2007) throughout the considered ground motion time series. Highest strains were checked at the RC member ends and the appropriate one of three performance levels namely immediate occupancy (IO), life safety (LS) and collapse prevention (CP) were noted on the frame. Infill walls were evaluated by the method suggested in ASCE/SEI-41 for life safety (LS) performance level. TEC2007 performance limits and their representation in following figures are given in Figure 3.22.

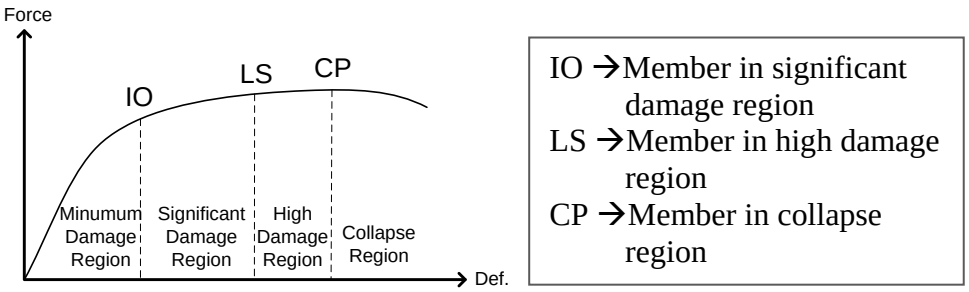

Figure 3.22: *Performance limits and their usage in performance evaluation figures*

Same procedure was applied for different scales of ground motion and results are shown in Figure 3.23. In the same figure observed damage on first story infill wall of actual test frame are also demonstrated (Kurt 2010). According to the analysis results 50% scale of ground motion did not yield any critical damage on the

frame members, while all the damage states remained in the IO range. Beams experienced cracking due to gravity loads. After applying 100% scale of ground motion, interior columns experienced some damage and they went beyond IO and CP levels. In addition to that, exterior columns and all the beams in the frame passed the IO performance level and first story infill wall went beyond LS performance level which indicates collapse of the infill wall. For the final scaling all the columns in first story lost their capability of carrying lateral loads and went beyond CP limit. At this stage element removal algorithm also became active because of crushing of the wall. Beams did not experience any more damage at this scale of ground motion. The weak column-strong beam concept is clearly seen from this result.

Hinge pattern of frame was also determined by checking strains on longitudinal reinforcements (Figure 3.24). Results showed that hinging first occurred on the beams due to distributed loading with steel blocks. With application of ground motion hinging was observed on the ends of interior columns at first story and beam ends of the stories.

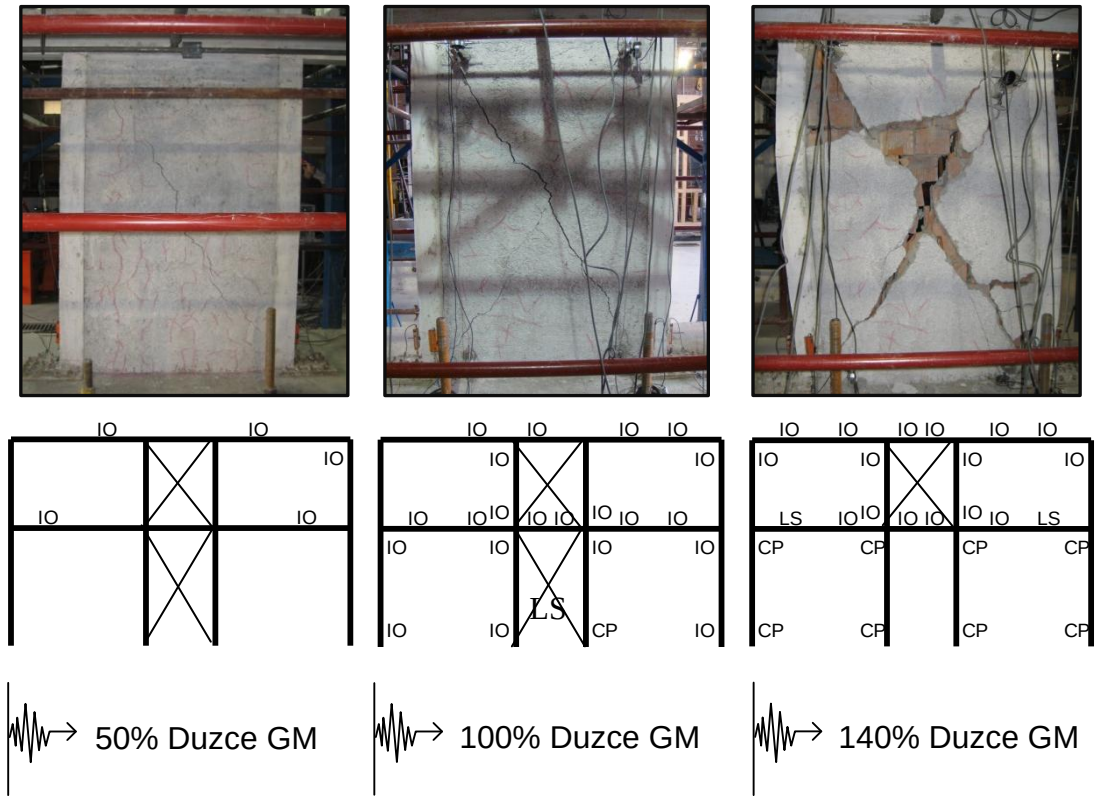

Figure 3.23: *Performance evaluation of RC frame members (Infill System)*

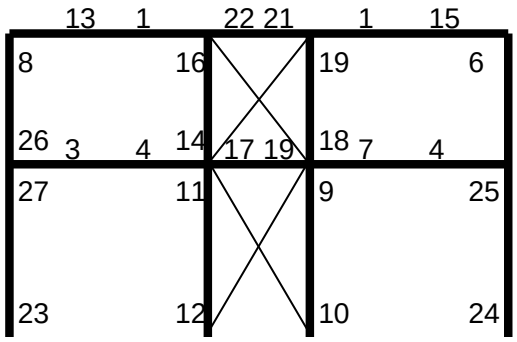

Figure 3.24: *Hinge pattern (Infill System)*

3.4.2 Case 2: RC Frame with Chevron Braces

Results of braced frame performance analysis showed that keeping frame under relatively low deformations prevented any significant damage on RC members. As a result none of the members went beyond code specified strain limits of IO for 50%, 100% and 140% scales (Figure 3.25). In the same figure observed damage on RC members and first story braces during the test are demonstrated (Ozcelik 2010). System started to take damage after applying 180% scale of ground motion and CP limit was observed on the interior column ends. It should be also mentioned that the location of possible hinging points on columns was slightly different than the observed in the test. In analytical model, gusset plates were connected to column bases (Figure 3.6) whereas they were connected to columns as show in Figure 3.3. This connection type increases the demand on the column ends and this may affect the location of hinging on column. For this level of scale two of exterior columns also experienced high damage and reached CP limit. Performance of braces was also evaluated by the method suggested in ASCE/SEI-41. According to results none of the braces experienced damage except the 180% scale of ground motion. Hinge pattern of the braced frame also indicated that hinging first occurred on beams, than on interior columns due to ground motion effects (Figure 3.26).

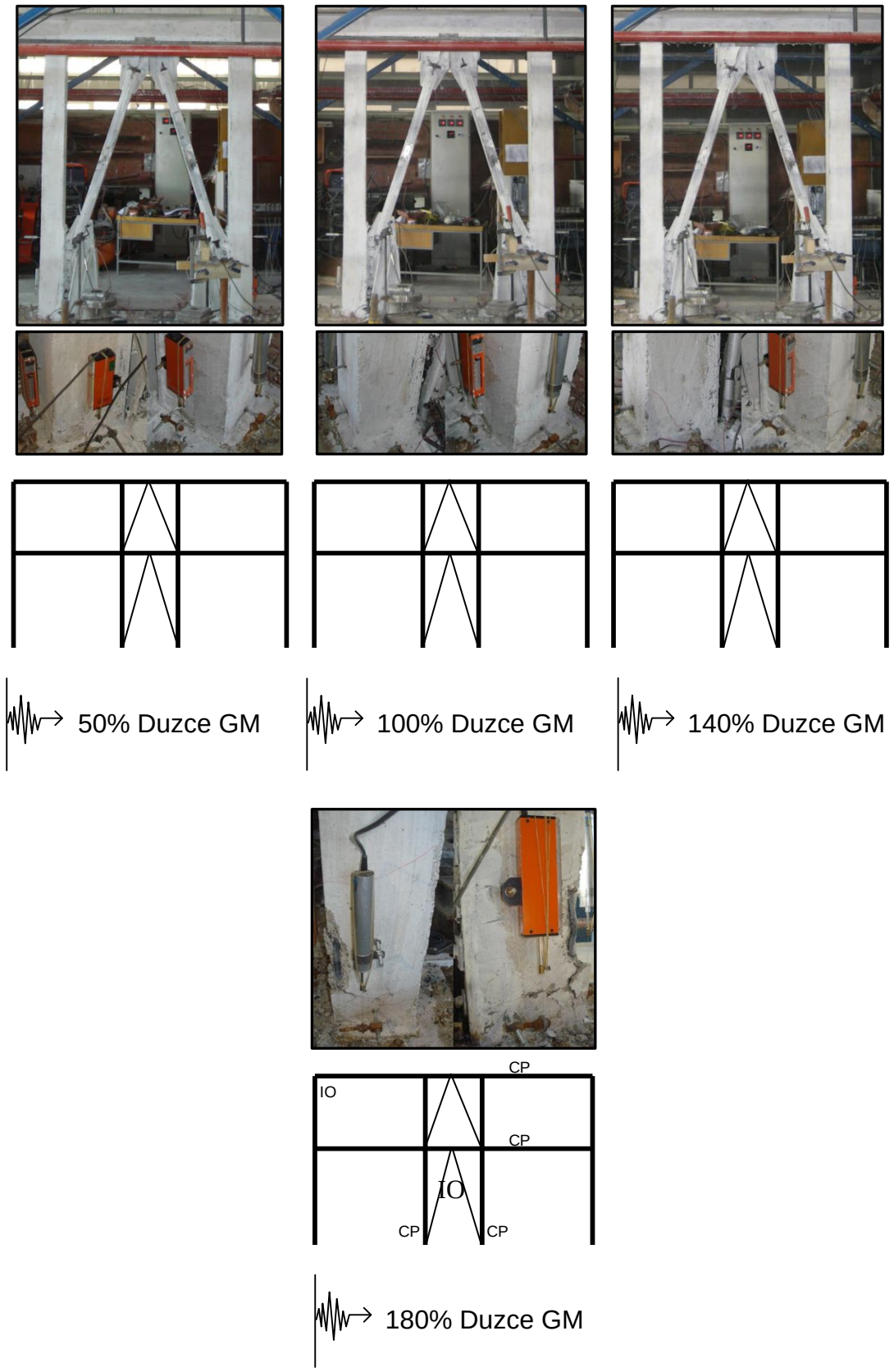

Figure 3.25: *Performance evaluation of RC frame members (Braced System)*

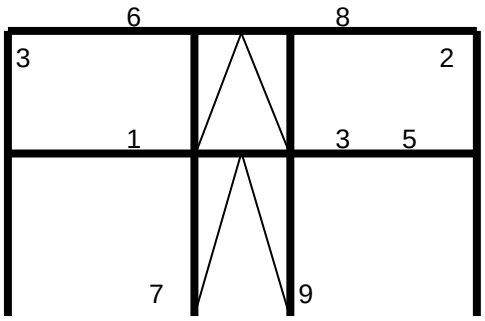

Figure 3.26: *Hinge pattern (Braced System)*

3.4.3 Case 3: RC Frame with Internal Steel Frames

Analysis results indicate that columns experienced significant damage for this case compared to chevron brace retrofitted frame (Figure 3.27). Application of 50% of ground motion resulted in occurrence of only IO performance level on the interior column of first story. For 100% scale of ground motion these columns experienced significant damage and passed beyond CP performance level. For 140% scale damage was distributed to exterior columns of the first story and they went to IO and CP performance limits. Beams did not experienced damage for these scales of ground motion. For the last scale all the columns in first story went to CP limit state. In addition to that second story columns started to experience damage and went to IO and CP limits. Observed damage on interior composite columns during the test are also demonstrated (Ozcelik 2010). Comparisons of observed damage and estimated performance levels indicate that code specified strain limits are somewhat conservative, but can be used safely, for the performance evaluation. A similar result to performance evaluation results of system was observed for the hinge pattern (Figure 3.28). Hinging was first occurred on the interior columns of the first story. That hinging was also observed on exterior columns of first and second story.

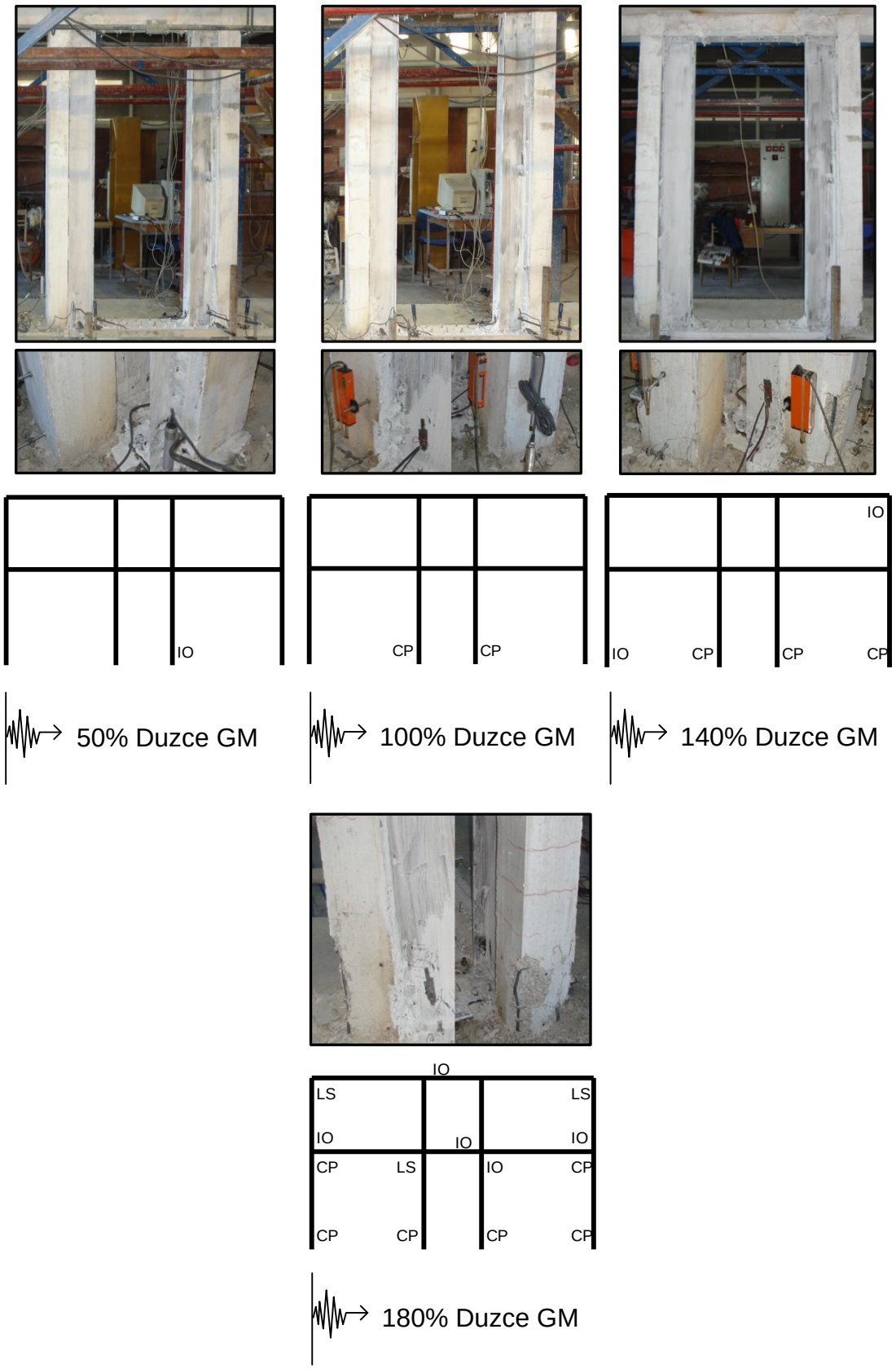

Figure 3.27: *Performance evaluation of RC frame members (ISF System)*

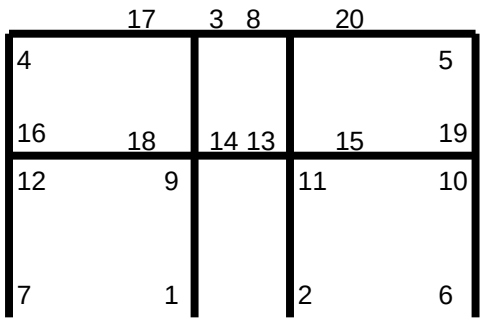

Figure 3.28: *Hinge pattern (ISF System)*

CHAPTER 4

CASE STUDY: STRUCTURAL STEEL RETROFIT OF A 4-STORY RC FRAME

4.1 Structure and Analysis Details

An exterior frame of a deficient existing 4-story 3-bay RC structure was analyzed by using various chevron brace sections with different inelastic post-buckling capacity and internal steel frames to observe the performance of seismic retrofits. Same structure was also analyzed with and without infill strut model to reflect the importance of infill modeling and element removal algorithm.

Uniaxial compressive strength of the concrete was 9 MPa and the yield strength of reinforcing steel was 220 MPa in tested structure. Tie spacing was 260 mm for beams and 280 mm for columns with a clear cover of 25 mm. The frame had 250x400 mm columns which were oriented in their strong axis for B-axis and their weak axis for A, C and D-axes. All the beam dimensions were 150x500 mm. Interior bay of the frame (B-C axes) were used for installing infill walls and strengthening members, namely internal steel frame and chevron braces. The frame general layout is shown in Figure 4.1 where the complete details of the analyzed frame are available in Binici et.al. (2006). The north-south component of the 1999 Duzce earthquake was used for the time history analysis (Figure 4.2). This figure also shows the spectral acceleration vs. time plot of the Duzce earthquake and spectrum defined in TEC

2007 and the fundamental period the analyzed frames. It can be observed that Duzce motion spectrum is expected to cause more demand in the constant acceleration region while being relatively close to the code specified spectrum.

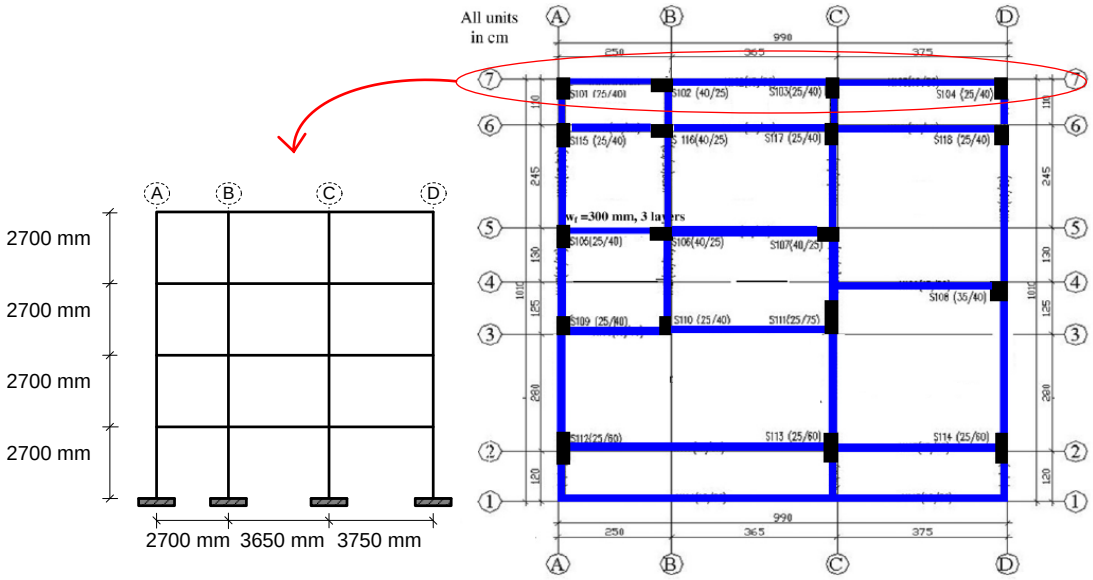

Column Sections:

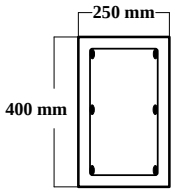

Column: *B-Axis*
Longitudinal : 6φ12
Transverse : φ8/270mm

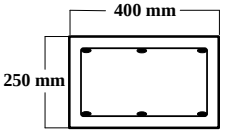

Column: *A/C/D-Axes*
Longitudinal : 6φ12
Transverse : φ8/270mm

Beam Sections:

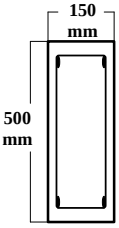

Beam: *All Axes*
Longitudinal : 4φ12
Transverse : φ8/280mm

Story	Gravity Load (kN) (1G+0.3Q)
1	110
2	233
3	233
4	235

Material Type	Material Strength (MPa)
Concrete	9
Reinforcement Steel	220
Confinement Steel	220

Figure 4.1: *Analyzed 4-story frame and beam, column details*

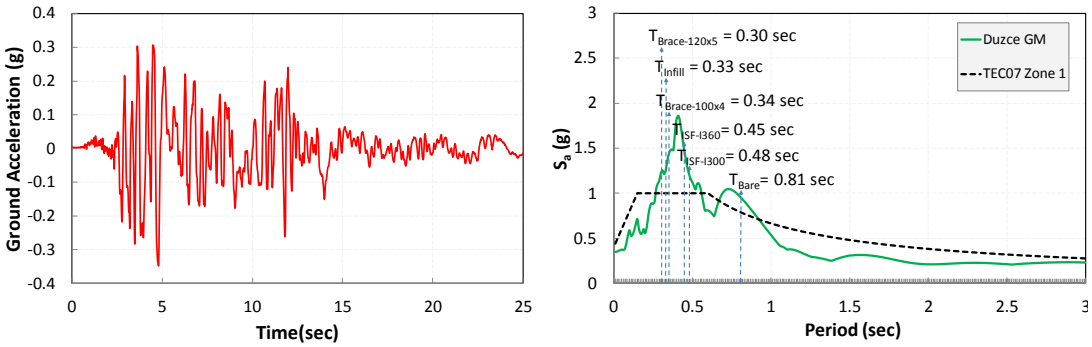

Figure 4.2: *Duzce ground motion and spectrum*

4.1.1 RC Frame With and Without Infill Walls

In order to compare effect of infill walls on bare frame two analyses were conducted; frame with and without infill walls. Bare frame analysis was conducted without adding any new structural component to the system. Then same frame were analyzed with previously explained truss model with element removal algorithm. It's assumed that infill wall had a width of 150 mm (110 mm brick, 40 mm mortar) which is same as width of beams in analyzed structure. Compressive strength of the mortar and the elastic section modulus of the infill wall were taken as 14 MPa and 10000 MPa, respectively. Corresponding strut properties were calculated by the procedure described in Chapter-3. Nodes were constrained to act as rigid diaphragms for all stories. Rayleigh critical damping of 5% was utilized during the analyses. The details of modeling and the properties of effective truss model are given in Figure 4.3.

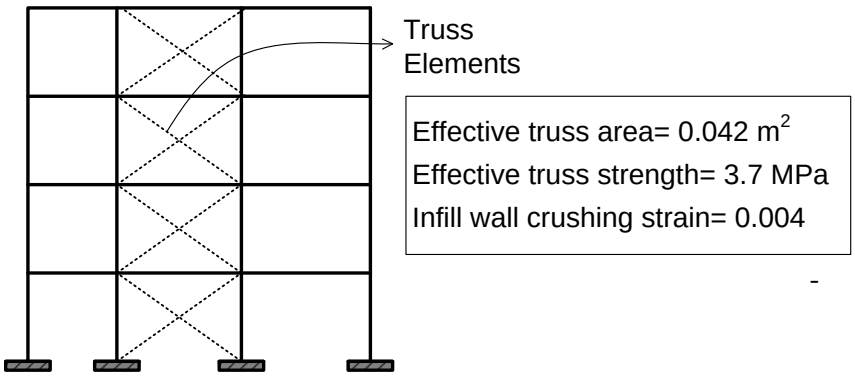

Figure 4.3: *Infill wall layout*

4.1.2 RC Frame with Chevron Braces

Frames were strengthened with chevron braces as represented in Figure 4.4. Two types of square HSS with dimension 100 mm and 4 mm thickness (HSS-100) and 120 mm and 5 mm thickness (HSS-120) with 235 MPa yield strength were installed in the middle bay of the frame. Rigid end zones were placed to brace ends to represent gusset plates. Slenderness ratios of braces were calculated with effective length of the braces as 62.1 and 50.8. Sinusoidal curved members were used with 1 mm initial imperfection at mid-span of the braces. Beams at the interior bay were supported by 10x150 mm steel plates which has 350 MPa yield strength. Same procedure that was explained in Chapter-3 was followed to model braces and their boundary conditions.

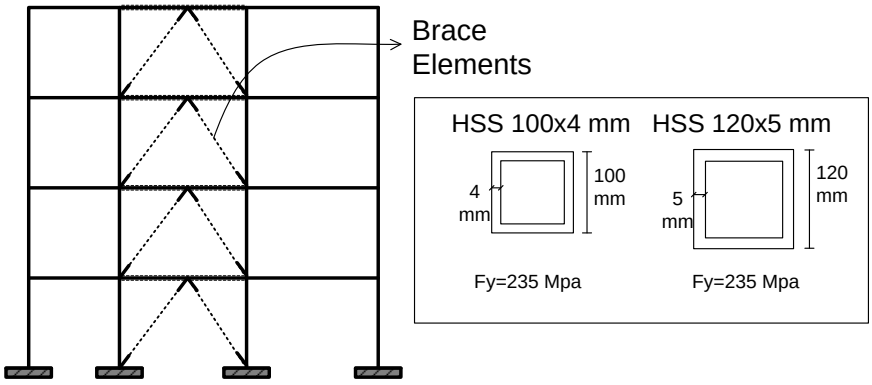

Figure 4.4: *Chevron brace layout*

4.1.3 RC Frame with ISF

Finally the test frames were strengthened with composite connected steel members (ISF). I300 and I360 steel sections were selected as strengthening members and they were installed to the interior columns of test frame (Figure 4.5). Additional steel plates were added to the interior beams as explained in previous section. Yield strength of I-beam sections and steel plates were taken as 235 and 350 MPa, respectively.

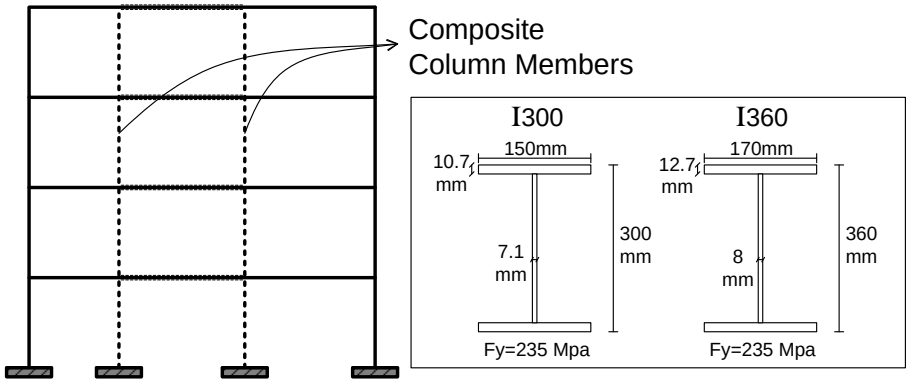

Figure 4.5: *ISF layout*

4.2 Analysis Results

4.2.1 RC Frame With and Without Infill Walls

The nonlinear time history analyses results of the bare frame and frame with infill walls are presented in Figure 4.6. For the structure without infill walls peak first-story drift ratio found as 3.6%. However, structure with infill walls experienced more than 8% DR and at 1.5% first-story DR level, struts at first story was automatically removed from the system. In other words, infill wall of first story was computed to be completely disintegrated. However infill walls of the upper stories did not take any significant damage and remained intact until the end of analysis. This condition created rigidity differences between first story and rest of the structure and caused soft-story formation. Structure with infill walls suffered higher drift ratios than the structure without infill walls and finally it collapsed under the extreme first-story drift ratio demands. Effect of soft-story formation could be seen more clearly in Figure 4.7. According to results structure without infill walls satisfied inter story drift ratio limits of TEC2007 for the CP limit state and remained in high damage region. Results reveal that neglecting infill walls for design purposes may not ensure designer to stay on the safe side for all the cases. However, for both cases such a structure is not capable of resisting the forces that are created by earthquake and should be strengthened.

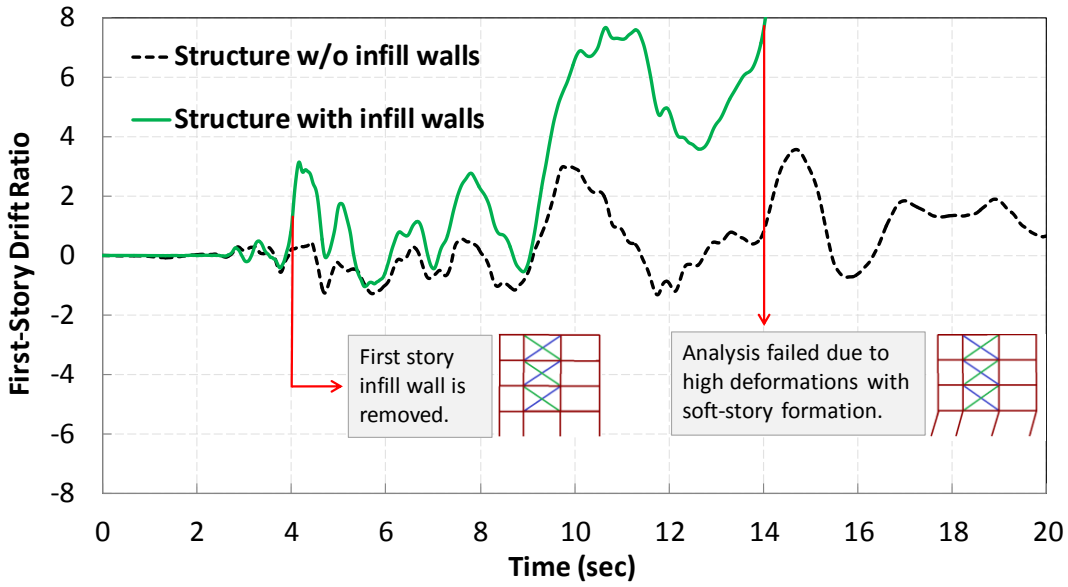

Figure 4.6: *Comparison of simulation results with and w/o infill walls*

Base shear versus top story DR responses are given in Figure 4.8. Results show that incorporating infill walls to the system increased both the stiffness and the lateral load capacity of the system significantly. However, after crushing of first story infill wall, this capacity dropped to the same level that was observed on the results of the bare frame. Therefore, capacity enhancement of infill walls to the system is not accountable at large deformation demands. The presence of an element removal algorithm clearly imposes more demand on the RC members than the case without the infill walls.

Performance evaluation of the both frames led to similar results for the first story (Figure 4.9). For the case without infill walls 75% of the columns passed beyond CP performance limit at first story. However, for the case with infill walls, all the first story columns of the test frame passed beyond CP performance limit as expected. Incorporating infill walls in the nonlinear time history analysis also changed the response on the upper stories. Bare frame mainly experienced damage at the interior columns of first and second stories and exterior beams of first story. Violation of CP performance limit was observed for these beams. For the case with

infill walls, formation of soft story oriented the distribution of damage to first story and prevented upper stories experiencing any significant damage. Both of the systems did not satisfy the overall performance criteria of TEC2007 and assigned to be in collapse region.

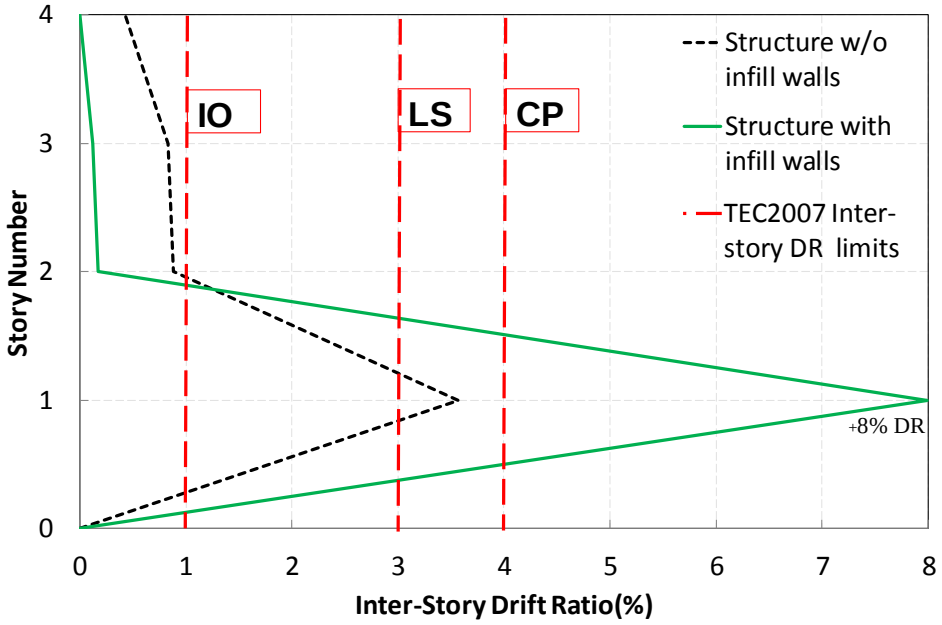

Figure 4.7: *Comparison of inter-story DR with and w/o infill walls*

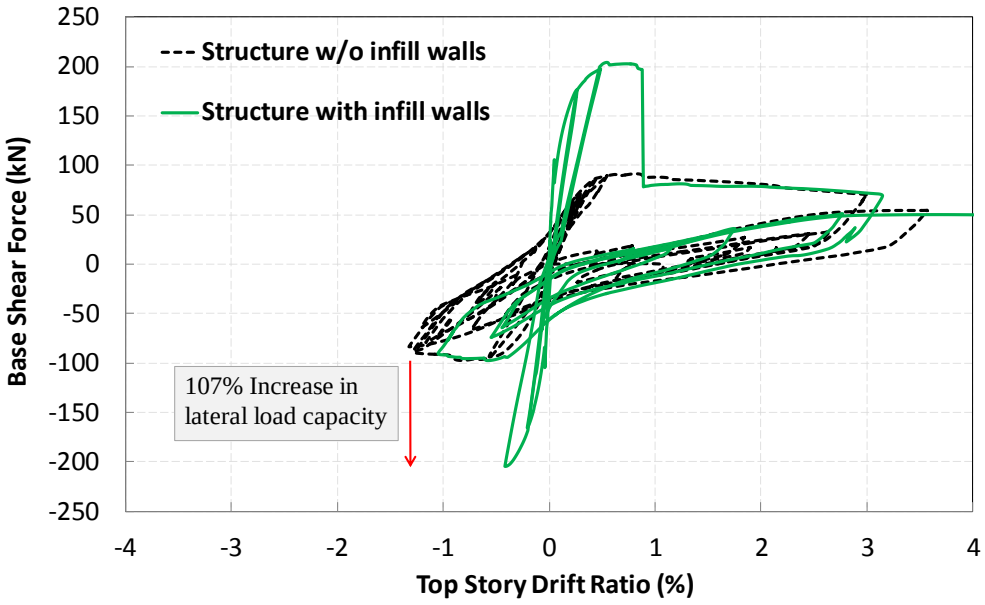

Figure 4.8: *Base shear versus top-story DR with and w/o infill walls*

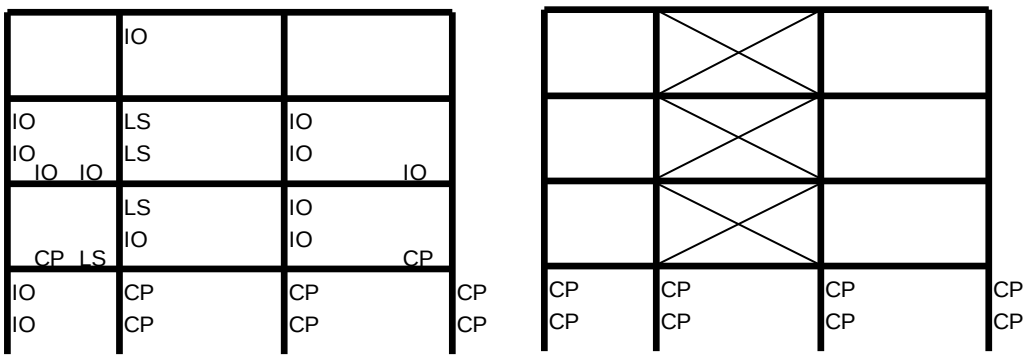

(a) Without infill walls (b) With infill walls

Figure 4.9: *Performance evaluation of RC frame members with and w/o infill walls*

4.2.2 RC Frame with Chevron Braces

The nonlinear time history analyses results of the braced frames with 100x4 and 120x5 mm sections are presented in Figure 4.10. Results of the frame without infill walls are also represented to reflect the original case of the structure. Results showed that 100x4 brace section was sufficient to keep the structure under 3% inter-story drift ratio which corresponds LS limit purposed by TEC2007. However according to inter-story DR limits that are shown in Figure 4.11, this size of braces pushed the frame to pass beyond IO performance limit. The 120x5 brace section kept the structure under 1% inter-story drift ratio for all the story levels.

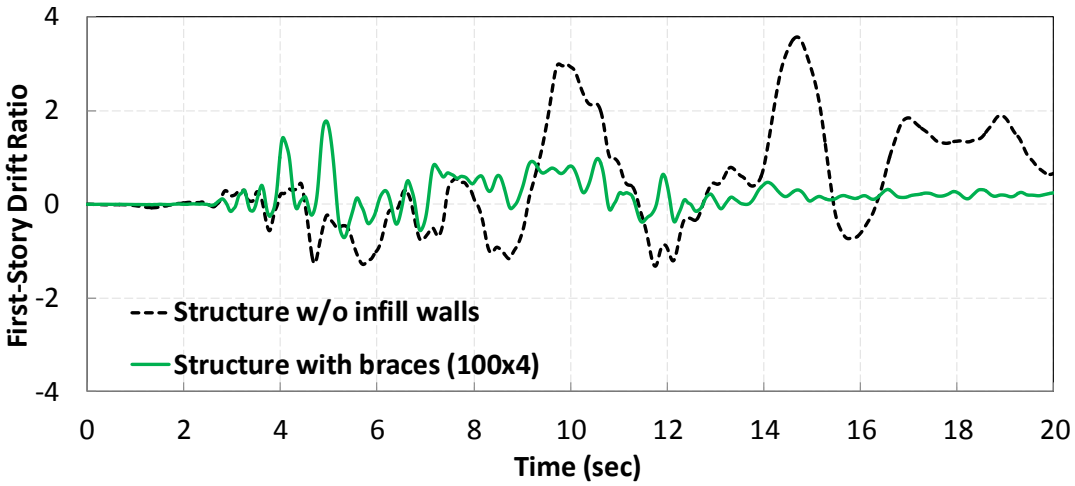

Figure 4.10: *(Continued)*

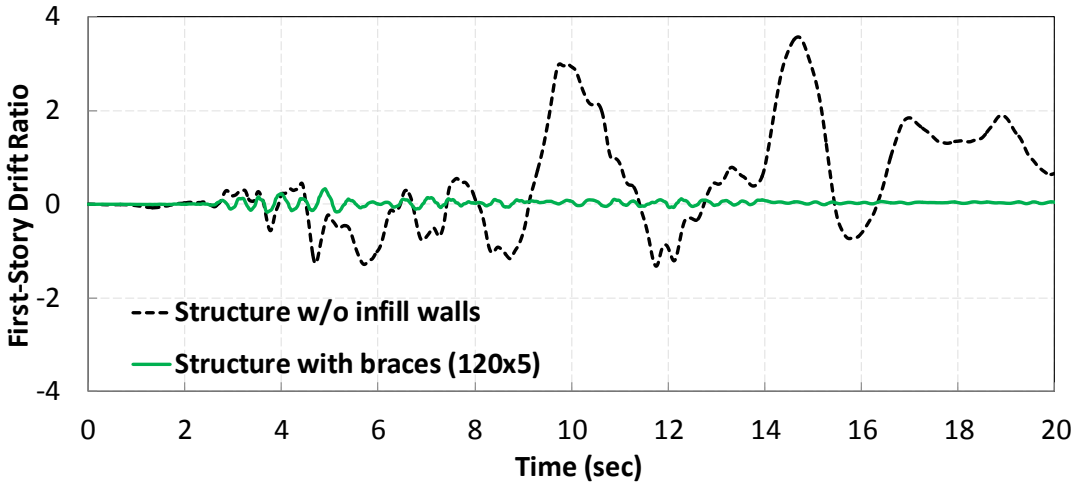

Figure 4.10: *Comparison of simulation results for braces*

Base shear versus top DR ratio results (Figure 4.12) shows that buckling occurred for 100x4 mm brace section whereas 120x5 mm brace sections remained elastic. However, both sections increased lateral loading capacity of the system significantly. Performance evaluation of the systems showed that interior columns experienced significant damage for 100x4 mm brace section due to high compression forces imposed on these members due to overturning (Figure 4.13). However case with 120x5 mm braces kept the system at very low lateral deformations so vertical members did not suffer any significant damage. Exterior beams of the test frame also experienced some damage for this case. State of damage in Figure 4.13 for the HSS120 chevron brace retrofitted frame can be deemed acceptable for LS performance criterion.

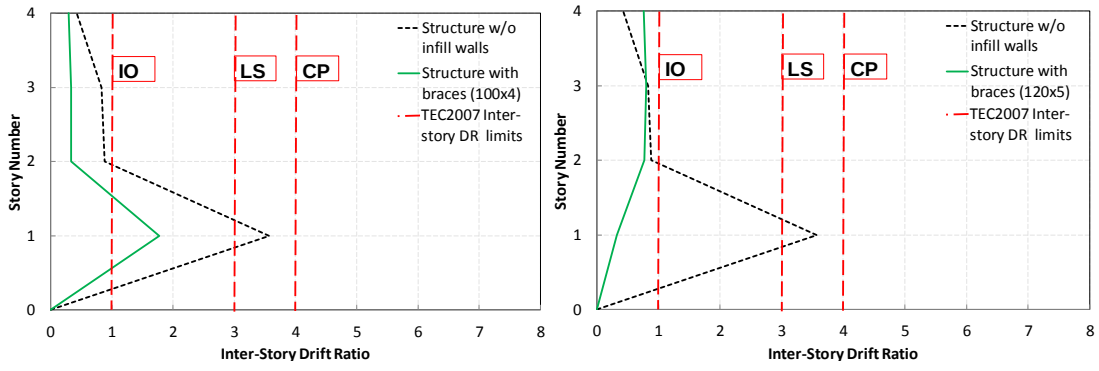

Figure 4.11: *Comparison of inter-story DR for braces*

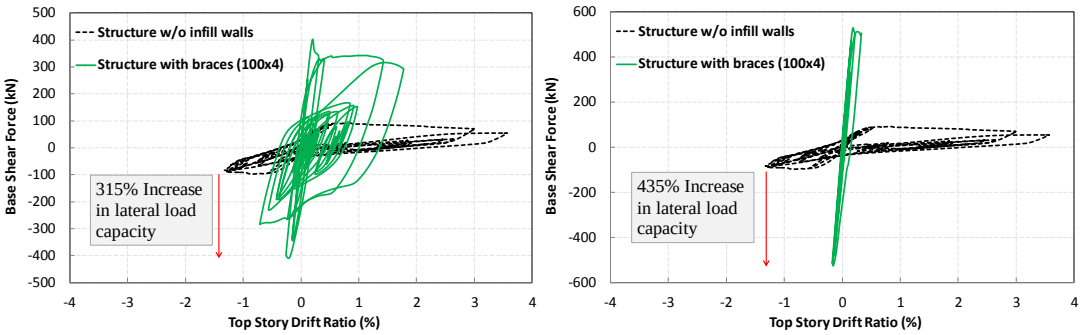

Figure 4.12: *Base shear versus top-story DR for braces*

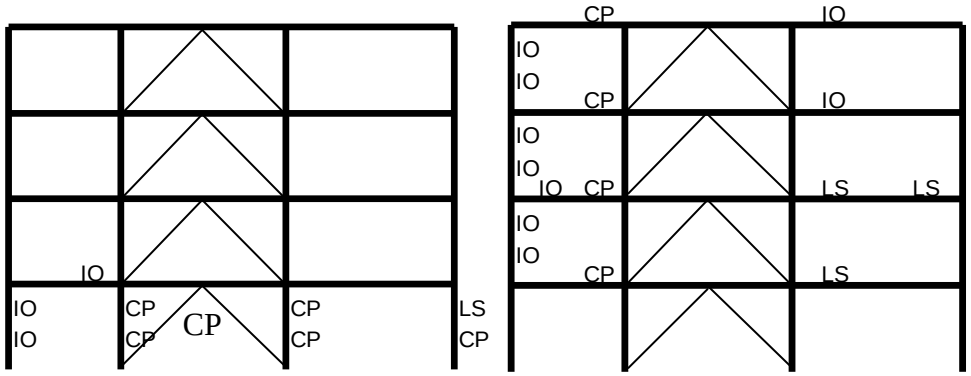

(a) HSS: 100x4 mm (b) HSS: 120x5 mm

Figure 4.13: *Performance evaluation of RC frame members for braced system*

4.2.3 RC Frame with ISF

For the last case, internal steel frame was used as strengthened method and its time history analysis results are given in Figure 4.14. Frame without infill wall results were again added to the figure as the control frame. Results showed that ISF with I300 section kept the system at about 1% inter-story DR and according to overall inter-story DR results (Figure 4.15). The frame slightly passed beyond IO performance level for first and second stories. Replacing steel sections with I360 ensured IO level in terms of inter-story drift ratios. This result indicates that ISF is a flexible strengthened method with respect to the bracing systems.

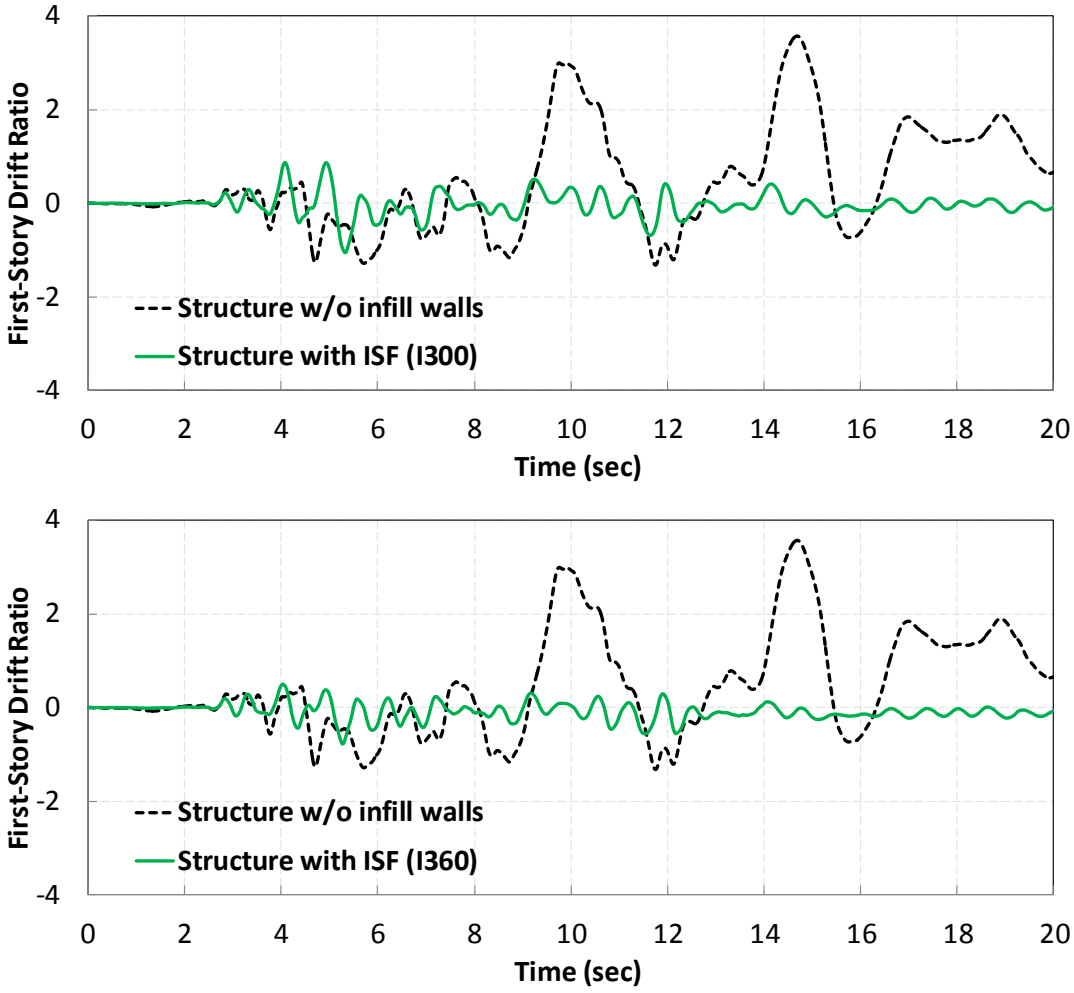

Figure 4.14: *Comparison of simulation results for ISF*

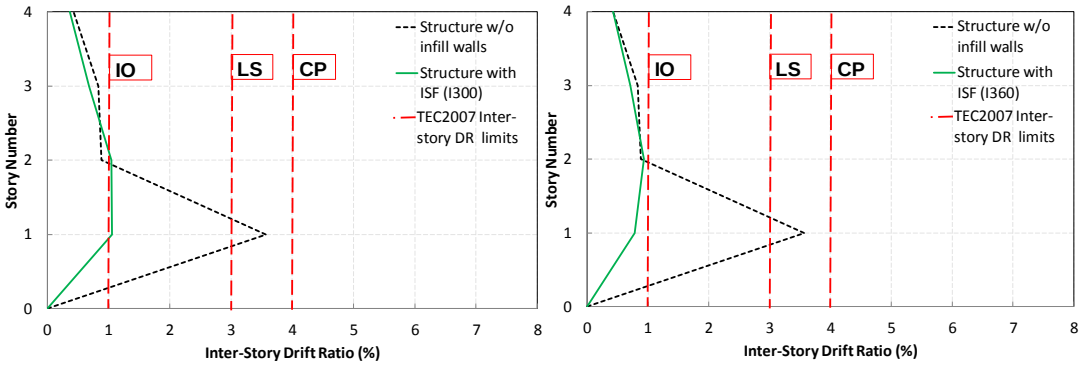

Figure 4.15: *Base shear versus top-story DR for ISF*

Lateral load capacity versus top-story drift ratio of the frame is given in Figure 4.16. Results showed that both steel sections increased lateral loading capacity significantly and I360 section almost remained elastic during the analysis. Performance evaluation of frame with ISF showed that internal columns of the first story were again critical and they went beyond CP performance limits for I300 section (Figure 4.17). Exterior beams of the first and second stories of test frame also experienced some damage for this case. Increasing steel section size helped to reduce damage on first story columns. However it slightly increased damage on beams. This phenomena also observed in analysis results of chevron braces strengthening.

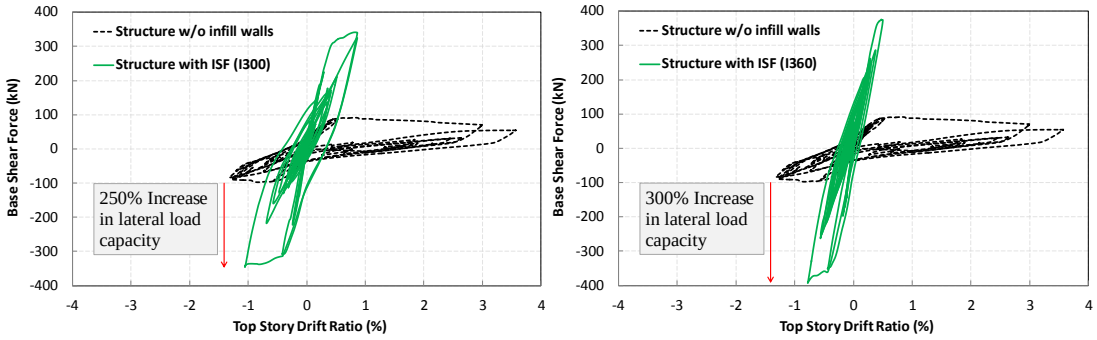

Figure 4.16: *Base shear versus top-story DR for ISF*

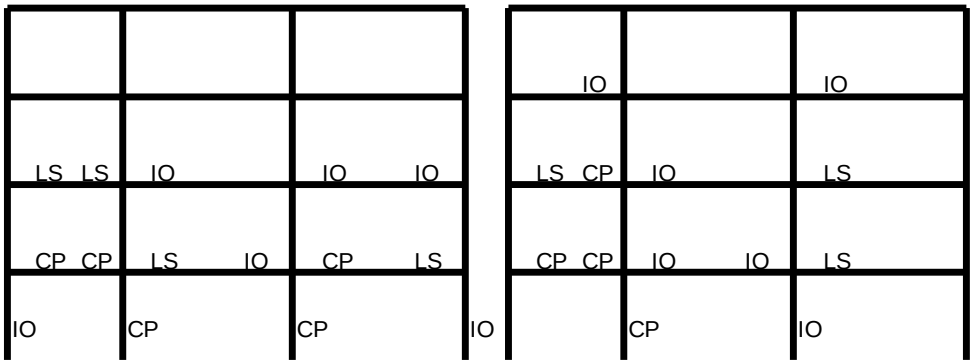

(a) I300 (b) I360

Figure 4.17: *Performance evaluation of RC frame members for ISF*

CHAPTER 5

CONCLUSION

This study aimed to simulate the nonlinear cyclic behavior of RC concrete frames with infill walls, chevron braces and internal steel frames. Numerical models were calibrated and later employed for the performance evaluations and a case study. Results and conclusions are given below:

Infill Wall Modeling

For design purposes, contribution of infill walls is usually neglected. However its effect should be included to have a better estimation of seismic behavior. Results showed that ASCE-SEI-41 recommendations for strut modeling may lead to satisfactory estimation along with the use of element removal algorithm. The formation of a soft story mechanism was found to be better simulated with the use of such a removal algorithm. Performance evaluation of the 4-story frame showed that after crushing of the infill wall, all the first story columns passed the CP limit state and crushed under extreme inter story DR levels. So, for design purposes neglecting infill walls would not always lead safe design or assessment results. However, according to results of both cases, it’s appear that such deficient structures should be strengthened otherwise collapse is inevitable.

Braced Frame Modeling

For braced frame analyses recommendations of Uriz et al. (2008) for brace modeling was found to be adequate. Contribution of rigid end zones and initial imperfection were found to be the important parameters that can affect the results and should be selected carefully. Pinching and degradation of reloading/unloading stiffness due to bond-slip of rebars could be modeled with the hysteretic material model incorporating such degradations. Results showed that buckling of braces has significant importance on performance of this retrofitting method. After buckling occurs, lateral load capacity of the system may drop dramatically. Performance limit states determined by deficient RC members and they found to be nearly independent from brace slenderness whereas dependent from axial load on columns. Brace performance limits defined by ASCE/SEI-41 and they almost coincided with RC member limits for all cases and this corresponds to about 1.5% DR level for CP limit state. Time history analysis showed that including correct boundary conditions can dramatically affect the response of these systems. According to the analysis results, keeping system under low deformations can lead RC members to take any significant damage. However, high axial forces can be transferred from upper story braces to first story columns due to overturning effects. That may increase damages on the first story columns which have share connection with braces. This condition was seen more specific in the case study results (interior columns in case study). Contribution of forces from upper stories caused to experience significant damage of interior columns due to high compression forces. So, for this type of retrofitting, overturning effects should be considered carefully.

ISF Modeling

According to one story frame results, contact between ISF and RC frame were correctly simulated for non-composite sections with applied modeling technique. Modeling RC and steel members as one composite section is also an acceptable modeling technique for this type of installing method. Modeling could be improved by using alternative boundary conditions and results could be matched better in terms of loading stiffness and cyclic behavior. These systems may extend

observed damage on RC members to a higher DR interval. They also provide decent ductility and high lateral loading capacity to the system. Strength capacity of these systems could be adjusted by changing steel section sizes and installing methods. Time history analysis of two-story frame showed that modeling ISF as composite section also provides sufficient performance for matching these test results. Performance evaluation of this system also revealed that RC portion of the composite sections usually experienced damage according to TEC2007 provisions. Case study results indicated that ISF system may capable have prevent destructive effects of ground motion however occurrence of damage in RC members of composite sections should be kept in mind.

Recommendations

Calibrating mathematical models with experimental results is essential to have reliable results for such case studies. However, changes in test setup complicates to adaptation of analytical model. For this study, there were differences in setup of investigated test results for one-story cyclic experiments and two-story PSD experiments. This may require major modifications on analytical model and its applications may not lead expected results. This condition prevents adaptation of analytical model for varied application cases. Another problem is although creating more complicate models leads more accurate results, sometimes they affects results adversely by making them highly sensitive to used parameters. This condition prevents its repeatability for different applications.

REFERENCES

[1] K. Ikeda and S. A. Mahin, "Cyclic Response of Steel Braces", ASCE, ISSN 0733-9445/86/0002-0342, Paper No. 20396, February, 1986.

[2] Marc Badoux and James O. Jirsa, "Steel Bracing of RC Frames for Seismic Retrofitting", Journal of Structural Engineering, ASCE, Vol. 116, No.1, Paper No. 24219, January, 1990.

[3] J.A. Pincheira and J. O. Jirsa, "Seismic Response of RC Frames Retrofitted with Steel Braces or Walls", Journal of Structural Engineering, ASCE, Vol. 121, No.8, August, 1995.

[4] Robert Tremblay, "Inelastic Seismic Response of Steel Bracing", Journal of Constructional Steel Research 58, 665–701, 2001.

[5] A.Ghobarah and H Abou Elfath, "Rehabilitation of a Reinforced Concrete Frame Using Eccentric Steel Bracing", Engineering Structures 23, 745-755, 2001.

[6] Murat Dicleli and Anshu Mehta, "Simulation of Inelastic Cyclic Buckling Behavior of Steel Box Sections", Computers and Structures 85, 446-457, 2007.

[7] Keh-Chyuan Tsai, Po-Chien Hsiao, Kung-Juin Wan, Yuan-Tao Weng, Min-Lang Lin, Ker-Chun Lin, Chui-Hsin Chen, Jiun-Wei, "Pseudo-dynamic Tests of a Full-Scale CFT/BRB Frame-Part I: Specimen Design, Experiment and Analysis", Earthquake Engineering Struct. Dyn. 37:1081–1098, 2008.

[8] Patxi Uriz, Filip C. Filippou and Stephen A. Mahin, "Model for Cyclic Inelastic Buckling of Steel Braces". Journal of Structural Engineering, ASCE / APRIL 628, 2008.

[9] Talaat, M., and Mosalam, K.M., "Modeling Progressive Collapse in Reinforced Concrete Buildings Using Direct Element Removal", Earthquake Engineering & Structural Dynamics, 38(5), 609-634, 2009.

[10] Ozcelik, R. and Binici, B., "Application of Steel Retrofit Schemes for Deficient Buildings in Turkey", Proceedings of the First European Conference on Earthquake Engineering and Seismology, ID 1030, 2006.

[11] Mazzoni, S., McKenna, H., Scott, M.H., and Fenves, G.L., "OpenSees Manual", Pacific Earthquake Engineering Research Center, http://opensees.berkeley.edu, 01/09/2010.

[12] Kent, D.C., Park, R., "Flexural Members with Confined Concrete", Journal of Structures Division, ASCE, ST7, 97, 1969–1990, 1971.

[13] Karsan, I.D., and Jirsa, J.O., "Behavior of Concrete under Compressive Loading." Journal of Structural Division, ASCE, ST12, 95, 2543-2563, 1969.

[14] Pinto, A.V., and Taucer F., "Assessment and Retrofit of Full-Scale Models Of Existing RC Frames." Advances in Earthquake Engineering for Urban Risk Reduction Book Series: Advances in Earthquake Engineering for Urban Risk Reduction, Editors Wasti, S.T. and Ozcebe, G. NATO Science Series, Earth and Environmental Sciences, Vol. 66, 353-367, 2006.

[15] Ministry of Public Works and Settlement, "Turkish Code for Buildings in Seismic Zones", Ankara, Turkey, 159 (In Turkish), 2007.

[16] American Society of Civil Engineers, "Seismic Rehabilitation of Existing Buildings, Report", No. ASCE/SEI 41-06, Reston, Virginia, 428, 2007.

[17] Elkhoraibi, T., and Mosalam K.M., "Towards Error-free Hybrid Simulation Using Mixed Variables", Earthquake Engineering & Structural Dynamics, 36(11), 1497-1522, 2007.

[18] Kurt, E., "Investigation of Strengthening Techniques Using Pseudo-dynamic Testing", Middle East Technical University, 2010.

[19] Ozcelik, R., "Strengthening Reinforced Concrete Frames Using Structural Steel Members", Middle East Technical University, 2010.

[20] American Concrete Institute, "Building Code Requirements for Structural Concrete and Commentary", ACI Committee 318, 430 pp, 2005.

[21] Popovics, S., "A Review of Stress–Strain Relationships for Concrete", American Concrete Institute Journal, 67(3) pp. 243–248, 1975.

[22] Madan A, Reinhorn AM, Mandar JB, Valles RE, "Modeling of Masonry Infill Panels for Structural Analysis", Journal of Structural Engineering ASCE; 123 (10):12951302, 1997.

[23] Ozcelik, R. and Binici, B., "Use of Internal V Braces for Strengthening Deficient Reinforced Concrete Frames.", 8th International Conference on Advances in Civil Engineering, CD Rom Proceedings, ID 246, 2006.